



VILNIUS GEDIMINAS TECHNICAL UNIVERSITY

FACULTY OF MECHANICS

DEPARTMENT OF MECHANICS AND MATERIALS ENGINEERING

ARIHARASUDHAN MUTHUSAMI

**DESIGN OF DELTA ROBOT**

Final Bachelor's Project

STUDY PROGRAMME MECHANICAL ENGINEERING,

CODE 612H33001

Vilnius, 2019

VILNIUS GEDIMINAS TECHNICAL UNIVERSITY  
FACULTY OF MECHANICS  
DEPARTMENT OF MECHANICS AND MATERIALS ENGINEERING

APPROVED BY  
Head of Department

*[Signature]*  
(Signature)

*[Name, Surname]*  
(Name, Surname)

*2019.05.31*  
(Date)

Ariharasudhan Muthusami

**DESIGN OF DELTA ROBOT**

Bachelor's degree final work 3

Mechanical engineering study programme, state code 612H33001

Machine design specialisation

Mechanical engineering study field

Supervisor *Dr. Signatas Petkevicius*

(Title, Name, Surname)

(Signature)

(Date)

*AD 19.05.30*

Consultant \_\_\_\_\_

(Title, Name, Surname)

(Signature)

(Date)

Consultant \_\_\_\_\_

(Title, Name, Surname)

(Signature)

(Date)

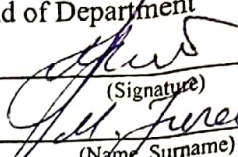
Vilnius, 2019

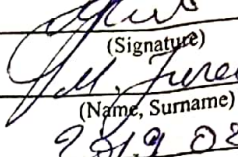
VILNIUS GEDIMINAS TECHNICAL UNIVERSITY  
FACULTY OF MECHANICS  
DEPARTMENT OF MECHANICAL ENGINEERING AND MATERIAL ENGINEERING

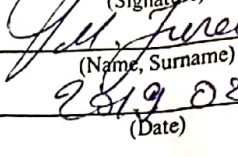
APPROVED BY

Head of Department

Mechanical Engineering study field  
Mechanical Engineering study programme, state code 612H33001  
Machine Design specialization

  
(Signature)

  
(Name, Surname)

  
2019 02 12  
(Date)

### OBJECTIVES FOR BACHELOR'S DEGREE FINAL WORK (PROJECT)

.....No. ....

Vilnius

For student ARIHARASUDHAN MUTHUSAMI

Final work (project) title: Design of Delta Robot

Approved on 04-12-2018 by Dean's degree No. 291 ME  
(day, Month, year)

The Final work has to be completed by 26th May 2019

#### THE OBJECTIVES:

Data: Dimension not exceeding (150\*100\*250) cm

Electrical Power: 0.2Kw (Average consumed)

Voltage supply: 220-230v

Controller: Arduino Programmed via Matlab

Explanatory note: Introduction; Analysis of similar devices; Argument of selected decisions; Necessary calculations of constructions; kinematics and stiffness calculations; Calculation of the drives; Description of control system; Technological part; Determination of the requirements of safety work using the device; Environmental requirements; Economical calculations; Conclusion, List of references.

Drawings: Drawing of general view (1 page A1); Technological sketches(1 page A1); Drawings of parts (1 page A1); Indicators of economics (0.5 page A1); control scheme (0.5 page A1).

Consultants of the final degree work (project): Design of Delta Robot

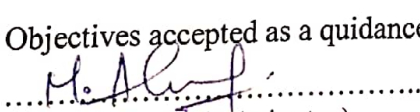
Academic Supervisor



(Signature)

Assoc. Prof.,Dr.SIGITAS PETKIVICIUS  
(Title, Name, Surname)

Objectives accepted as a quidance for my Final work (project)

  
(Student's signature)

ARIHARASUDHAN..MUTHUSAMI

(Student's Name, Surname)

13-2-2019

(Date)

(the document of Declaration of Authorship in the Final Degree Project)

**VILNIUS GEDIMINAS TECHNICAL UNIVERSITY**

Ariharasudhan Muthusami, 20151711

(Student's given name, family name, certificate number)

Faculty of Mechanics

(Faculty)

Mechanical Engineering, MPfuc-15

(Study programme, academic group no.)

**DECLARATION OF AUTHORSHIP  
IN THE FINAL DEGREE PROJECT**

May 30, 2019

I declare that my Final Degree Project entitled „Design of Delta Robot“ is entirely my own work. The title was confirmed on February 18, 2019 by Faculty Dean's order No. 69me. I have clearly signalled the presence of quoted or paraphrased material and referenced all sources.

I have acknowledged appropriately any assistance I have received by the following professionals/advisers:  
Doctor Sigitas Petkevičius.

The academic supervisor of my Final Degree Project is Doctor Sigitas Petkevičius.

No contribution of any other person was obtained, nor did I buy my Final Degree Project.

  
(Signature)

Ariharasudhan Muthusami  
(Given name, family name)

Pirmosios pakopos studijų **Mechanikos inžinerijos** programos bakalauro baigiamasis darbas 3  
Pavadinimas **Delta roboto projektavimas**  
Autorius **Ariharasudhan Muthusami**  
Vadovas **Sigitas Petkevičius**

Kalba: anglų

**Anotacija**

Baigiamajame bakalauro darbe sukurtas „Delta robotas“. Darbe apžvelgjama literatūra ir panašūs prietaisai, naudojami pramoneje ir moksliniuose tyrimuose. Išankstinio ir atvirkštinio kinematikos skaičiavimai yra skirti pateikiems pradiniams duomenims rinkti ir išrinkti, o iš pradžių analizuojami ir siūlomi keli irenginiai, atitinkantys technologinius skaičiavimus, kuriuose yra diržas, guolis, variklis, kinematika, kurie yra atrinkti šiame skyriuje . Kontrolės algoritmo ir Elektros schemas projektavimas atliekamas pagal pasirinktus komponentus, pateikiami aplinkosaugos saugos nurodymai saugiam prietaiso naudojimui pagaliau, ekonominiai skaičiavimai, tokie kaip bendra, fiksuotos išlaidos ir baigtos išvadomis.Darbą sudaro 8 dalys: literatūros apžvalga, skaičiavimai, kinematikos skaičiavimai, valdymo algoritmas, elektros schema, ekonominiai rodikliai, išvados, nuorodosDarbo apimtis - 67 puslapiai, teksto be priedų, 27 paveikslai, 10 lenteliu, 16 bibliografinių ir kitų nuorodų.

**Prasminiai žodžiai:** Additive Manufacturing,Curved Layer Fused Deposition Modeling,Differential algebraic equation,Denavit – Hartennburg,Degrees of freedom,Forward kinematics principle,Ground positioning system,Linear delta robots,Proportion-integral-derivative,Parallel Kinematic structure,Robotic operating system

Bachelor Degree Studies Mechanical Engineering study programme Bachelor Graduation Thesis 3

Title

Design of Delta Robot

Author

Ariharasudhan Muthusami

Academic supervisor

Sigitas Petkevičius

Thesis language: English

**Annotation**

In the final bachelor's work, designed a "Delta Robot." The work provides an overview of the literature and similar devices used in industries and research. Calculations for the forward and inverse kinematics is designed for pick and place operations for the given initial data provided, and initially few devices are analysed and proposed a design accordingly to technological calculations which contain belt, bearing, motor, kinematics which are on the electronics selected in this section. Design of Control algorithm and Electrical scheme is performed according to the selected compensates in the calculations part followed by environmental safety instructions are provided for safe usage of device finally economic calculations like total, fixed costs and concluded with the conclusions.

The work comprising 8 parts: Literature Review, Calculations, Kinematics Calculations, Control Algorithm, Electrical Scheme, Economical indicators, Conclusions, References

The thesis consists of 67 pages, text without appendixes, 27 figures, 10 tables, 16 bibliographic references.

**Keywords:** Additive Manufacturing, Curved Layer Fused Deposition Modeling, Differential algebraic equation, Denavit - Hartennburg, Degrees of freedom, Forward kinematics principle, Ground positioning system, Linear delta robots, Proportion-integral-derivative, Parallel Kinematic structure, Robotic operating system

## TABLE OF CONTENTS

INTRODUCTION .....	11
1. LITERATURE REVIEW .....	12
2. REVIEW OF ANALOGIC CONSTRUCTIONS .....	20
2.1. FANUC M-1/0.5SL.....	20
2.2. IGUS delta robot .....	21
2.3. YASKAWA MOTOMAN MPP3S .....	22
2.4. Justification of Technical Solution.....	23
2.4.1. Arguments.....	23
2.4.2. Methodology & Implementation .....	24
3. CALCULATIONS .....	25
3.1. Belt Drive Calculation.....	25
3.1.1. Motion Quantities .....	25
3.1.2. Motion calculations.....	26
3.1.3. Drive Calculations .....	27
3.2. Spherical Bearings.....	32
3.2.1. Dynamic load.....	33
3.3. Linear Bearing Calculations.....	36
3.4. Motor Selection.....	41
3.5. Micro-stepping .....	42
3.5.1. Motion requirement and motion quantities.....	43
3.5.2. Determining the positioning resolution of load .....	43
3.5.3. Determining the motion profile .....	43
3.5.4. Determine the required motor torque:.....	44
3.5.5. Select & Confirm the Stepping Motor & Driver System.....	45
4. KINEMATICS CALCULATIONS .....	46
4.1. Forward Kinematics .....	50

5.	CONTROL ALGORITHM .....	52
6.	ELECTRICAL SCHEME .....	54
7.	REQUIREMENTS OF WORK SAFETY AND ENVIRONMENT .....	56
7.1.	Design Consideration for safeguards .....	56
7.2.	Installation environment.....	57
7.3.	Wiring safety .....	59
8.	ECONOMIC INDICATORS.....	60
8.1.	Calculations of fixed assets and production costs.....	60
8.2.	Calculation and determination of fixed costs .....	63
	CONCLUSIONS .....	65
	REFERENCES .....	66
	APPENDIX .....	68

## LIST OF FIGURES

<b>Figure 1.1.</b> Delta robot (Roantech, 2018).....	12
<b>Figure 1.2.</b> Delta robot (Bortoff, 2018).....	15
<b>Figure 1.3.</b> Structural scheme of Delta robot (Yeshmukhametov, A. 2017).....	17
<b>Figure 1.4.</b> Workspace of Delta type robot (Yang, X. 2017).....	18
<b>Figure 2.1.</b> FANUC M-1/0.5SL (FANUC, 2018) .....	20
<b>Figure 2.2.</b> IGUS delta robot (IGUS, 2018) .....	21
<b>Figure 2.3.</b> Graph for Mass vs. Picks (IGUS, 2018) .....	22
<b>Figure 2.4.</b> YASKAWA MOTOMAN MPP3S (YASKAWA, 2018).....	23
<b>Figure 3.1.</b> RPM versus Power (Elatech, 2018) .....	29
<b>Figure 3.2.</b> Mass versus acceleration (Elatech, 2018).....	30
<b>Figure 3.3.</b> Dimensions of spherical bearing (HIRSCHMANN, 2018).....	32
<b>Figure 3.4.</b> The action of load; $F_r$ - radial load; $F_a$ - axial load (HIRSCHMANN, 2018). ....	33
<b>Figure 3.5.</b> Y factor (HIRSCHMANN, 2018).....	34
<b>Figure 3.6.</b> Types of loads (HIRSCHMANN, 2018) .....	34
<b>Figure 3.7.</b> Operating factors (HIRSCHMANN, 2018) .....	35
<b>Figure 3.8.</b> Specific surface pressure (HIRSCHAMNN, 2018) .....	35
<b>Figure 3.9.</b> Dimensions of Linear bearing (SKF, 2019).....	36
<b>Figure 3.10.</b> $C_1$ -Determination from reliability (SKF, 2019).....	39
<b>Figure 3.11.</b> Inner diameter versus viscosity (SKF, 2019).....	39
<b>Figure 3.12.</b> Factor $f_s$ for linear bearings (SKF, 2019) .....	40
<b>Figure 3.13.</b> Graph determining deflection versus pressure ratio (SKF, 2019) .....	41
<b>Figure 3.14.</b> Velocity versus time graph (SURESTEP, 2018) .....	42
<b>Figure 4.1.</b> Schematic explaining the parts .....	46
<b>Figure 4.2.</b> XY Plane in the bottom view.....	47
<b>Figure 5.1.</b> Structure of Control Algorithm.....	52
<b>Figure 6.1.</b> Electrical Scheme .....	54
<b>Figure 7.1.</b> Interlocked 3d Printer .....	58

## LIST OF TABLES

<b>Table 3.1.</b> Factors for belt calculation (Forbo movements, 2018) .....	28
<b>Table 3.2.</b> Data from the manufacturer (HIRSCHMANN, 2018) .....	33
<b>Table 3.3.</b> Capacity and load factor (HIRSCHMANN, 2018). ....	34
<b>Table 3.4.</b> Dimension values for figure 3.9 (SKF, 2019). ....	37
<b>Table 3.5.</b> Initial data for calculations (SKF, 2019). ....	38
<b>Table 3.6.</b> Initial data for the calculation of basic life hours (SKF, 2019):.....	40
<b>Table 8.1.</b> Initial investments of the company producing the mechanisms.....	60
<b>Table 8.2.</b> The mechanism component price list.....	60
<b>Table 8.3.</b> Variable direct and non-direct costs for manufacturing one product.....	63
<b>Table 8.4.</b> Fixed costs of the company .....	64

## **NOMENCLATURE**

AC	-	Alternating Current
AM	-	Additive Manufacturing
CLFDM	-	Curved Layer Fused Deposition Modeling
CNC	-	Computer numeric control
DAE	-	Differential algebraic equation
DC	-	Direct current
DH	-	Denavit - Hartennburg
DOF	-	Degrees of freedom
FKP	-	Forward kinematics principle
GPS	-	Ground positioning system
LDRs	-	Linear delta robots
LED	-	Light emitting diodes
PID	-	Proportion-integral-derivative
PKM	-	Parallel Kinematic structure
ROS	-	Robotic operating system
WHO	-	World Health Organization
CAD	-	Computer Aided Design

## INTRODUCTION

It is a parallel kind of manipulators in which several links connected in the closed kinematic chain where the articulated traveling plate is attached to the bottom of link in a common type of parallel manipulator called Delta robots, but there are several modified Delta robots which provide 3,4,6 DOF according to their orientation of linkages. These types of robots which are getting popular now-a-days because of their high acceleration due to low inertia, high stability and precision due to multiple ties connecting articulated traveling plate, these types of robots used in pick and place operations of lightweight materials, medicinal packaging, micro-electronics assemblies, and parallel manipulators have several advantages over serial kind of manipulators like acceleration and high stiffness, high repeatability.

Its usage is increased by developing the mobility of the robot, and its architecture plays a vital role in Delta type 3d printers due to which it is one of the high accurate 3d printers and some researchers even made four-axis milling machine using this architecture as a base. Initially Delta robot was founded by researcher Clavell in École Polytechnique fédérale de, Lausanne Switzerland for a pick and place of chocolates for an industry thereafter several optimizations were done by researchers and students, one several kinds of optimization is used for surgery where robots link length has been nearly tripled, and kinematics and dynamics were altered accordingly for the required purpose (Gurgen, M. 2016). The above robots have been optimized by calculating forward and inverse kinematics so that efficient way of manipulating the robots successfully in the required area, each above-optimized robots work envelope changes accordingly, and it is inscribed radius in delta robots which is going to be optimized in this thesis and several other things to things to be optimized which we will see in forthcoming part.

Aim of the work: To design a delta robot with 3 DOF for wider workspace by introducing a spherical joint between articulated traveling plate and the link connecting it, necessary calculations like selection of bearings and belt, motor and kinematic analysis of the robot. Control algorithm and electrical scheme for working of the robot and environment safety requirements for the device and the operator, economic calculations like fixed costs, production costs variable costs which are analyzed through plotting graphs.

## 1. LITERATURE REVIEW

One of the most standard parallel manipulator designs is the DELTA platform, initially developed by Swiss team lead by Raymond Clavell, driven by 3 revolute joints located on the base, motion is transmitted through three parallelogram arms to a semi-triangular finish piece, called the delta plate figure 1.1 Delta robot (Roantech, 2018) explains the delta robot parts.

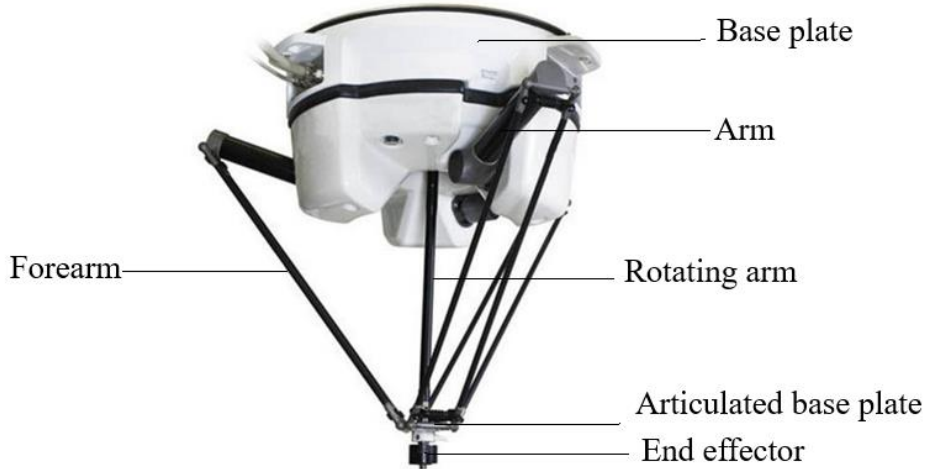


**Figure 1.1.** Delta robot (Roantech, 2018)

In this (figure 1.1) base plate contains an actuator directly actuates actuators and arm, forearms are actuated by link connecting arm, rotating arm is connected directly to the motor which rotates the articulated base plate connecting the end effector.

The defining facet of Delta manipulators is their parallelogram arms. Two long links are connected to the adjacent links by spherical joints at each end, forming a 4-bar mechanism. This setup ensures that two connected links remain parallel, effectively removing one degree of freedom from the system. By using three 4-bar mechanisms, Delta platforms lock the pitch, roll, and yaw of the Delta plate, such as the articulated traveling plate includes a constant orientation no matter position. There are various Delta platform configurations, including linear Delta robots, which swap the revolute joints of the original Delta platform for prismatic joints. In most cases, motion is achieved through the utilization of lead screws and rotational motors, though other linear actuation methods are also used.

The Delta parallel robot is one of the most successful parallel robot designs to its intrinsic properties, based on the type of actuator, the 3-DOF Delta robot falls into two groups, namely, revolute-input and prismatic-input. So far, different kinematic sensitivity indices have been proposed and by employing different kinematic sensitivity indices such as manipulability, dimensionally kinematic sensitivity, and weighted kinematic sensitivity indices. The cytostatic performance of the

robots compared over a specific workspace. The sensitivity of prismatic Delta robot is high in the center of the workspace, and the sensitivity increases when the articulated traveling plate moves to edges from the center. However, the sensitivity of the revolute Delta robot is different. It is high on the sides, and it decreases by moving to the center. Weighted kinematic sensitivity results show that geometrical features of the robots are essential, and it changes the sensitivity values and trend significantly.

Moreover, to enhance the kinematic performance of the robots, the configuration of the robots is redesigned using optimization of the kinematic sensitivity indices. The kinematic sensitivity indices can be employed in the design step of the robot to reach an optimal kinematic sensitivity in the workspace. The kinematics sensitivity indices are mathematical expressions defining the kinematic performances of the manipulator such as velocity and acceleration, which are related to the design parameters.

Generally, a high or very low kinematic sensitivity of the manipulator is undesirable. More precisely, a high sensitivity would describe that a small change at the actuator joint space would be amplified into a massive orientation change of the end-effector. On the other hand, a very low kinematic sensitivity would indicate that the orientation of the end-effector is not controllable because a change in the joint coordinates would cause no effect on the end-effector orientation. Kinematic modeling of revolute and prismatic 3-DOF Delta manipulator implemented. Formulation of manipulability, dexterity, kinematic sensitivity, and weighted kinematic sensitivity is presented. Different sensitivity indices are calculated and weighted kinematic sensitivity of 3-DOF parallel Delta. To compare the kinematic sensitivity of these two robots, different criteria such as manipulability, dimensional, and weighted kinematic sensitivity indices are used for evaluating the robots. A rectangular mesh of robot workspace was considered, and the indices were derived over the workspace. Based on the kinematic sensitivity indices, the kinematic performance of two robots was compared. Dimensional and weighted kinematic sensitivity indices showed a totally different trend for two different robots. to satisfy different sensitivity criteria, it is essential to choose a proper precision to make sensitivity in the critical points negligible. Moreover, as an application of the kinematic sensitivity, by means of optimization of the sensitivity indices, the design parameters of a robot (Behzad 2017).

Parallel robots are composed of several kinematic chains that connect the end-effector to the base, thus forming multiple closed-loop chains. This structural characteristic allows for load-sharing on each kinematic chain yielding several advantages such as increased accuracy, rigidity, and velocity of the articulated traveling plate when compared to serial robots. Furthermore, all the actuators are fixed to the base of the manipulator so that the weight of the motors is not supported by the kinematic

chains, thus resulting in a lighter structure. Therefore, an increased payload capacity relative to the total robot mass is obtained when compared to serial robots. Due to their advantages, parallel robots have recently drawn a lot of interest in a growing range of applications (medical, machine-tools, packaging, pick and place, etc.).

On the other hand, their use is still sporadic due to several open problems inherent to their control. Indeed, there is no standard technique to calculate the forward kinematics (FKP) for a generalized parallel robot. Even though particular FKP solutions may exist, their calculation is rather time-consuming. Furthermore, an algorithm to discriminate between feasible and non-feasible solutions (e.g., going through a singular configuration, causing interference, etc.) is necessary. A related issue is the calibration of the kinematic model, which is often required to control the system. Errors caused by uncertainties in manufacture and assembly of the links make it difficult to obtain an accurate Jacobian which is needed in most control approaches, which in turn result in articulated traveling plate positioning errors. To minimize these errors, the calibration of the architecture parameters is necessary.

The larger the number of parameters, the more difficult it is to calibrate the system. In general, parallel robots require the calibration of a more significant number of structural parameters when compared to serial robots. For example, when using the DH method, each link actuated by a single degree of freedom (DOF) actuator is uniquely defined by 3 parameters and one variable. Thus, in the case of a 3-DOF serial robot, having 1 link per DOF, 9 parameters need to be specified to define the kinematics of the robot accurately. The delta robot (one of the simplest parallel robots) is also a 3-DOF robot but has 7 links, and therefore requires the specification of 21 parameters. Due to the use of a linear camera model, the approach yields low computational cost, which makes it suitable for real-time implementation. A single iteration of the control approach can be performed in 89 milliseconds even though this time can vary depending on the hardware and software used in the implementation (Enrique, 2017).

Delta robots are designed to satisfy the need for rapid, precise, relatively mild-weight pick out-and-location adaptable environment by mounting. cycle time of 3 cycles-per-second with payload capacity less than 1kg is common however, delta robots, and parallel mechanisms more usually, offer blessings over extra common serial-link manipulators, inclusive of lower mass and excessive stiffness, with a view to causing them to suitable for applications besides pick-and-place, such as robotic assembly. And extensions to the original design are addressing kinematic limitations by growing the numbers of DOF. Delta robots and similar parallel mechanisms have drawn the attention of the studies network for many years to cope with the demanding situations of kinematic and dynamic modeling and manage. Unlike the kinematics of serial chain robots, the ahead kinematics of

the delta robot (the function from actuated joint angles to the location of the give up effector) cannot be expressed analytically. This makes the formulation of dynamic and inverse dynamic equations of movement greater hard. equations of motion may be derived using a ramification of methodologies consisting of the precept of virtual work, the Newton-Euler components, or LaGrange and Hamiltonian energy-based approaches on. But, there is no single correct kinematic, dynamic or inverse dynamic model of a Delta robot or any robot, for that matter. different methodologies result in different models, and each has merit depending on the use-case, e.g., some methods may be more efficient for the process of model synthesis, while others result in greater efficient code, and nonetheless, others are greater useful for feedback manipulate machine layout. developing a more general modelling framework, and extra concretely, model libraries, which are useful for time-area simulation, dynamic evaluation, numerous kinds of optimization, and manage gadget layout of not only a robotic, however in the long run an entire assembly line, which includes the robot's tasks that go beyond pick-and-place, and at varying DOF.

The below figure 1.2 explains the nomenclature of delta robots like distal links proximal links, base plate and end effector for a reference in the below explanation.

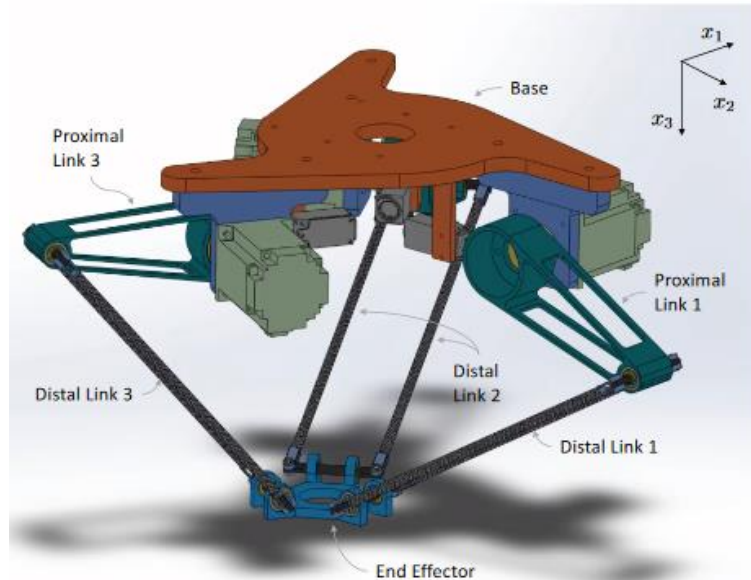


**Figure 1.2.** Delta robot (Bortoff, 2018)

The above figure 1.2 delta robot's nomenclature is concerned for the with explanation of below paragraph.

Our vision and indeed technical approach are kin to the ideas and mathematical rigor in including designing, calculations, economical estimations. It is important to emphasize that modeling is expensive and time-consuming, and we seek a framework in which we can reuse models for a variety of different use-cases, such as control system design at its various hierachal levels (e.g., low-

level feedback loops and also higher-level sequences), possibly as part of the control law itself, e.g., using Model Predictive Control, for model-based estimation, mechanism co-design, and even for uses that are not immediately foreseen today. First by defining the dynamics for each independent arm, assuming it is unconstrained, and then derive the dynamics of the robot by adding a holonomic coupling constraint representing the end effector.

The resulting index-3 Differential Algebraic Equation (DAE) is stabilized using Baumgarten's method, giving an index-1 DAE that is useful directly for simulation, dynamic analysis, control system design, and is extendable to other uses such as force control (Bortoff, 2018). The main disadvantage of the parallel robots (in this case the linear delta robot) compared to commonly used cartesian systems in additive manufacturing, is the reduced working space they provide relative to the overall size of the robot. In this way, the workspace becomes a design parameter that requires special attention. Then a method that allows finding the minimum dimensions for the structure of the robot according to a prescribed workspace is necessary. Over the years different parallel robots have emerged, many of these architectures are truly innovative; however, the linear delta robot has become by far the most popular and used in pick and place operations, packaging, welding, CNC operations and of course, additive manufacturing (AM). Raymond Clavell proposed the first robot with delta configuration in 1985. Basically, three DOF (Degrees of Freedom) linear delta robot is formed by two platforms connected through three identical kinematic chains, where one of the platforms is usually defined as mobile, and each kinematic chain is constituted by links parallelogram with spherical joints. This kind of architectures exhibits excellent performance in terms of high speed, low inertia, and accuracy. In AM applications, linear delta robot enables the manufacturing of Curved Layer Fused Deposition Modeling (CLFDM), which is an AM technique with dynamic tool-path containing dynamic z-values within each layer (Alberto, 2018).

It is worth noting that maximum industrial manipulators have a serial kinematic architecture, that is, their hyperlinks are organized serially, resulting in a cantilever kind shape. The serial kinematic association of hyperlinks produces massive workspace but suffers from high positioning errors and reduced stiffness. Another well-known fact, but far less widespread kinematic architecture is the fully parallel one for which the output hyperlink is hooked up to the ground through numerous legs. Completely-parallel kinematic architectures are recognized for their high stiffness and low positioning mistakes but suffer for a relatively small workspace. They had been used for a long-time in-flight simulator and, more recently, in robotics and gadget device packages. The concept of mixing the above two sorts of kinematic arrangement in a single hybrid structure is poorly exploited, despite the potential benefits which could be gained with such architecture. Combination of 3-DOF serial and Delta parallel manipulator will be investigated in terms of design analysis, kinematics, dynamics, and

control system. The most evaluated robot characteristics are precision, payload capacity, speed, and simplified kinematics equation. In this study, we propose Hybrid manipulator Yambot 10 with 7 DOF, 1 DOF from the slider, 3-DOF comes from the following part, and 3- DOF provides Delta manipulator.

The below figure 1.3 is show the structural scheme of delta robot where parts are numbered, and numberings are explained in the below lines

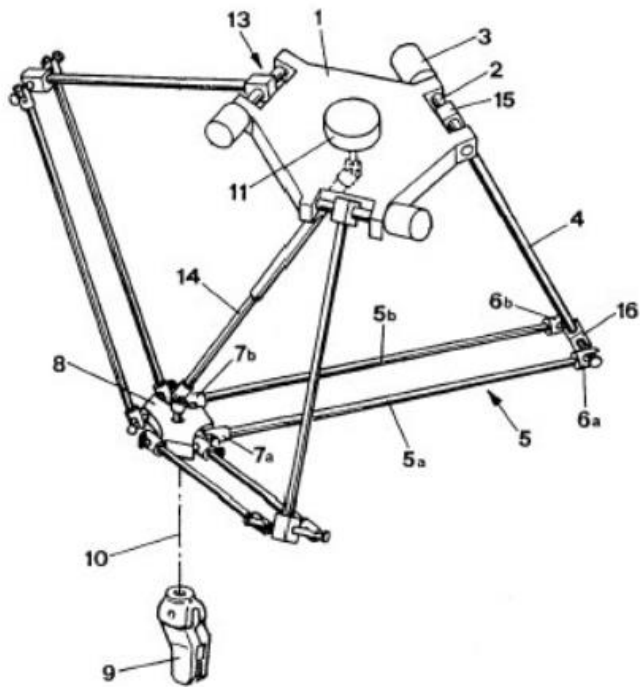


**Figure 1.3.** Structural scheme of Delta robot (Yeshmukhametov, A. 2017)

(9 - End effector; 14 - pneumatic line; 8 - articulated traveling plate; 16,13 - revolute joint; 1,11 - base plate; 4- forearm; 5a, 5b – arm; 7a,7b,13,15 – joint end; 2 – joint support; 3 – motor; 6b- joint support, 10 line for assembly of end effector).

One of the most challenging parts of this work is combining all constraints and determination of workspace. This mean that, proactive actions and vibrations could directly affect to robot's precision and accuracy, because of Delta robot mostly exploits only in vertical position and Delta robot is one of the fastest robots in the world, furthermore in this work Delta robot would be able to work in horizontal direction as well, which creates some technical problems related with dynamics and robot frequency. About robot frequencies, the serial and parallel part should be synchronized rate and speed to decrease possible inaccuracy during work. Moreover, this research will propose a technical solution to eliminate the dynamic effect. The second main concern of this

work is hybrid robot size ration; this means the ratio between parallel and serial manipulator (Yang, X. 2017). Because of the high torque of Delta, manipulator work translates to the whole robot body, which could create unstable and non-balanced robot work. After their inception within the past two decades as possible alternatives to conventional computer numerical controlled (CNC) machine tools systems that dominantly adapt serial structures, parallel kinematic machines PKM had been anticipated to shape a foundation for a brand-new era of destiny machining centers. But, this desire fast faded out as maximum troubles associated with this type of systems persist and could not be solved entire satisfactorily.

This especially turns into more apparent in machining packages in which accuracy, stress, dexterity, and ample workspace are essential necessities. although the PKMs possess advanced mechanical traits to serial systems, especially in phrases of high stress, accuracy, and dynamic reaction, however, the PKMs have their very own drawbacks along with singularity troubles, inconsistent dexterity, irregular workspace, and confined variety of motion, mainly rotational movement (Yeshmukhametov, A. 2017).

The below figure explains the typical workspace of delta type robots in X and Y axis of a Delta type robot

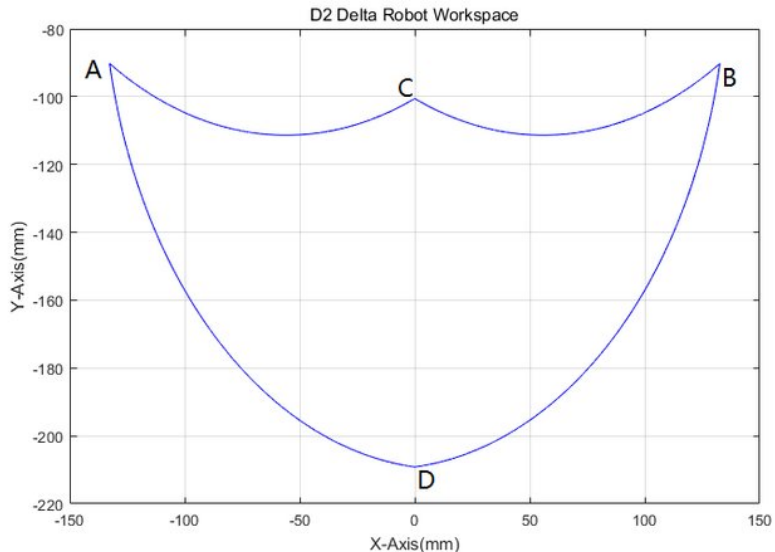


**Figure 1.4.** Workspace of Delta type robot (Yang, X. 2017)

A, B, C, D are the maximum points reached by the end effector of a delta type of robot and these positions are evaluated using software for best results.

The above figure 1.4 explains the workspace or inscribed radius of delta robot in X and Y axis as we can observe that it has maximum of 220 mm in Y-axis and 150 mm in X-axis which is very less these kinds of robots are used only for small work area but we can observe a curve meets at peak

point at C at the same time maximum end at point D in Y-axis but these workspace can be altered accordingly using joint types and design changes. But the above figure 1.4 workspace is taken from delta robot using restricted joint type because usual delta robots inscribed radius will be half circle without distractions like points D in figure 1.4 suppose assume that a 3 DOF robot is designed and the workspace can be clean half circle with some radius so from these we can say that joint types or in other words design changes or end effector positions can also alter the workspace so before designing to some required workspace the above parameters like joint angle limits, link lengths, end effector positions should be considered.

## 2. REVIEW OF ANALOGIC CONSTRUCTIONS

### 2.1. FANUC M-1/0.5SL

It is a FANUC M-1/0.5SL robot which is compact and enter a replacement dimension in high-speed small parts handling. With the 4<sup>th</sup> axis this of high-speed assembly robot with inscribed radius of up to 420 metric linear unit and because of ultra-variable mounting positions they can be put in directly into the foremost compact area (figure 2.1) explains the FANUC M-1/0.5SL delta robot parts (FANUC, 2018).



**Figure 2.1.** FANUC M-1/0.5SL (FANUC, 2018)

This figure 2.1 robot has base plate close configured which make it useful in the areas of chemical exposure and water resistant but here the arm connecting the base plate and forearm to the arm which is lighter, and rotational arm is connecting the base plate to plate connecting the end effector.

Its payload of maximum 1 kilogram and this robot uses four-bar kinematic closed chain mechanism each arm is actuated by an actuator which operates the base plate accurately to the required position which makes inscribed radius of 420 mm and 150 mm height in Z-axis which is shown in figure 2.1, and repeatability of  $\pm 0.02\text{mm}$ , which is the most accurate for low payloads in these kinds of delta robots, FANUC 3D area sensors enable robots to recognize and obtain positioned objects straight from a picking area. Automating the processes like object-recognition technology represents an efficient manner of accelerating productivity and reducing prices on an enormous vary of general material handling applications, “iRPickTool” visual line tracking technology enhances productivity by providing single or multiple robots with the ability to identify and pick and place items on a moving conveyer belt. which can be controlled via “iPendant” touch teach pad, which makes easily usable, and it requires a voltage of 220-230V and average power supply of 0.2 KW (FANUC, 2018).

So basically, it is the most accurate and with high repeatable rate robot due to their additional constraint in the structure and support to their articulated traveling plate which is connected to the base plate but for only fewer payloads with high accelerations and links are very light otherwise it will create more inertia which can reduce the acceleration

## 2.2. IGUS delta robot

It is a robot with three links. They are attached in a pyramidal shape and 3 axis Dof in which locking the articulated traveling plate rotation along the Z axis and each link is driven by corresponding actuator Figure 2.2 IGUS delta robot (IGUS, 2018) explaining the workspace of IGUS delta robot.

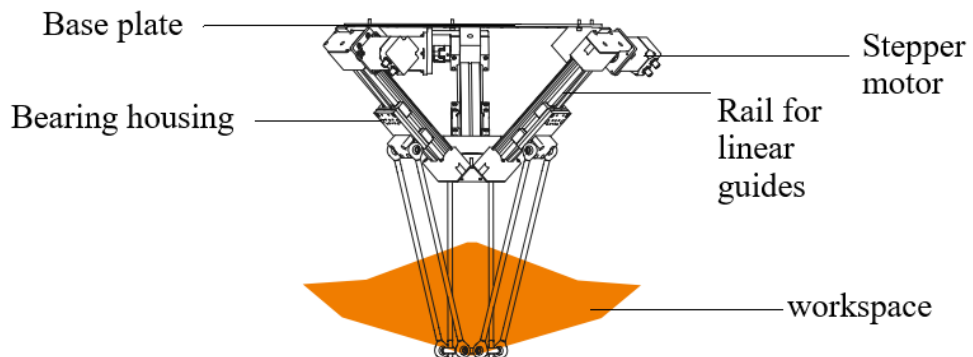


**Figure 2.2.** IGUS delta robot (IGUS, 2018)

In this figure, 2.2 base plate is open configured and forearm connecting directly to the actuator which is connected to the stepper motors no arm and rotational arm is present, the orange part of this figure representing the inscribed radius of this robot.

The belt drive is used for positioning and adjustment tasks. The lubrication-free W profile guide acts as a linear guide. The stroke is individually selectable. It is a lightweight design using plastic and aluminum, belt axes have low mass inertia, making them highly efficient and belt drive offers the ideal solution in both confined spaces and applications that require a high caliber of torque support. Stepper motor “NEMA 23XL” with steep angle  $1.8\pm 5\%$  and maximum axial load of 15N and a maximum radial load of 63N is used for actuating links because of their high accuracy (IGUS, 2018).

This robot can carry payload up to 5 kilograms with medium accuracy of  $\pm 0.5\text{mm}$  with the workspace of 360mm with 75 mm of the forearm, and it can be suitable for the acceleration of  $60 \text{m/s}^2$  because of higher payloads which give more inertia. Picks per minute are also affected by the mass of the object due to inertia, which is explained in the above paragraph, these dynamic relations

can be graphically shown in figure 2.3. The articulated base plate is attached to the bottom with spherical joints in which rotation is locked. By placing the frame for supporting this pyramidal shape robot vibration of  $0.5 \text{ m/s}^2$  which is not a significant factor affecting the positioning accuracy figure 2.3 shows the dynamics relations that are mass(g) versus pics/min.

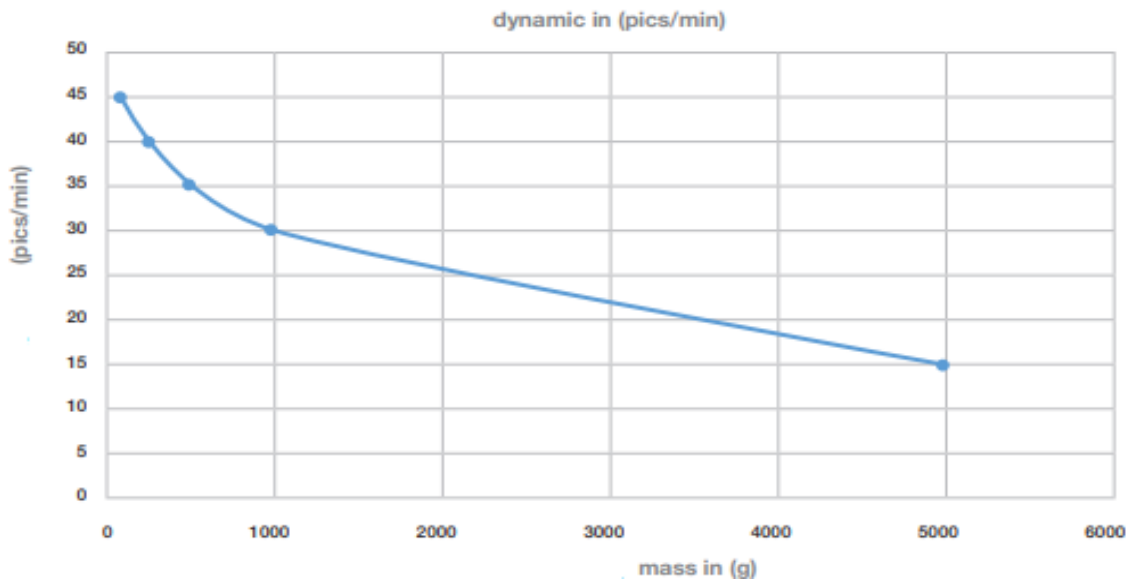


**Figure 2.3.** Graph for Mass vs. Picks (IGUS, 2018)

As we can see that in the dynamic graph that when payload load increases pick per minute decreases compensating vibration factor caused by inertia. So, to maintain the picks per minute. This robot has encoders in the stepper motor-shaft, so position accuracy can be eliminated for the tolerance value of 0.5 mm.

### 2.3. YASKAWA MOTOMAN MPP3S

The robot is a 4-axis robot with parallel kinematic system combines the speed of the open kinematic chain design with a high payload capacity and a broad working range. Due to the high torque to the fourth axis, the so-called wrist axis moves payloads of up to 3 kg at high speed. In this robot, three links are driven by three different actuators in which actuators use stepper motor for driving the link connecting forearm and arm for good positioning accuracy. Likewise, in parallelogram structure and additional rotation of wrist axis, is added to this structure, and inscribed radius of 800 mm because of increased linkage length. When comparing all the above robots, this one has a higher work envelope because of higher linkage length but with the position accuracy with  $\pm 0.1\text{mm}$  which is comparatively better. Pick per minutes is dependent on payload completing 150 cycles per minute with 3 kilograms of load and 185 cycles per minute for 1 kilogram of the load. It has various advantages like position tracking and conveyor tracking facility and programmed via

teach-pedant or with ROS programming (figure 2.4 “YASKAWA MOTOMAN MPP3S”) explains the link lengths and workspace of the robot.

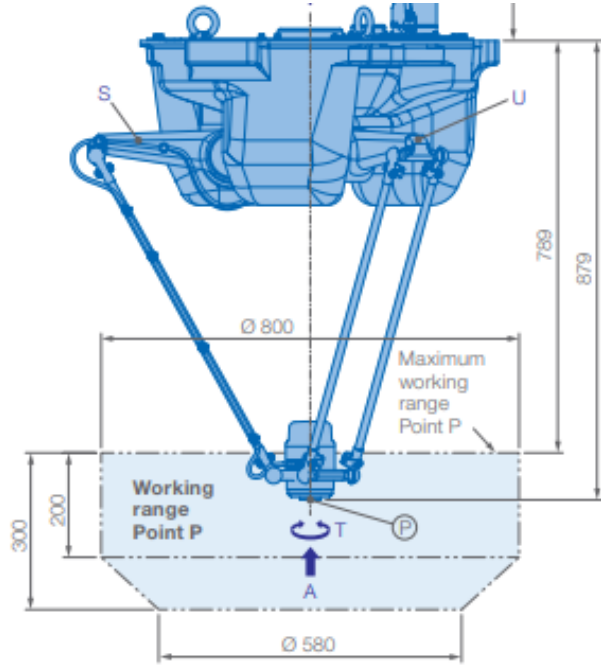


**Figure 2.4.** YASKAWA MOTOMAN MPP3S (YASKAWA, 2018)

In this figure 2.4, the arms are connected to the base plate, and one side of the forearm to arm and other to the base plate and articulated base plate contains the wrist arm for the end effector which adds to the rotation along the Z axis, the blue part representing the workspace of the robot.

Observing this robot has 4-axis with both higher payloads and good accuracy because of wrist arm attached to the articulated base plate with exceptional behavior opposing the inertial phenomena by achieving a low inertial design in a robot so designing factor plays an essential role in reducing many factors.

## 2.4. Justification of Technical Solution

### 2.4.1. Arguments

When gathering all the above parameters like the center of mass, kinematics, and positioning accuracy system because of traditional lever-based design, the motors must deliver high torque to counteract the increasing force applied by the payload on the shaft. This is the reason for low payloads to most of the Deltas. There's a huge torque on the motors that get translated all the way down to the wrist of the robot. So, because of that offset and distance away from the motor itself, we are moving link that can be more than 1000 mm. So, the idea here is when the motors are subjected to high-torque, we have this offset that we must deal with it. To maintain speed, we limit the payload. Comparing all the robots commonly in delta robot linear guides with a belt is driven system assures

us to be more accurate and provides us more payloads even though a lot of manufacturers and researchers working with lead screws which do not need maintenance. In the case of IGUS delta robot mentioned in the IGUS delta robot section of page number 19, that when the mass increases picks per minutes get affected compensating the vibration factor caused by the inertia to maintain these both we can make design changes to robot work for both.

#### 2.4.2. Methodology & Implementation

I am going to design a delta robot with a single link from each side interacting with the objects and for wider inscribed radius with 80 average picks per minute. So, in this thesis, a hexagonal structure is chosen in which three articulated traveling-plate is connected to forearms which are directly connected to three different actuators actuated by belt drive system connected to bearing housing with rail shaft and stepper motor because this can provide higher maximal loads. As it is compared to the above statement, the lead screw type of guides is not used because the belt is cost-efficient. As our project is for medium payloads we should eliminate the inertial factor that is to make the linear guide system in aluminum and links should have optimal tension resists and to be weightless which is chosen to be carbon fiber and for reducing joint failures we should design ball joints in a weigh less way but must have high withstanding capability.

In the base plate area, there is no much weight for reducing the vibration factor so the need for the frame is required in enough manner that it must be enclosed by frame covering the inscribed radius of the robot. So, the bottom plate requires additional support to reduce the vibration, which will be also be designed if required after evaluating the design for vibrations.

Software for designing, SOLIDWORKS is used, and its workspace and kinematics calculations are carried out in MATLAB, Strength and stiffness requirements, the rigidity of links, joint failures are done through ANSYS workbench. Software like ADAMS is used for selecting the length of the efficient link and for finding out possible errors due to linkage lengths vacuum type of grippers are used which does not need any separate power or additional sensors and for positioning-accuracy we are going to use position tracker sensor which is going to be programmed via MATLAB and controlled via ARDUINO and several other microcontrollers. Open source firmware would be used because it is not the time-consuming way, and errors can be avoided. Encoders are used for motor shafts are used these encoders can give position errors from shafts of motors which would help to get feedback for position errors. The project outcome would-be low-cost automation.

### 3. CALCULATIONS

#### 3.1. Belt Drive Calculation

The selection of belt requires necessary calculations to perform flawless drives so, before certain calculation parameters are taken for our requirements which are mentioned as initial data in the below lines and their short abbreviations are noted with a respective term which will be used for further calculations. Our belt is chosen from the Forbo movements manufacturer, so their catalog is used as a reference for this belt calculation (Forbo movements, 2018).

Initial data are:

- center distance for travel ( $d$ ) = 350 mm;
- required speed ( $s$ ) = 1.4 m/s;
- maximum acceleration ( $a$ ) = 6 m/s<sup>2</sup>;
- maximum deceleration ( $d$ ) = 6 m/s<sup>2</sup>;
- mass to be lifted ( $m$ ) = 1 kilogram;
- gravity ( $g$ ) = 9.8 m/s<sup>2</sup>;
- no of belts to be introduced for single side = 1;
- frictional force from shaft and bearing ( $F_R$ ) = 80 N;
- maximum pulley pitch diameter ( $d_o$ ) = 32 mm;
- center distance of pulley ( $e$ ) = 610 mm;
- frictional coefficient ( $\mu$ ) = 0.5.

Initial consideration of pulley diameter, belt pitch, belt width is chosen from the graphs available that is without the tension so, therefore, the belt with a T5 metric standard and 5mm pitch.

##### 3.1.1. Motion Quantities

The motion quantities are calculated to know about the drive speeds, RPM, for the system to achieve the requirements, and it will be helpful for choosing the suitable belt and motor for our system.

Revolutions per minute of the pulley are calculated using the formula  $n$ :

$$n = \frac{v \times 19.1 \times 10^3}{d_o} = \frac{1.4 \times 19.1 \times 10^3}{32} = 835 \text{ min}^{-1} \quad (3.1)$$

where,  $v$  - velocity (m/s);  $d_o$  - pitch diameter of the pulley (mm).

The speed required to achieve the given position is given by the formula:

$$v = \frac{d_o \times n}{19.1 \times 10^3} = \frac{32 \times 835}{19.1 \times 10^3} = 1.4 \text{ m/s}, \quad (3.2)$$

where  $d_o$  - pitch diameter of the pulley (mm);  $n$  - revolutions of the pulley.

Acceleration to cover the required distance is calculated by considering the distance traveled and the time to reach in the given distance:

$$a = \frac{s}{t^2 \times 0.5} = \frac{0.350}{0.35^2 \times 0.5} = 6 \text{ m/s}^2 \quad (3.3)$$

where,  $u$  - initial velocity (m/s);  $a_b$  – acceleration ( $\text{m/s}^2$ );  $t$  – time (s).

Power required to achieve the required motion is calculated by considering the force and velocity so, the formula for calculating the power is:

$$P = \frac{F_U \times v}{9550} = \frac{15.6 \times 1.4}{9550} = 0.00229 \text{ KW}, \quad (3.4)$$

where,  $F_U$  - force required to pull (N);  $v$  – velocity (m/s).

The torque required for the system is calculated using the formula:

$$T = \frac{F_U \times d_o}{2000} = \frac{15.6 \times 32}{2000} = 0.32 \text{ Nm}, \quad (3.5)$$

where,  $F_U$  - the force required to pull (N);  $d_o$  - pitch diameter of the pulley (mm).

### 3.1.2. Motion calculations

Motion quantities are calculated to know acceleration time, velocity, deceleration, and other quantities which are helpful to select belt size.

The time required to accelerate indirectly time required to reach the constant velocity is calculated by using the formula:

$$t_{ab} = \frac{v}{a_b} = \frac{1.4}{6} = 0.23 \text{ s},^{-1} \quad (3.6)$$

where,  $v$  – velocity (m/s);  $a_b$  – acceleration ( $\text{m/s}^2$ ).

Distance traveled during the acceleration is calculated to avoid the error in the total distance traveled which would be calculated using the formula:

$$S_{ab} = \frac{a_b \times 1000 \times t_{ab}^2}{2} = \frac{6 \times 1000 \times 0.35}{2} = 158.8 \text{ mm}, \quad (3.7)$$

where,  $a_b$  – acceleration ( $\text{m/s}^2$ );  $t_{ab}$ - acceleration time (s).

Distance traveled during braking is calculated to know the distance so that error can be avoided during total distance travel for calculating the braking travel is calculated using formula:

$$s_d = \frac{a_v \times 1000 \times t_{cb}^2}{2} = \frac{6 \times 1000 \times 0.23^2}{2} = 158.7 \text{ mm}, \quad (3.8)$$

where,  $a_v$  – deceleration ( $\text{m/s}^2$ );  $t_{cb}$ - deceleration time (s).

### 3.1.3. Drive Calculations

In the drive calculations, we will know about the force from acceleration, pulling force, the torque required to pull so observing the parameter from the motion quantities the following drive calculations are performed. Effective pull  $F_U$  (N) to be transmitted by the belt are calculated using certain factors like accelerating force and frictional force, which are calculated in below lines.

Force generated from acceleration is calculated using the mass and acceleration which is given by the formula:

$$F_A = m \times a_v = 1 \times 6 = 6 \text{ N}, \quad (3.9)$$

where,  $m$  – mass (kg);  $a_v$  – acceleration ( $\text{m/s}^2$ ).

Lifting power or lifting force is calculated by considering the mass and inclination angle so lifting force is calculated by the formula:

$$F_H = m \times g * \sin(\alpha) = 1 \times 9.81 \times \sin(50) = 7.51 \text{ N}, \quad (3.10)$$

where,  $m$  - mass to be lifted (kg);  $g$  – gravity ( $\text{m/s}^2$ );  $\alpha$  - Inclined angle (degrees).

Force due to frictional is considered due to sliding motion so, the coefficient of friction is considered therefore for calculating the frictional force:

$$F_R = m \times \mu \times g = 1 \times 0.5 \times 9.81 = 4.9 \text{ N}, \quad (3.11)$$

where,  $m$  - mass (kg);  $\mu$  - coefficient of friction;  $g$  - gravity ( $\text{m/s}^2$ ).

Considering the forces generated from all source summing to get the total force which is given by the formula:

$$F_U = F_A + F_H + F_R = 18.41 \text{ N}, \quad (3.12)$$

where,  $F_A$  - accelerating force (N);  $F_H$  - lifting power (N);  $F_R$  - frictional force (N).

Several Factors are considered below, which are taken from the belt manufacturer, which will be useful for calculating the maximum effective pull.

**Table 3.1.** Factors for belt calculation (Forbo movements, 2018)

Acceleration factor	$C_3 = 0$
Operational factor	$C_1 = 1$
Teeth in mesh factor	$C_2 = 1$

Number of teeth of pulleys is preferred by designer and belt pitch is chosen from graph 3.2, by mass and acceleration so, Number of teeth of pulley ( $Z_{min}$ ) - 20 teeth, Belt pitch ( $t$ ) – 5mm from graph 3.2.

The maximum effective pull is calculated by considering the operating factors like and teeth in mesh factor and operational factor from the table1.1 which is given by:

$$F_{Umax} = F_U \times (C_2 + C_3) = 18.419 \times (1^2 + 0) = 18.41 \text{ N}, \quad (3.13)$$

where,  $C_2$  - teeth in mesh factor;  $C_3$  - acceleration factor.

Here the graph 3.1 explaining the rpm of the pulley (rpm) versus power (KW) for choosing the belt pitch which is assumed to be T5 because power in our case is 0.0029 KW and rpm is 835.

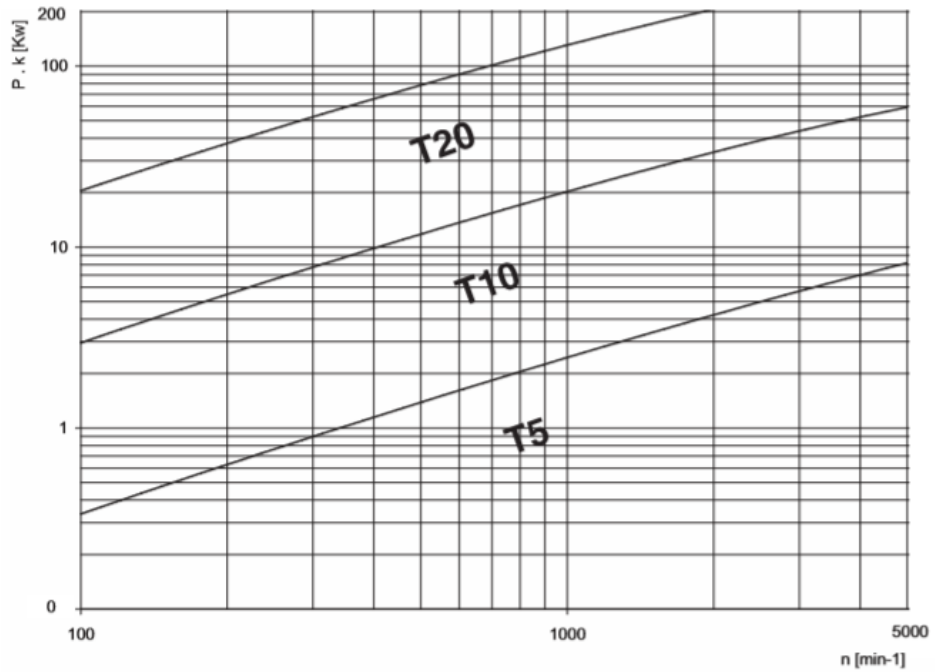


**Figure 3.1.** RPM versus Power (Elatech, 2018)

Specific effective pull required is calculated by using the formula with the help of  $C_1$  operational factor:

$$F_{Ureq} = \frac{F_{Umax}}{C_1} = \frac{18.419}{1} = 18.41 \text{ N}, \quad (3.14)$$

where,  $F_{Umax}$  - maximum effective pull (N);  $C_1$  - operational factor.

Considering all the factors and choosing the belt T5 belt with 5 mm pitch and 10 mm width as a standard metric belt with the effective pull of chosen belt is 160N which is very much assured to withstand tension, so the belt failure and strength calculations are performed below.

Here the Graph 3.2 mass (kg) is plotted against acceleration ( $\text{m/s}^2$ ) for determining the belt width as our mass is 1.5kg and acceleration is  $6\text{m/s}^2$ , so the chosen belt width is 10mm

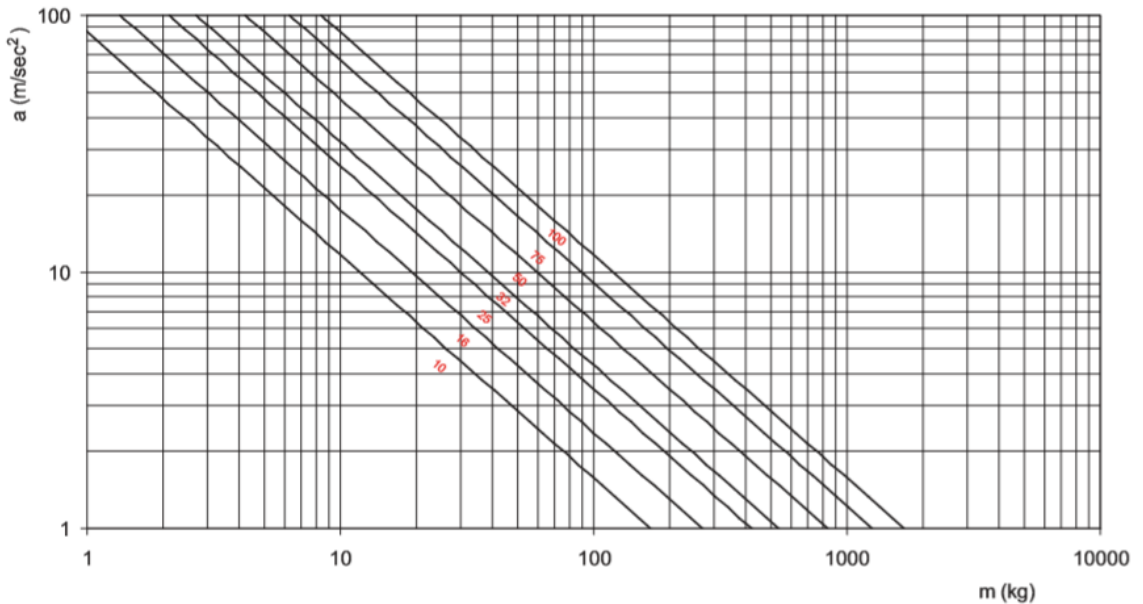


**Figure 3.2.** Mass versus acceleration (Elatech, 2018)

After choosing the belt now we must calculate the belt for load applications like a failure and other factors like tearing and shearing and an allowable tensile load of the chosen belt is  $F_{Per} = 160\text{N}$  so, we must check the tension and other factors.

Number of teeth in the pulley is calculated using the initial assumption of pitch circle diameter of pulley and chosen belt pitch:

$$Z = \frac{d_o \times \pi}{t} = \frac{32 \times 3.141}{5} = 20 \text{ teeth}, \quad (3.15)$$

where,  $d_o$  - pitch diameter of pulley (mm);  $t$  - belt Pitch (mm).

Several teeth in pulley according to standard pulley dimensions are selected pulley with pitch circle diameter of 32mm.

Belt length is calculating be considering the center distance of pulley and the pitch diameter of the pulley so the formula for finding the belt length would be:

$$L = 2 \times e + \pi \times d_o = 2 \times 609 + 3.14 \times 32 = 1320 \text{ mm}, \quad (3.16)$$

where,  $e$  - center distance of pulley (mm);  $d_o$  - pitch diameter (mm).

As belt density is  $0.021 \text{ kg/m}$  so, belt weight would be 200 grams for 1320 mm length, and together with pulley mass exceeding not more than  $0.250 \text{ kg}$  so mass inertia due to pulley and belt is neglected.

Selecting pretension force from the maximum effective pull of the belt so that belt is not over tensioned:

$$F_V \geq 0.5 \times F_{Umax} = 30 \text{ N}, \quad (3.17)$$

where,  $F_{Umax}$  - maximum effective pull (N).

Force determining the belt selection would be given by summing the maximum effective pull and pretension force:

$$F_B = F_{Umax} + F_V = 18.419 + 30 = 48.4 \text{ N}, \quad (3.18)$$

where,  $F_V$ -pretension Force (N);  $F_{Umax}$  - maximum effective pull (N).

Permissible force on each strand is considered from the belt manufacturers catalog:

$$F_{per} = 160 \text{ N (Forbo movements, 2018)}. \quad (3.19)$$

Tension member service factor is evaluated from the permissible force and maximum effective pull to be transmitted by the belt:

$$S_{tm} = \frac{F_{per}}{F_B} = 1.031 \geq 1, \quad (3.20)$$

where,  $F_{per}$  - Permissible force on each strand (N).

Take-up range is the elongation in belt due to tension caused by force and considering the belt clamping:

$$\Delta e = \frac{F_V \times l}{2 * C_{Spec}} = \frac{30}{2 * 80000} = 0.2 \text{ mm}, \quad (3.21)$$

where,  $F_V$ -pretension force (N);  $C_{Spec}$  - specific spring constant (80000 N).

Chosen belt tension is less than the required effective pull, and the pre-tensioning case is also verified so that belt failure can be avoided.

### 3.2. Spherical Bearings

The spherical joints are used for rotation so, we need to consider the bearing for angle restrictions and load sustainability and lubrication because no rod end can offer frictionless drive and therefore, the following lines contain the initial data for calculations of the load. As our spherical joints are chosen from HIRSCHMANN spherical bearings, so their manual is chosen as a reference (HIRSCHMANN, 2018)

Here the following figure 3.3 explains the dimensions of spherical joints or rod ends their dimensional values are defined below the figure 3.3 Dimensions of spherical bearing (HIRSCHMANN, 2018).

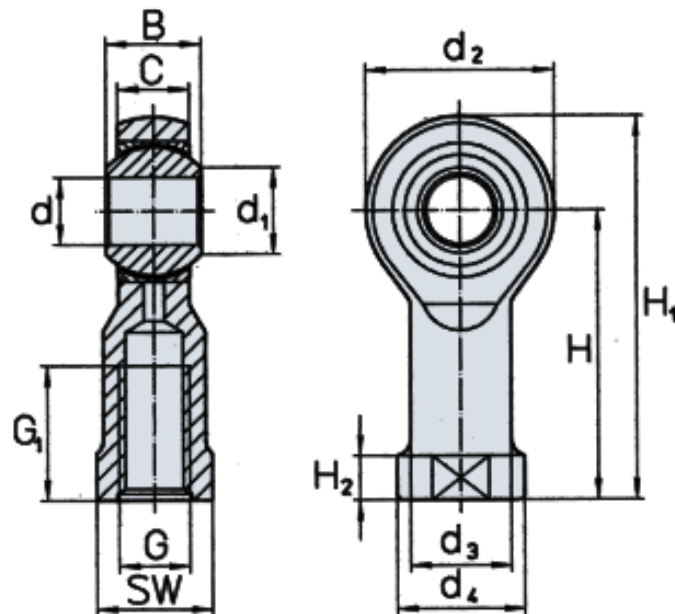


**Figure 3.3.** Dimensions of spherical bearing (HIRSCHMANN, 2018).

Dimensions mentioning the above bearing:  $d - 6 \text{ mm}$ ;  $B - 9 \text{ mm}$ ;  $C - 6.75 \text{ mm}$ ;  $d_1 - 8.9 \text{ mm}$ ;  $d_2 - 20 \text{ mm}$ ;  $d_3 - 10 \text{ mm}$ ;  $d_4 - 13 \text{ mm}$ ;  $H - 30 \text{ mm}$ ;  $H_1 - 40 \text{ mm}$ ;  $H_2 - 5 \text{ mm}$ ;  $G_1 - 12 \text{ mm}$ ; ball diameter ( $K$ ) -  $12.7 \text{ mm}$ ; thread( $G$ ) - M6;  $SW - 11 \text{ mm}$ .

Our design values are dictated by manufacturer and these values are reviewed before designing for our requirements;

**Table 3.2.** Data from the manufacturer (HIRSCHMANN, 2018).

swing angle ( $\beta$ )	30
operating temperature $C$ ( $^{\circ}\text{C}$ )	40
dynamic capacity (N)	109000
static capacity $C_o$ (N)	7000

These values are dictated by the design where the constant dynamic radial load  $F_r$ -80 N; constant axial load  $F_a$  -30 N; swing frequency  $f$  -120 rpm. Requirements on rod end SFCP 6mm. Radial load  $F_r$  must be smaller than the permissible load  $P_{permissible}$  to avoid permanent deformation. The service life  $G_h$ , the requirement should be at least 6000 operating hours.

### 3.2.1. Dynamic load

The inner ring includes out a swinging or pivoting movement in relation to the bushing. Here the following figure 3.4 explains the action of the load to our joints and the direction of swinging frequency the action of load (HIRSCHMANN, 2018).

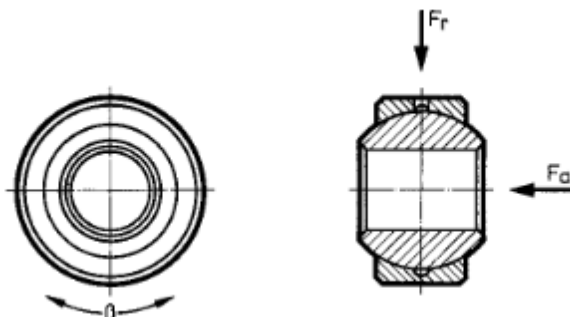


**Figure 3.4.** The action of load;  $F_r$  - radial load;  $F_a$  - axial load (HIRSCHMANN, 2018).

The dynamically equal bearing load  $P$  for rod ends, and spherical bearings with constant dynamic loads are calculated as follows:

$$P = F_r + (y \times F_a) = 80 + 1.5 \times 30 = 125 \text{ N}, \quad (3.22)$$

$$y = \frac{F_a}{F_r} = 0.3 \text{ because } \frac{F_a}{F_r} \text{ is from (figure 3.5).}$$

The below figure 3.5 is used for evaluating the Y factor, which will be used for calculating equivalent bearing load, and this figure 3.5 is chosen from manufacturer's catalog Y factor (HIRSCHMANN, 2018).

Load-relation	$\frac{F_a}{F_r}$	0,1	0,2	0,3	0,4	0,5	> 0,5
Axial-factor	Y	0,8	1	1,5	2,5	3	not suitable

**Figure 3.5.** Y factor (HIRSCHMANN, 2018)

Here the following table contains several factors for calculation of permissible load which are considered from figures and table:

**Table 3.3.** Capacity and load factor (HIRSCHMANN, 2018).

Static bearing capacity ( $C_O$ )	7000N (from table 3.2)
Temperature factor ( $b_2$ )	1 (from figure 3.7)
Load factor ( $b_4$ )	1 (from figure 3.7)

Permissible rod end load is calculated using the static bearing capacity and temperature factor:

$$P_{permissible} = C_O \times b_2 = 7000 \times 1 = 7000 \text{ N}, \quad (3.23)$$

according to the requirement  $P = 125 \text{ N} < P_{permissible} = 7000 \text{ N}$ .

The following (figure 3.6) explains types of load where invariable load is in our case so  $b_4$  is 1 which will be used in further calculations. Types of loads (HIRSCHMANN, 2018).

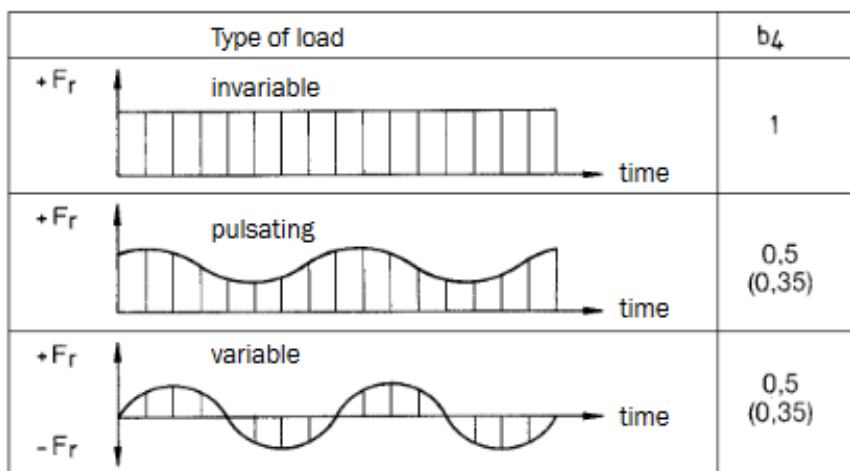


**Figure 3.6.** Types of loads (HIRSCHMANN, 2018)

Here are initial data for calculation;

- dynamic bearing capacity  $C = 10900 \text{ N}$ ;
- dynamic bearing load  $P = 125 \text{ N}$ ;
- inner ring diameter  $K = 6 \text{ mm}$ ;

- swing angle<sup>-1</sup>  $\beta = 30^\circ$ ;
- loading direction factor  $b_1 = 0.3$  From figure 3.7;
- temperature factor  $b_2 = 1$  From figure 3.7;
- material factor  $b_3 = 2$ .

The below figure 3.7 is reference for choosing the load direction factor and temperature factor by knowing the operating factor where in our case bearing type is maintenance free and alternating load direction so load direction factor would be 0.3 and temperature factor would be 1 because operating temperature is not more than 80° Celsius which will be used in further calculations operating factors (HIRSCHMANN, 2018).

Operating-factors	Load direction factor $b_1$		Temperature factor $b_2$					
	Bearing type	single direction	alternat. direction	80	100	150	200	250
lubricated	1	2,5	1	1	1	0,8	0,5	
maintenance-free	1	0,3	1	1	0,8	0,5	0,3	

**Figure 3.7.** Operating factors (HIRSCHMANN, 2018)

To calculate the service life that is the life hours after to be serviced or not usable is useful for changing the bearing in the correct time:

$$G_h = \frac{b_1 \times b_2 \times b_3}{k \times \beta \times f} \times 10^7 \times \frac{C}{P} = \frac{1 \times 0.3 \times 2}{6 \times 30 \times 120} \times 10^7 \times \frac{10900}{125} = 30000 \text{ hours}, \quad (3.24)$$

where,  $G_h$  - service life (h);  $C$  - dynamic bearing capacity (N);  $P$  - dynamic equivalent bearing load (N);  $K$  - inner ring diameter (mm);  $b$  - swing angle<sup>-1</sup> (degrees).

Now checking the lining for overheating because of continuous operation so, before we need surface specific pressure which is chosen below, Specific surface pressure  $K_C = 150 \text{ N/mm}^2$  from figure 3.8 Specific surface pressure (HIRSCHAMNN, 2018).

Type of bearing	Specific surface pressure $k_C$ [N/mm <sup>2</sup> ]
lubricated	50
maintenance-free	150

**Figure 3.8.** Specific surface pressure (HIRSCHAMNN, 2018).

Surface pressure is evaluated again by considering the pressure to dynamic bearing load and dynamic bearing capacity using the formula:

$$p = k_c \times \frac{P}{c} = 150 \times 0.0114 = 1.71 \text{ N/mm}^2 \quad (3.25)$$

where,  $k_c$  - specific surface pressure ( $\text{N/mm}^2$ );  $p$  - dynamic equivalent bearing load (N);  $c$  - dynamic bearing capacity (N).

Mean running speed is calculated by considering the inner ring diameter swing angle and swinging frequency so, the formula for calculating the mean running speed follows:

$$v = k \times \beta \times f = 1.745 \times 10^{-5} \times 30120 = 0.37 \text{ m/min}, \quad (3.26)$$

where,  $K$  - inner ring diameter (mm);  $\beta$  - Swing angle (degrees);  $f$  - Swing frequency (rpm)

Finally,  $p \times v$  factor is considered to check the overheat:

$$p \times v = 1.71 \times 0.37 = 0.637. \quad (3.27)$$

Our calculated  $p \times v$  factor is less than the allowable  $p \times v$  factor that is 60 m/mm, and no overheating is expected as our spherical joint is maintenance free.

### 3.3. Linear Bearing Calculations

Four Linear bearings are pulled by mass through linear rail shaft so totally eight linear bearings are used, and LBCR linear bearings are used because it has a dynamic load capacity of 490N and static load capacity of 355N which is much more than the required so choosing LBCR bearing and checking for the application of load. As our linear bearings are chosen from SKF manufacturer their linear bearings manual is used as a reference for below calculations (SKF, 2019).

Here the following figure 3.9 linear bearings are shown schematically explaining dimensions

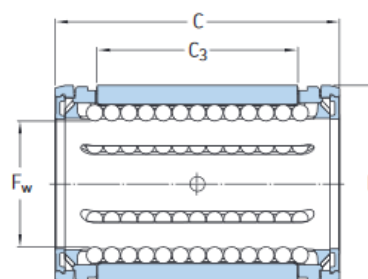


**Figure 3.9.** Dimensions of Linear bearing (SKF, 2019).

Data from LBCR 8mm bearing the following notations are explaining the above dimensions which are used in our machine.

The following table 3.4 contains dimensional values for figure 3.9, and load ratings are dictated by the manufacturer:

**Table 3.4.** Dimension values for figure 3.9 (SKF, 2019).

Inner diameter ( $F_W$ )	8 mm
Outer diameter ( $D$ )	16 mm
Length of bearing ( $c$ )	25 mm
Short length ( $C_3$ )	14 mm
Number of rows of balls ( $N$ )	4
Dynamic load rating ( $C$ )	490 N
Static load rating ( $C_0$ )	355 N
Mass (m)	0.009 kg

As the bearings slide in the rail shaft we must consider the frictional factors from the rail shaft because of stroke length is considered. So, the data for drive calculation is performed below.

- Stroke length ( $s$ ) -350 mm;
- stroke frequency ( $n$ ) -120 min<sup>-1</sup>;
- frictional factor ( $\mu$ ) - 1.5;
- viscosity( $\nu$ ) - 250 mm/s<sup>2</sup>.

The basic dynamic load rating of linear ball bearing since two bearings are used on a single side of lifting closure basic dynamic load rating is multiplied by factor 2:

$$C = 2 \times 490 = 980 \text{ N.} \quad (3.28)$$

The effective dynamic load rating can be obtained by using the basic dynamic load rating of linear ball bearing:

$$C_{eff} = f_h \times f_i \times C = 720 \text{ N,} \quad (3.29)$$

where,  $f_h$  - surface hardness of shaft;  $f_i$  - number of loaded bearings per unit factor  $f_i$  has already been considered in the dynamic load ratings quoted for SKF linear bearing units. Therefore  $f_i = 1$ ;  $C$  - basic dynamic load rating linear ball bearing.

To calculate the equivalent dynamic load factor for load direction, since the line of load acts through the zone of maximum load carrying capacity of the linear ball bearing  $f_i = 1$ . Since self-aligning linear ball bearings are used in this linear unit. Despite this, the calculation of misalignment is to be demonstrated here:

**Table 3.5.** Initial data for calculations (SKF, 2019).

The factor for misalignment ( $f_i$ )	1
Four bearings are used ( $f_m$ )	$\frac{F}{4} = 5 \text{ N}$
Centre distance ( $a$ )	350mm
Shaft diameter ( $d$ )	8 mm
Shaft length ( $l$ )	620 mm

The constant mean load is calculated by considering the load at each point acted at their respective distance, so the formula would be:

$$F_m = \left[ \frac{F^3 \times S_1 + F^3 \times S_2 + F^3 \times S_3 + \dots + F_N \times S_N}{S} \right]^{\frac{1}{3}} = 22 \text{ N}, \quad (3.30)$$

where,  $F$  - constant load (N);  $S_l$  - length during the action of load (mm).

Now, calculating the equivalent dynamic load by considering the factor for misalignment and maximum load carrying capacity of the linear ball bearing:

$$P = f_m \times f_i \times F_m = 1 \times 1 \times 22 = 22 \text{ N}, \quad (3.31)$$

where,  $f_m$  is a factor for misalignment  $f_m$  is 1 since, self-aligning linear ball bearings are used in this linear unit;  $f_i$  is 1 (factor for load direction, since the line of load, acts through the zone of maximum load carrying capacity of the linear ball bearing);  $F_m$  - Constant mean load (N).

Thus, the adjusted rating life can be obtained by considering the factor  $C_l$  for reliability,  $C_l$  is 1 from graph 3.10 because reliability is 90% according to the manufacturer  $C_l$  -Determination from reliability (SKF, 2019).

Reliability %	$L_{ns}$	$c_1$
50	$L_{50s}$	5,04
60	$L_{40s}$	3,83
70	$L_{30s}$	2,77
80	$L_{20s}$	1,82
90	$L_{10s}$	1
95	$L_{5s}$	0,62
96	$L_{4s}$	0,53
97	$L_{3s}$	0,44
98	$L_{2s}$	0,33
99	$L_{1s}$	0,21

**Figure 3.10.**  $C_1$  -Determination from reliability (SKF, 2019)

To calculate the velocity by the rod end, we must consider the mean running speed and revolution per minute of the rod end, the velocity of rod is given by the formula,

$$v = \frac{2 \times s \times n}{60} = 1.4 \text{ m/s} \quad (3.32)$$

where  $s$  -mean velocity (m/s);  $n$  - number of strokes per minute (rpm).

When the lubrication is considered viscosity plays an important factor so, the viscosity is  $400 \text{ mm/s}^2$  mean velocity is  $1 \text{ m/s}$ , so  $F_w$  is 1 from graph 3.11 Inner diameter versus viscosity (SKF, 2019).

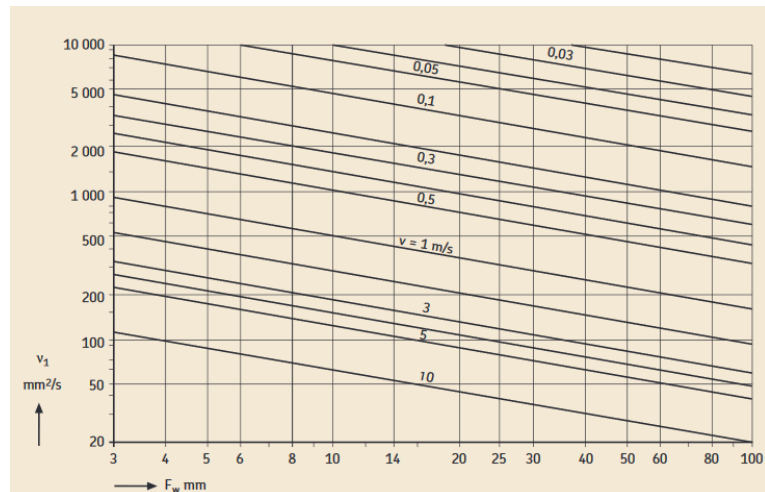


**Figure 3.11.** Inner diameter versus viscosity (SKF, 2019)

Several factors like operating temperature and viscosity ratio are considered for calculation of basic life rating the following table contains initial data for basic life hours calculation, the following table 3.6 contains initial data for calculation of basic life hours,

**Table 3.6.** Initial data for the calculation of basic life hours (SKF, 2019):

operating temperature( $t$ )	35°C
viscosity ratio ( $K$ )	$\frac{V}{v} = 0.2$ from graph 3.11
$C_2$ for operating conditions from the stroke length and number of strokes per minute	$C_2 = 0.1$

Here the following figure 3.12 is considered from the manufacturer for evaluating the factor  $f_s$  ball with comparing  $\frac{l_s}{l_t}$  the ratio is 1, so;  $f_s$  ball is 1, which will be used in further calculations Factor  $f_s$  for linear bearings (SKF, 2019).

$l_s / l_t$	$f_{s, \text{ball}}$
1,0	1,00
0,9	0,91
0,8	0,82
0,7	0,73
0,6	0,63
0,5	0,54
0,4	0,44
0,3	0,34
0,2	0,23
0,1	0,13

**Figure 3.12.** Factor  $f_s$  for linear bearings (SKF, 2019)

Life of the bearings is calculated by considering the operational factor, dynamic load, effective dynamic load and the basic life hours is given by the formula:

$$L_{10h} = \frac{C_1 \times C_2 \times 5 \times 10^7 \times (\frac{C_{eff}}{P})^{1/3}}{S \times n \times 60} = 55365 \text{ hours}, \quad (3.33)$$

where,  $c_1$ - factor for reliability may be used for a life achieved or exceeded by 90 % of the bearings;  $c_2$ = between 0,18 and 0,6 6 (the lower value applies to mineral oils without additives and the upper value to mineral oils with approved EP additives);  $C_{eff}$  - effective dynamic load rating;  $S$ - mean velocity (m/s);  $n$  = number of strokes per minute (rpm).

Finally checking the safety factor which is given by the formula:

$$S_o = f_{10} \times f_{h0} \times \frac{C_o}{P_o} = 0.0788, \quad (3.34)$$

where,  $f_{l0}$  = factor for direction of load;  $f_{h0}$  = factor for surface hardness of shaft;  $C_o$  = basic static load rating (N);  $P_o$  = equivalent static load (N).

Here, the following graph 3.13 represents the elastic deformation free linear ball bearings in the ball contact zone, so we can choose the pressure relation for our bearings which will be used for the following equations.

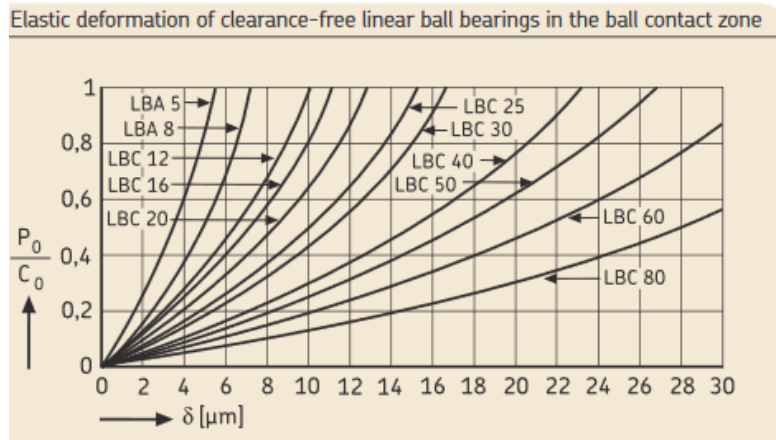


**Figure 3.13.** Graph determining deflection versus pressure ratio (SKF, 2019)

For a linear ball bearing LBCR 8, assumed to be clearance-free, an elastic bearing deflection of 2  $\mu\text{m}$  from above graph 3.13. can be obtained from  $\frac{P_o}{C_o} = 0.8$ .

### 3.4. Motor Selection

Steppers have their torque reducing capacity significantly increasing speed, and above some speed, the torque became too low it can barely turn the motor. The functionality of a stepper to run fast is related to its construction, and the resistance to changing the current in a stepper is translated in a parameter called Inductance, expressed in mH (millihenry).

- The speed limit is associated with the electric characteristics of the stepper, which makes the electrical current change of direction difficult. To ease the exchange of cutting-edge in the stepper, there are two solutions:
- Increase the voltage supply, which is efficient. This is one of the reasons you see more high-end machines supplied in 24V (there are other motives).
- Have a dissimilar winding for the same form factor, say use less turns on the coils, which reduce the inductance significantly increase the nominal current.

There is no alternative; stepper faster speed requires either higher voltage or higher current (or both, e.g., for CNC machine)

### 3.5. Micro-stepping

A very common type of resolution for stepper motors is 200 steps per revolution 1.8 degrees per step. We will use this decision, for example, in the rest of this post. Often 200 steps in keeping with revolution may not be enough to achieve the accuracy required by the robot. To increase accuracy, we should enable micro-stepping. This will improve the number of steps per revolution with a factor of  $2^n$  ( $n$  is an integer). Micro-stepping up to 8x (i.e., 8 times the full step resolution – resulting in 1600 steps with the revolution in our example above) is common but we may even find stepper systems with 256x micro-stepping. One very important drawback with micro-stepping we should take into consideration is that the holding torque drastically decreases as the micro-stepping factor increases. According to micromo.com a micro-stepping factor of 8x will give only 19.51% holding torque compared to what you get from no longer permitting micro-stepping (256x micro-stepping will give you as little as 0.61 percent of the original holding torque. As our motor is chosen from the “SURESTEP” stepper motors, their “SURESTEP” Stepping Systems User Manual is used as a reference for below calculations (SURESTEP, 2018).

Here's a simple equation used to calculate steps per mm for linear motion with belts and pulleys so, the steps per mm is calculated using the formula:

$$\frac{S_{rev} \times f_m}{N_t \times p} = \frac{200 \times 2}{500 \times 20} = 4 \text{ steps per mm,} \quad (3.35)$$

where,  $S_{rev}$  - number of steps per revolution of the motor (rpm);  $f_m$  -micro-stepping factor;  $p$  – pitch (mm);  $N_t$  - number of teeth on the pulley attached to the motor shaft.

The selection of a stepping system follows a defined process. let's undergo the process and define a few beneficial relationships and equations. we can use this data to paint some regular examples alongside the way.

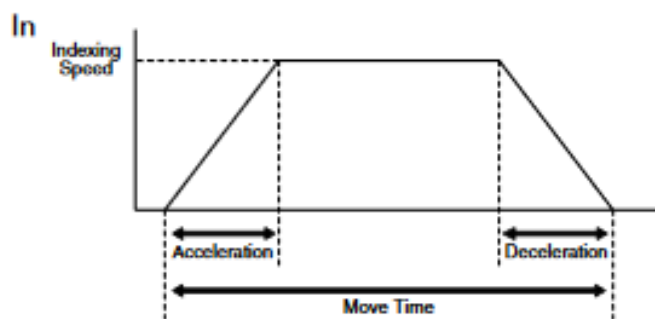


**Figure 3.14.** Velocity versus time graph (SURESTEP, 2018).

The above (Figure3.14) explains velocity versus time that our system follows that's starting acceleration time is 0.15 second and constant velocity time is 0.3 second and deceleration time is 0.15 second that is total time for reaching 350 millimeters is 0.5 second and maximum velocity that our system reaches is 1.4 m/s.

### 3.5.1. Motion requirement and motion quantities

Here are the data for selection of stepper motor that is our required torque, payload, time characteristics.

- weight =  $m \times g = 9.81$  kg;  $m$ - mass of object,  $g$ - gravity;
- frictional coefficient of sliding surface = 0.5;
- belt and pulley efficiency = 0.8;
- pulley diameter = 32 mm;
- pulley thickness = 15 mm;
- pulley material = aluminum (density = 0.002 g/cm<sup>3</sup>);
- desired resolution = 4 mm/step;
- stroke = 350 mm;
- move time = 0.5 second;
- acceleration and deceleration time = 0.3 second.

### 3.5.2. Determining the positioning resolution of load

For determining the positioning resolution first, we should determine,  $d_{load} = \pi \times d_o$  then the following equation evaluates the position resolution which is given by:

$$\theta_{step} = \frac{d_{load}}{L_o} = \frac{32\pi}{0.4} = 251 \text{ steps/revolution}, \quad (3.36)$$

where,  $d_{load}$  -  $\pi \times d_o$ .

Stepping system can be set at 252 steps/revolution to exceed the required load positioning resolution slightly.

### 3.5.3. Determining the motion profile

The total pulses to make the desired move is considered as  $P_{total}$  so, we need to consider the total distance for one stroke and steps per revolution:

$$P_{total} = \frac{D_{total}}{d_{load}} \times \theta_{step} = 1044.98 \text{ Pulses}, \quad (3.37)$$

where,  $D_{total}$  - Total distance for one stroke (350mm);  $d_{load}$  -  $\pi \times$ pulley diameter (100.48mm);  $\theta_{step}$  - 251 steps/revolution.

The running frequency for a trapezoidal pattern is calculated by the following formula by considering the total pulses and total time for upward direction and formula is given by:

$$f_{trapezoidal} = \frac{P_{total}}{t_{total}-t_{tramp}} = \frac{1044}{0.2} = 5224.9 \text{ Hz}, \quad (3.1)$$

where,  $P_{total}$ - 1044.98 pulses;  $t_{total}$  -the total time during travel upward (0.5);  $t_{tramp}$  -time for braking(0.2s).

### 3.5.4. Determine the required motor torque:

For determining the motor torque so, first we need to calculate the total moment of inertia of load for that inertia from the payload is required, and inertia from pulleys are required.

So, calculating inertia from the load is given by:

$$J_{load} = \frac{weight}{g \times efficiency} \times r^2 = \frac{15}{9.81 \times 0.8} \times 0.0032^2 = 0.001957 \text{ kgmm}^2 \quad (3.38)$$

where, weight – 15 kg;  $g$  - 9.81; efficiency - 0.8.

Now calculating the inertia of the pulleys is calculated by the formula is given by:

$$J_{pulleys} = \left( \frac{\pi \times t \times \rho \times r^4}{2 \times g} \right) \times 2 = \frac{\pi \times 0.015 \times 0.002 \times 0.0016^4}{2 \times g} \times 2 = 0.00251 \text{ kgmm}^2 \quad (3.39)$$

where,  $t$  - thickness of pulleys (mm);  $\rho$  - density of Aluminium ( $\text{g/cm}^3$ );  $r$  -radius of pulley (mm);  $g$  - gravity ( $\text{m/s}^2$ ).

The inertia of the load and pulleys to the motor is calculated by considering the inertia from pulleys and inertia from the load which is given by:

$$J_{total} = (J_{pulleys} + J_{load})_{to\ motor} = 0.00251 + 0.001957 = 0.01166 \text{ kgmm}^2 \quad (3.40)$$

Now, the torque required to accelerate the inertia is given by the formula:

$$T_{acc} = J_{total} \times \left( \frac{speed}{time} \right) = 0.01166 \left( \frac{1.4}{1} \right) = 0.0128 \text{ Nm.} \quad (3.41)$$

Running torque is calculated by multiplying the force and pitch circle radius of the pulley which is given by:

$$F \times r = 20 \times 0.032 = 0.64 \text{ Nm.} \quad (3.42)$$

The total force is evaluated by considering the forces generated from all sources which are gravitational, frictional, gravitational force the formula calculating is given by:

$$F_{total} = F_{ext} + F_{friction} + F_{gravity}, \quad (3.43)$$

where,  $F_{ext} = 0$ .

The frictional force is given by the multiplying the coefficient of friction, mass to be lifted and gravity:

$$F_{friction} = \mu \times m \times g \times \cos\theta; \quad (3.44)$$

where,  $\mu$  = coefficient of friction;  $m$  = mass to be lifted (kg);  $g$  = gravity.

Gravitational force is given by multiplying the mass and gravity,

$$F_{gravity} = m \times g = 1.5 \times 9.81 = 14.715 \text{ N.} \quad (3.45)$$

where,  $m$  - mass;  $g$  - gravity.

Therefore, the total force would be given as from equation 3.43,

$$F_{total} = F_{ext} + F_{friction} + F_{gravity} = 24.715 \text{ N.} \quad (3.46)$$

Considering the frictional force and re-evaluating torque required to accelerate,

$$T_{run} = \frac{(24.715 \times 0.15)}{5} = 0.741 \text{ Nm.} \quad (3.47)$$

Finally, the required motor torque is evaluated by considering the acceleration torque and  $T_{run}$ :

$$T_{motor} = T_{accel} + T_{run} = 0.0128 + 0.741 = 0.7538 \text{ Nm.} \quad (3.48)$$

where,  $T_{accel}$  - 0.0128 Nm;  $T_{run}$  - 0.741 Nm.

### 3.5.5. Select & Confirm the Stepping Motor & Driver System

It looks like an affordable choice for a motor could be the “NEMA 17” motor. This motor has inertia of  $J_{motor} = 0.0175 \text{ Kgmm}^2$  and torque upto 5 Nm.

## 4. KINEMATICS CALCULATIONS

There are several ways to analyze the original kinematics of the delta robot. I realize that inverse kinematics for rock stock is already to be in firmware and is probably described somewhere on the Internet if I look long enough, but I like to understand things myself.

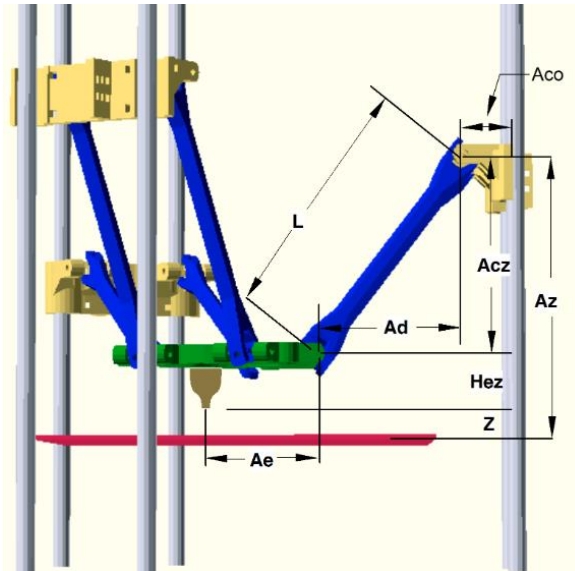


**Figure 4.1.** Schematic explaining the parts

( $A_{cz}$  - length from bearing housing to base;  $A_e$  - length from centre of articulated travelling plate and pivot points;  $L$  - length of link;  $A_d$  - length from top pivot point to base pivot point;  $H_{ez}$  - Length from end effector to base;  $A_{cz}$  - length from top pivot point articulated travelling plate;  $A_{co}$  - Length of Bearing housing).

One important set of the formulation may be derived via looking at that the arms and the vertical rise form a right-angle triangle where the third leg is in the plane of the effector platform. Now we need to understand how the third leg relates to our X, Y point in the middle of the effector platform. My first thought turned into that our line of motion passes through the center of the effector platform. But this is not true. The line from the middle of the effector platform to an aspect of the effector platform where the line of motion meets the effector platform is perpendicular to the edge. Since the edge is parallel to connection factors at the carriage, the line on the effector platform will maintain the equal orientation in the x y plane. It is a fixed vector. We will call these vectors  $A_e$ ,  $B_e$  and  $C_e$  by our definition, they possess the same length, and the direction is determined by the orientation of the corresponding column. Since vector addition is commutative, we can display that these vectors can be moved from the end of the arc and carried out to the column positions. This changes the pivot factor to a virtual column role that the factors of interest shape an arc round,

simplifying the mathematics when doing kinematic calculations. so, the space from the edges to the center of the effector platform become a constant applied once when initializing software.

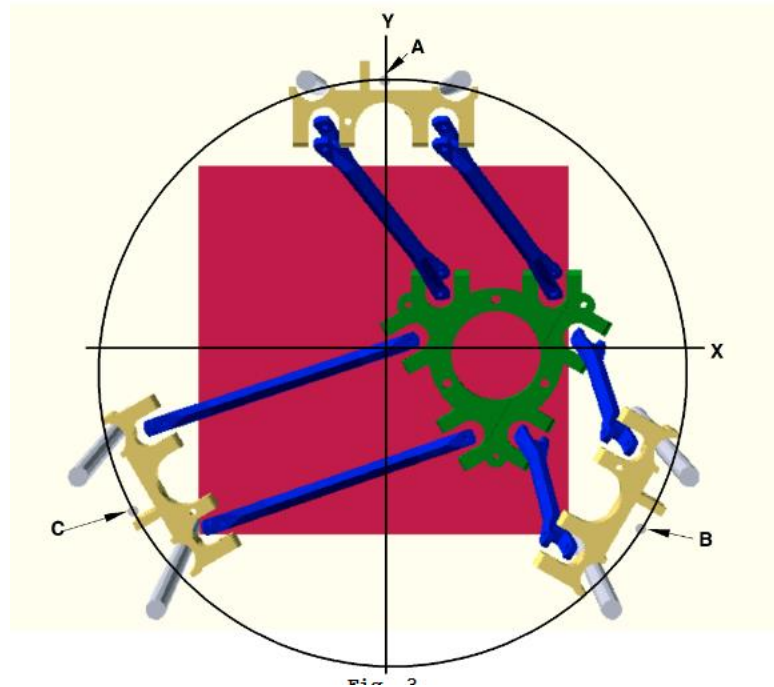


**Figure 4.2.** XY Plane in the bottom view

(Inscribed radius circle in X, Y plane and A, B, C are centre of pivot points).

Now to determine the formulas we can derive from the right-angle triangles formed by each arm, the vertical rise, and leg in the X-Y plane. We will name the distances of the triangle vicinity to the point below the carriage pivot point) in XY plane Ad, Bd, and Cd. Using the Pythagorean theorem, we get the formulae;

Length of legs can be calculated from Pythagoras theorem since it is placed like a triangle Pythagoras theorem is applicable so, length of the link is calculated using formula:

$$Ad^2 + Acz^2 = L_1^2 = \sqrt{155^2 + 250} = 294 \text{ mm.} \quad (4.1)$$

Similarly, for other length of the link:

$$Bd^2 + Bcz^2 = L_2^2 = \sqrt{155^2 + 250} = 294 \text{ mm.} \quad (4.2)$$

Similarly, length of the third link:

$$Cd^2 + Ccz^2 = L_3^2 = \sqrt{155^2 + 250} = 294 \text{ mm.} \quad (4.3)$$

Now let's relate our links to the X, Y plane. The first important thing is to describe the locations of the base of the columns A, B, and C in the X, Y plane. we are able to name the physical locations  $Ax, Ay; Bx, By$  and  $Cx, Cy$ . By observation, we can see that the real pivot factors are the points exactly below where each line of movement terminates on its carriage. we can calculate those locations via subtracting a vector from every column, which represents the carriage offset. we can name these pivot locations  $Apx, Apy; Bpx, Bpy$  and  $Cpx, Cpy$ . We will use those values for now, but later we can reduce the number of unknowns by moving these places to virtual column positions. for this assessment, we keep Z constant, so we're prescribing our effector platform to a given XY plane. The line of motion for each column pivots across the factor on the carriage. When the carriage is at a given peak position above the effector platform, the possible locations in the XY plane where the brink of an effector platform meets a given line of motion is an arc throughout the pivot issue. if the vector is ae, be and ce have been 0, and the strains of motion meet at the middle of the effector platform our X, Y coordinates would be the intersection between these arcs. but on account that ae, be and ce are not 0; the problem is a little more complicated.

let's make some equations to relate  $Ae, Be$  and  $Ce$  to our (x, y) coordinates allows call the coordinates in which the lines of movement meet the effector platform  $Acx, Acy; Bcx, Bcy$ , and  $Ccx, ccy$ . we recognize that a vector can be represented through a delta X and delta Y, so we are able to cancel the vectors right down to  $Aex, Aey; Bex, Bey$  and  $Cex, Cey$ . we can outline the vectors as pointing from the brink to the middle of the effector platform. so, we have the subsequent family members, the maximum reach in X plane is calculated using the formula:

$$X = Acx - Aex = Bcx - Bex = Ccx - Cex = 250 - 60 = 190 \text{ mm.} \quad (4.4)$$

Similarly, maximum reach in Y direction is calculated using the formula:

$$Y = Acy - Aey = Bcy - Bey = Ccy - Cey = 250 - 60 = 190 \text{ mm.} \quad (4.5)$$

Based on our above lines, the line of action travels on an arc. The formula for an inscribed circle is  $CR$ :

$$(X - CX)^2 + (Y - CY)^2 = CR^2; \quad (4.6)$$

$$CR = \sqrt{(190 - 95)^2 + (190 - 95)^2} = 135 \text{ mm.} \quad (4.7)$$

Where  $CX$ ,  $CY$  is the center of the circle, and  $CR$  is the radius in mm. We should be able to remedy the equations for one column and determine the other two by similarity. So, looking at column A, where  $Ad$  is the linear distance between the articulated traveling plate and bearing housing in mm:

$$(Acx - Apx)^2 + (Acy - Apy)^2 = Ad^2. \quad (4.8)$$

Solving for  $Acx$  and  $Acy$  that is length from bearing housing to articulated traveling plate by substituting we get:

$$Acx = X + Aex = 190 + 60 = 250 \text{ mm}. \quad (4.9)$$

From the above equations,  $Acy$  that is length from bearing housing to articulated traveling plate is evaluated by replacing  $Aex$  to  $Acy$ , so we get  $Ad$ :

$$Acy = Y + (X + Aex - Apx)^2 + (Y + Aey - Apy)^2 = Ad^2; \quad (4.10)$$

$$(X + Aex - Apx)^2 + (Y + Aey - Apy)^2 = Ad^2; \quad (4.11)$$

$$Ad = \sqrt{(220 + 60 - 30)^2 + (220 + 40 - 30)^2} = 353 \text{ mm}. \quad (4.12)$$

We see a simplification; we can deal with the pivot points of the circle as we will call this point  $Avx$ ,  $Avy$ . So, we will define the following from manipulation:

$$Avx = Apx - Aex; Avy = Apy - Aey. \quad (4.13)$$

We will call the following geometric relations for the pivot points of the circle,

$$\begin{aligned} Avx &= Apx - Aex, Avy = Apy - Aey, Bvx = Bpx - Bex, Bvy = \\ &Bpy - Bey, Cvx = Cpx - Cex, Cvy = Cpy - Cey. \end{aligned} \quad (4.14)$$

Now, with our simplified version, we have the following formulation for linear length from bearing housing to articulated traveling plate:

$$(X - Avx)^2 + (Y - Avy)^2 = Ad^2 = L^2 - Acz^2. \quad (4.15)$$

Solving for  $Acz$  length from bearing housing to articulated traveling plate from equation 4.16 we get these relations:

$$Acz^2 = L^2 - (X - Avx)^2 - (Y - Avy)^2; \quad (4.16)$$

$$Acz = \sqrt{(L_2 - (X - Avx))^2 - (Y - Avy)^2}; \quad (4.17)$$

$$Acz = \sqrt{(L_2 - (X - Avx))^2 - (Y - Avy)^2} = 250 \text{ mm}. \quad (4.18)$$

By similarity the formulas for the carriage height above the effector platform  $Bcz$  and  $Ccz$ :

$$Bcz = \sqrt{(L_2 - (X - Bvx))^2 - (Y - Bvy)^2} = 250 \text{ mm}; \quad (4.19)$$

$$Ccz = \sqrt{(L_2 - (X - Cvx))^2 - (Y - Cvy)^2} = 250 \text{ mm}. \quad (4.20)$$

The real values required is the distance of each carriage above the base. These formulae were given above. Here they are again:

$$Az = Z + Acz + Hcz = 190 + 250 + 100 = 540 \text{ mm}; \quad (4.21)$$

$$Bz = Z + Bcz - Hcz = 190 + 250 + 100 = 540 \text{ mm}; \quad (4.22)$$

$$Cz = Z + Ccz - Hcz = 190 + 250 + 100 = 540 \text{ mm}. \quad (4.23)$$

#### 4.1. Forward Kinematics

Forward kinematics is the formulas which determine the X-Y-Z coordinates of the effector platform when given the carriage positions. They are a little extra difficult than the inverse kinematics. Our mathematical version using the virtual column positions is still beneficial. If we use the virtual column position middle of the effector platform is the point this is far from each carriage position on the virtual column. This gives the following equations.

Length of the link is calculated by using the following relations:

$$L = \sqrt{(X - Avx)^2 + (Y - Avy)^2 + A_{cz}^2} = 290 \text{ mm}; \quad (4.24)$$

$$L = \sqrt{(X - Bvx)^2 + (Y - Bvy)^2 + B_{cz}^2} = 290 \text{ mm}; \quad (4.25)$$

$$L = \sqrt{(X - Cvx)^2 + (Y - Cvy)^2 + C_{cz}^2} = 290 \text{ mm}. \quad (4.26)$$

Where  $A_{cz}$ ,  $B_{cz}$  and  $C_{cz}$  are the length of each carriage above the plane of the effector platform and related to Z as follows,

$$A_{cz} = Az - Z - Hez = 579 - 189 - 100 = 290 \text{ mm}; \quad (4.27)$$

$$B_{cz} = Bz - Z - Hez = 579 - 189 - 100 = 290 \text{ mm}; \quad (4.28)$$

$$C_{cz} = Cz - Z - Hez = 579 - 189 - 100 = 290 \text{ mm}. \quad (4.29)$$

$Az$ ,  $Bz$ , and  $Cz$  are the Z quantities of the given carriage positions. We have three equations and three unknowns, however the squares make these difficult equations to solve. I had originally used an answer for the forward kinematics based on the circumcenter, but thanks to Michael Pauwe from New Zealand, I have now used a better method based on Trilateration. Trilateration means finding a point in 3D space based on the distances from three known points. This is exactly how GPS works. Our three known points are the carriage positions.

## 5. CONTROL ALGORITHM

This robot has three degrees of freedom, allowing the end-effector to rotate across the vertical axis. The moving platform continually remains parallel to the bottom.

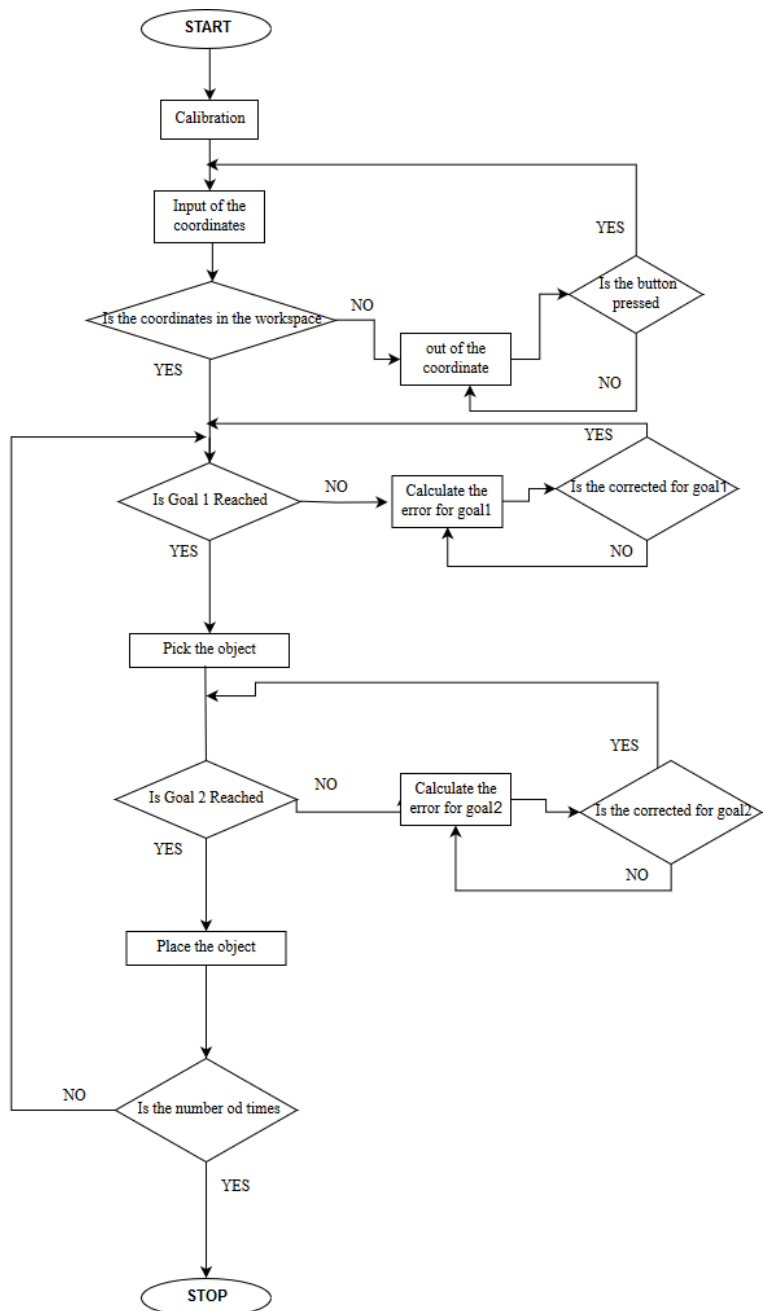


**Figure 5.1.** Structure of Control Algorithm

It is connected to the bottom by means of three equal kinematic chains having an R-(RR)-(RR) architecture. The parallel chains are actuated by means of the revolute joints, that are close to the base, using DC motors constant to the bottom. with this structure, the delta has a totally low inertia and can manipulate light pieces within a very short cycle time, robot start and calibrates for error to

reach such high robot accuracy, it is necessary to avail sturdy and dependable calibration strategies, which is quite difficult to obtain from both theoretical and sensible factor of view, even if it could be performed off-line. Robot accuracy can be suffering from increasing backlash because of robot operation, thermal effects, robot control, robot dynamic, manufacturing errors and element deformation sensor with encoders installed in the robot determines the relative position of the robot with respect to a spherical object fixed in the working area of the robot. The positions of the end effector are related to the incremental positions of resolvers of the robot motors. A kinematic model of the robot is used to find a new group of parameters, which minimizes errors in the kinematic equations. The goal of the kinematic calibration process is to obtain the constraints of quite large measured poses called calibration poses to determine which geometry is distances or angles of elements of the robot.

Once the calibration the robot waits for input of goal coordinates to pick and place with respect to the base frame of the forward kinematics in the robot and the number of times the robot repeats the operation of reaching the goal coordinates. And when the robot receives the input check for whether the coordinates are in the workspace of the robot. This test is done with the kinematic model that was created with the inverse kinematics. It also checks for redundancy to avoid multi-inverse kinematic solutions. The solution with easy reach is selected to move on. If the coordinates are out of the workspace, it indicates with a red led light in the system with an instruction to press the button that makes the robot to wait for the goal coordinates again which loops until it gets a goal coordinate in the workspace.

If the goal coordinate is in the workspace and the robot moves to the goal, this goal reaching is controlled with a PID-controller with an error to the goal coordinates in the opposite error control. The error can be obtained from the encoders in the motor. This happens until the robot reaches the goal. Once it is the goal coordinate is reached, the robot performs the action od pick. And returns to the goal place to coordinate with the same principle. This happens until the number of times is reached to the goal number of times and stops the operation.in this whole process is there is any error mistake the robot stops and blinks a black-led in the circuit of the robot.

## 6. ELECTRICAL SCHEME

For the delta robot, I have planned it away to open source hardware for controller Arduino Mega 2560, which has 54 digital output and input pins that can be used to connect the motor drive.

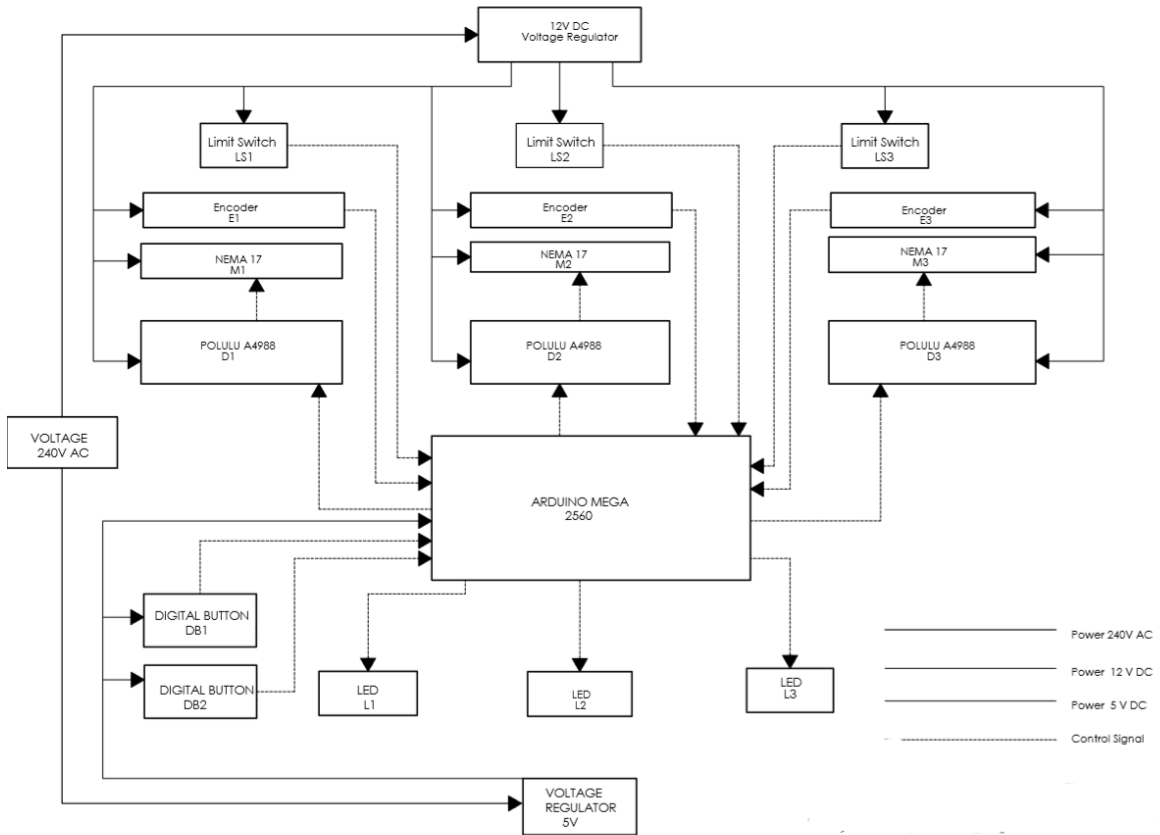


**Figure 6.1.** Electrical Scheme

As the robot use more power to operate I used a 5V DC regulator to convert the main current to use it for the robot motor and the controller Arduino Mega 2560 and use the motor drive “Pololu A4988” to convert the signals from the Arduino to the motor “NEMA17” which has an encoder in it to checks for its position of rotation. The LED are connected to notify the user about the robot function that was explained above. Arduino can be programmed with the header files and custom programming in the Arduino IDE. I have selected Arduino 2560 mega because it has 54 digital I/O pins for controlling as most parts of the system are controlled by the digital output from the controller. And Nema17 because it can deliver a precise movement for the belts that can move the end effector. With the limit switch at the end of the limit of the moment in the axis of the controller can receive the signal from it. The encoder is attached to the motor which can send discretely and continues signals about the position of the motor in encoder value that must be converted to the real value in the movement. With a digital button in the robot can send the digital input to the system. Led light provides the systems state in control algorithm. The robot must be powered with a input of 240V AC

which then converted to 12V DC and 5V DC with the regulators respectively. The 12V DC power is provided to the motor encoder and motor driver as they use high power and higher voltage than the Arduino. With the 5V DC Arduino is the power to gives to digital and analog power to its direct controlled electrical elements.

## **7. REQUIREMENTS OF WORK SAFETY AND ENVIRONMENT**

Delta Robot safety is also understood in various ways, including preventing the automation from damaging its environment, notably the human involvement of that surroundings, and easily preventing injury to the robot itself. While not correct precautions, a robot experiencing a fault or failure can cause serious injuries to people and injury equipment in or around a work cell. Industrial robots are programmable units designed to form expected actions. Lamentably, the movements of folks WHO work with robots cannot be expected, creating automaton safety very important. Most robot-related accidents occur throughout programming, maintenance, repair, setup, and testing. All these tasks involve human interaction and necessitating correct safety training for workers and therefore, the proper use of acceptable safeguards. Note that robots, depending on the task, might generate paint mist, attachment fumes, plastic fumes, etc. Robots, on occasion, are utilized in environments or duties too dangerous for staff, and as such, creates hazards not specific to the robots, however specific to the task. Industrial robots are programmable gadgets designed to shape predicted movements. Unfortunately, the movements of those who are working with robot cannot be predicted, making robot safety vital. Most robot-related accidents occur throughout programming, maintenance, repair, setup, and testing. All these tasks involve human interaction, necessitating correct safety coaching for workers and therefore, the proper use of acceptable safeguards. Note that robots, relying on the task, might generate paint mist, attachment fumes, plastic fumes, etc.

Considering the above hazards, our safety procedures are manipulated accordingly with our robot. Following are work safety procedures to be followed by an operator or instructor to run a machine without any disaster.

### **7.1. Design Consideration for safeguards**

The first step in designing a secure robot tool is to understand the hazards that exist in the system. The hazards can be categorized based on the subsequent criteria: severity, potential injury, frequency of access to the hazard, and the opportunity of avoidance. Proper structures and employees safeguarding necessities exist at every level in the development of a robot and robot's environment. At each stage, hazard evaluation must be executed. a robot machine design idea, which can account for protection, should include the following elements.

- Restricting the movement range;
- provide safety measures for end effector (gripper, etc.);
- end effectors must be oriented, designed and manufactured so that they cause no hazards (such as a loose workpiece or load) even if power (electricity, air pressure, etc.) is shut off or power fluctuations occur;

- if the object gripped by the end effector might possibly fly off or drop, then provide appropriate safety protection considering the object size, weight, temperature, and chemical properties;
- provide adequate lighting;
- install an operation status light.

## 7.2. Installation environment

If there is a threat to the operator, maintenance employees, or other personnel from robotic motion within the restricted or running area, this area ought to also be safeguarded. Area safety scanners and mild curtains are often utilized in these areas, as the scanner coverage area is wider and greater flexibly programmed than with different devices. Again, these safeguarding devices need to be placed at a distance that provides an adequate stopping time of the machine and bills for the rate of approach from the personnel in the area as well as a depth penetration aspect, as defined inside the ANSI/RIA R15.06-1999 standard.

- Do not use in strong magnetic fields.
- Do not use in locations problem to feasible electromagnetic interference, and so forth.
- Do not use the robot in places situation to electromagnetic interference, electrostatic discharge, or radio frequency interference. The robot may malfunction if utilized in such places creating risky situations.
- Do not use in places exposed to flammable gases.
- In the installation work or in case of an emergency, do not hold the arm by your hand. It may cause malfunction.

For the planning stage, set up and next operation of a robotic or robot system, the following need to be considered. Safeguarding devices Personnel ought to be safeguarded from hazards related to the restricted envelope (space) using one or more or more safeguarding devices, consisting of:

- Mechanical limiting devices.
- Non-mechanical limiting devices.
- Presence-sensing safeguarding devices;
- Fixed barriers (which save you touch with moving elements).
- Interlocked barrier guards; like in figure 7.1 Interlocked 3d Printer.

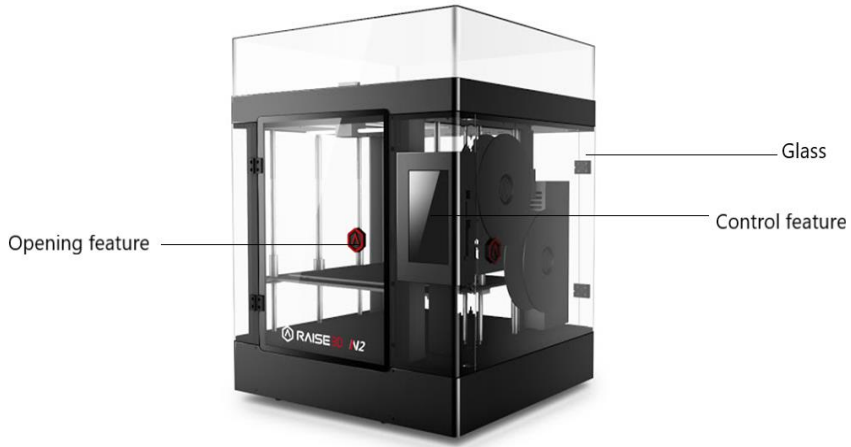


**Figure 7.1.** Interlocked 3d Printer

This figure 7.1 explains the interlocking feature through a transparent glass with opening and several features outside the working area.

Awareness devises typical awareness devices include chain or rope barriers with supporting stanchions or flashing lights, signs, whistles, and horns. These are usually used at the side of other safeguarding gadgets. safeguarding the teacher, special consideration needs to receive to the instructor or person who is programming the robot. When systems are huge and complex, it is able to be smooth to activate improper functions or sequence functions improperly. Since the person doing the education may be inside the robot's restricted envelope, such mistakes can result in accidents. Mistakes in programming will result in accidental movement or actions with similar results. For this reason, a restrained pace of 250 mm must be placed on any parts of the robot during education to decrease capability accidents to teaching employees. Several other safeguards are to be referred to in the ANSI/RIA R15.06-1992 standard to reduce the hazards associated with coaching a robotic machine. operator safeguards.

The system operator should be protected from all the source of hazards during operations performed by a robot. When the robotic is operating mechanically, all safeguarding gadgets must be activated, and at no time should any part of the operator's properties be within the robot's safeguarded area. The ANSI/RIA R15.06-1992 standard provides additional operator safeguarding suggestions. Attended continuous operation. When a person is authorized to be in or near a robot's restricted envelope to evaluate or check the robot's movement or different operations, all non-stop operation safeguards must be in force. During this operation, the robotic need to be at low velocity, and the operator should have the robot in the teach mode and take the full control of all operations. Other

safeguarding requirements are referred in the ANSI/RIA20R15.06-1992 standard. Maintenance and repair person when maintenance and repair operations are being held, the robot should be placed in the manual mode, and the maintenance personnel ought to perform their work within the safeguarded area and out of doors the robot's constrained envelope.

Additional safeguarding techniques and approaches to guard preservation and restore personnel are listed in the ANSI/RIA R15.06-1992 standard Safety training. The user of a robot must be nicely-skilled, especially concerning the use of safety equipment and procedures. Users must be aware of the feasible dangers and need to have an overview of the entire application. Robotic programmers and Engineers need to be conscious that they may be reasonable for a hazard when a robot machine is programmed or configured within the incorrect manner. Therefore, they should be acquainted with the safety statistics on the manipulator and control system. Adjustment by removing a cover requires specialized technical knowledge skills and may also involve hazards if attempted by an unskilled person. These tasks must be performed only by persons who have enough ability and qualifications in accordance with local laws and regulations.

### 7.3. Wiring safety

After checking the specified combination of the robot and controller, connect the robot and controller. Always shut off all levels of the energy supply externally before starting installation or wiring work failure to do this could cause electric surprise, or product damage Do not apply excessive impacts or loads to the connectors whilst making cable connections. this could bend the connector pins or damage the inner C board. When disconnecting the cable from the robot, do not hold the cable and pull it out by hand. Loosen the screw on the connector (if fastened with the screws), and then disconnect the cable when trying to detach by pulling on the cable itself may damage the connector or cables, and poor cable touch will motive the controller or robot to malfunction. Do not modify the cables and do no longer place any heavy objects on them handle them carefully to avoid damage. Damaged cables may purpose malfunction or electrical shock.

Be sure to store the cables connected to the robot in the conductor clamp them securely in place. If the cables are not saved in a conduit or well clamped, excessive play or movement or mistakenly pulling at the cable can also damage the connector or cables, and poor cable contact will cause the controller or bottom function. Always ground the robot body earth terminal failure to do so may result in electric shock.

## 8. ECONOMIC INDICATORS

Manufacturing activity is an indicator of the kingdom of the economic system this affects the GDP (gross home product) strongly; a boom in which shows greater demand for patron goods and, in turn, a wholesome economic system moreover, in view that people are required to manufacture new items, increases in production interest additionally enhance employment and in all likelihood wages as nicely. All the calculations presented below are not precise and presented as if any company will start to produce the body frame and assemble the machine. The calculations of costs, revenues, profits, and other parameters will be performed in this chapter. The goal of these calculations is to find the minimum production level that will bring profit and define the payback period for the estimated volume of production. For that reason, total fixed and variable costs, variable costs per unit, total costs and revenues, break-point and payback period will be used to perform calculations.

### 8.1. Calculations of fixed assets and production costs

The beginning of the production starts with some investments. They are made once and are not changed during a long period of time.

**Table 8.1.** Initial investments of the company producing the mechanisms

Type of the long-time fixed costs	Price of the investment, euro
Office and manufacturing premises	1 80 000
Machinery (Cutting, drilling and polishing machines, welding and other equipment)	30 000
Lifting/loading equipment	20 0000
Office and manufacturing premises furniture	2 000
Software	6 000
<b>Total:</b>	<b>2 38 000</b>

The next step is to calculate the variable and fixed production costs. The price list of components is presented in Table 1.3:

**Table 8.2.** The mechanism component price list

No:	Component Name	Quantity	Price of one piece, Euro	Total Price, Euros
1.	T5 mm Pulley	6	10	60
2.	Belt 5mm Pitch (Forbo movements)	3	10	30

End of table 8.2

No:	Component Name	Quantity	Price of one piece, Euro	Total Price, Euros
3.	Aluminium Profile for 4×20mm for Base	12	5	60
4.	LBCR 8mm Bearing	12	15	300
5.	Spherical Joint	8	20	160
6.	Nema 17 Motor	3	30	90
7.	Aluminium Profile for Side (20×600mm)	6	5	30
8.	Shaft Holder 8mm	6	1.5	9
9.	Link Rod (8×250mm)	6	2	12
10.	Linear Rail Shaft (8mm×632mm)	6	8	48
11.	Hex Bolt Grade ab-ISO (73×30×12)	24	1	24
12.	Hexlobular Socket Cheese Head-ISO	6	2	12
13.	Hex nut Style Grade ab-ISO	6	1	6
14.	Slot Head Pan Head Screw	24	0.5	12
15.	Aluminum Profile Support	12	1	12
16.	Hex Screw grade ab-ISO	24	0.50	12
17.	Pan Head Cross Recess Screw ISO	12	1	12
18.	Encoders	3	20	60
19.	Polulu A4988	1	5	5
No:	Component Name	Quantity	Price of one piece, Euro	Total Price, Euros
20.	RGB	3	0.50	1.5
21.	Arduino MEGA 2560	1	35	35
22.	5V regulator	1	10	10
<b>Total</b>				<b>1000.5</b>

The total price of the entire components and materials for mechanism manufacturing II = 1000.5 Euro.

The salary of the company's employee must be calculated. Supposed that there are needed four workers to manufacture and assemble one product: cutting machine operator, drilling and polishing operator, and two assemblers. To manufacture one product, the first worker needs 6 hours, the second one – 8 hours and the assemblers need 6 hours to transport and assemble the device. The average monthly wage in the Republic of Lithuania in the IV quarter of the 2018 year was 970.3 euro (<https://www.finansistas.net/vidutinis-darbo-uzmokestis.html>). The price of the workplace was calculated using the calculator (<http://www.bss.biz/atlyginimo-ir-mokesciu-skaiciuokle/>) and is 1 272.84 euro. In the Republic of Lithuania, the workday consists of 8 hours and 40 hours per week. An average number of working days per month is 20. For the 8-hour working day, the employee will receive:

$$I_2 = \frac{1 272.84}{20} \times 1 = 63.6 \text{ Euro.} \quad (8.1)$$

To manufacture one part, the second employee needs a whole working day and receives 63.6 euros, while operator and assembly workers – 53 euros (per 6-hour working day). The energy costs are also included in the manufacturing price. To produce one device, the following equipment is used: cutting, drilling, and polishing machines, as well as portable welding station. The total power of the for all the equipments is 120 KW. Supposing all required equipment is used for 10 hours to produce the final product. The price of 1 kWh is 0.130 euro (<https://letiekimas.lt/namams/elektra-namams-2/tarifu-planai-ir-kainos/>). The total cost of electric energy for one product is:

$$I_3 = 120 \times 10 \times 0.130 = 156 \text{ Euro.} \quad (8.2)$$

During the production process, they are used additional materials like wires for welding materials, cables, and wires, lubricants, packing materials, etc. Expenses for those materials regularly appear during the production process. To continue the calculations, suppose that those costs are  $I_4 = 25$  euro for one product. Moreover, the wearing of tools (drills, welding equipment parts, etc.) of manufacturing equipment also creates some costs for the company to replace and maintain. They are supposed that technological wearing costs for production of one device will be:  $I_6 = 25$  euro. The products will be delivered to an order by the assemblers. It means that the fuel will be used, likely more than the average as the weight and size of the device transported are big. We can assume that it would be  $I_5$  is 25 Euro for one product if the product is assembled in Lithuania and more if the product is assembled abroad.

The variable direct costs consist of the materials and components costs, energy costs, and workers' salaries. The variable non-direct costs consist of the costs of additional materials, transportation costs, and costs of the technological wearing of tools. Table 8.3 presents these costs.

**Table 8.3.** Variable direct and non-direct costs for manufacturing one product

No	Direct costs	Amount, euro
1.	Components and materials	1000.5
2.	Wages of the company's employees	63.6
3.	Energy	156
4.	Non-direct costs	25
5.	Additional materials	25
6.	Transportation costs	25
7.	The technological wearing of tools	25
<b>Total variable costs (AVC)</b>		<b>1 320.1</b>

## 8.2. Calculation and determination of fixed costs

The next step in the economic calculations is to evaluate fixed costs, which primarily consist of administration and general staff wages. As the complexity of the structure is not high, we can assume that there are 10 employees who participate in the production process of those mechanisms. The workplace's price of one employee is 1 272.84 Euro. The salaries of 10 employees per year will cost the company the next amount of money:

$$I_7 = 1272.84 \times 10 \times 12 = 1 52 740.8 \text{ Euros} \quad (8.3)$$

The offtake of the company heavily depends on the advertising of the product. There is no sense to rent a billboard in the center of the city because the manufactured mechanisms are not the mass-consumption product. It was decided to advertise the product on the Internet. The price of advertising is 200€ per month (three times per day in the 50 qualified proclaiming lists) + GOOGLE advertising (<https://pigiaireklama.lt/kainos>). The cost of advertising per year will be:

$$I_3 = 200 \times 12 = 2 400 \text{ Euro.} \quad (8.4)$$

CAD design software is necessary for the company. The Solid works and AutoCAD programs are used by designer and production engineer. The cost of the licenses for both programs per year is

$I_9 = 6000$  euro. Sometimes the cost of CAD design software can be eliminated by using the open source software.

The manufacturing premises should be serviced every year. Amortization costs are included in the fixed costs and calculated according to the following formula:

$$I_{10} = \frac{P_1 - P_2}{T} \quad (8.5)$$

where,  $I_{10}$  – amortization costs per year (Euros),  $P_1$  – the price of the obtained manufacturing and office premises (Euros),  $P_2$  – the price of the liquidated fixed assets (Euros).

$T$  - a time of exploitation (the building is wearing normative  $T = 15$  years according to 2008 04 10 LR law Nr. X-1484 of fixed assets wearing or amortization normative). The calculated wearing amortization costs of the premises are:

$$I_{10} = \frac{P_1 - P_2}{T} = \frac{180000 - 18000}{15} = 10800 \text{ Euros.} \quad (8.6)$$

The clerical expenses, costs of communicational service (telephone, Internet) and utility rates are also included in the fixed costs and supposed that clerical and communicational expenses will be  $I_{11} = 5000$  euro and utility rates  $I_{12} = 4000$  €. The list of the fixed costs of the company that is planning to produce sealing-cutting mechanisms is presented in Table 4.

**Table 8.4.** Fixed costs of the company

No	Fixed costs	Amount, Euro
1.	Administration and general staff employees' salaries and social insurance	1 52 740.8
2.	Advertising	2 400
3.	Software	6 000
4.	Office and manufacturing premises amortization	2 000
5.	Utility rates	5 000
6.	Clerical and communicational expenses	4 000
	<b>Total fixed costs (FC)</b>	<b>1 76 640.8</b>

## CONCLUSIONS

1. As we can observe from the literature review and finds that delta robot has been optimized for various usage like surgery and other tasks with links larger, hence design for larger workspace is no more exceptional, so in this work design of delta robot for wider workspace is going to be implemented.
2. It is found from review of analogic constructions when forearms become larger the accuracy decreases because of inertia and moment so this work proposes lower linkages length comparing to conventional delta robots.
3. Belt actuation method is chosen because it has low mass inertia and it can produce high caliber of torque support so reducing one arm which reduces a joint, by this moment can be reduced, which can be used for higher payloads of 2 kg by maintaining medium accuracy of  $\pm 0.2$  mm.
4. During belt drive calculations mechanical torque is ought to be 0.32 Nm but after belt is chosen considering the inertia from the belt the required torque is 0.758 Nm which makes motor selection in the same category “NEMA 17” where second line of conclusion has become true.
5. In the control algorithm section our robot control structure is designed upto 25 logical steps with consideration of calibration where errors can be avoided by doing it so successful implementation is possible by introducing this structure.
6. In electrical scheme minimum number of components are used in connections for minimizing errors and easy troubleshooting and with the minimum number of components ought to be cheaper.
7. From economical calculations mechanical parts contributes 80% of the total cost for producing the device which is comparatively higher than electrical components but repairing costs of mechanical components when compared to replacement of electrical components is cheap and efficient way and breakpoint occurs at 422 units.

## REFERENCES

- [1] Alberto, J. A., 2018. Development of the linear delta robot for additive manufacturing. *Journal of 5th International Conference on Control, Decision, and Information Technologies (CoDIT'18)*. ResearchGate (Alberto, 2018).
- [2] Behzad, M., 2017. Kinematic sensitivity evaluation of revolute and prismatic 3-DOF delta robots. *International conference on robotics and mechatronics*. ResearchGate (Behzad, 2017).
- [3] Bortoff, S. A., 2018. Object-Oriented Modeling and Control of Delta Robots. *Journal of intelligent and robotic systems*. Mitsubishi electric research laboratories (Bortoff, 2018).
- [4] Elatech, 2018. *Drive calculation catalog* (Elatech, 2018).
- [5] Enrique, C, 2017. Vision-based control of delta parallel robot via linear camera manipulation. *Journal of the intelligent and robotic system*. Springer link (Enrique, 2017).
- [6] FANUC, 2018. Datasheet M-1iA-05SL. *FANUC datasheet* (FANUC, 2018).
- [7] Forbo movements, 2018. *Forbo movements belt drive catalog* (Forbo movements, 2018).
- [8] Gurgen, M, 2016. Parametric design of delta robot. *Journal from CBU international conference in innovation and science and education*. Research gate (Gurgen. M, 2016)
- [9] HIRSCHMANN spherical bearings, 2018. *Rod ends/spherical bearings pdf* (HIRSCHMANN, 2018)
- [10] IGUS, 2018. *IGUS datasheet* (IGUS, 2018).
- [11] Roantech, 2018. *Roantech Delta robot datasheet*. (Roantech, 2018).
- [12] SKF, 2019. *Linear bearings manual*. (SKF, 2019).
- [13] SURESTEP, 2018. *SURESTEP Stepping Systems User Manual*. Selecting the Sure Step Stepping System (SURESTEP, 2018).
- [14] Yang, X. 2017. Delta robot structural design and kinematic analysis. Journal from IOP conference. ResearchGate (Yang, X. 2017).
- [15] YASKAWA, 2018, *YASKAWA MOTOMAN MPP3S datasheet* (YASKAWA, 2018).

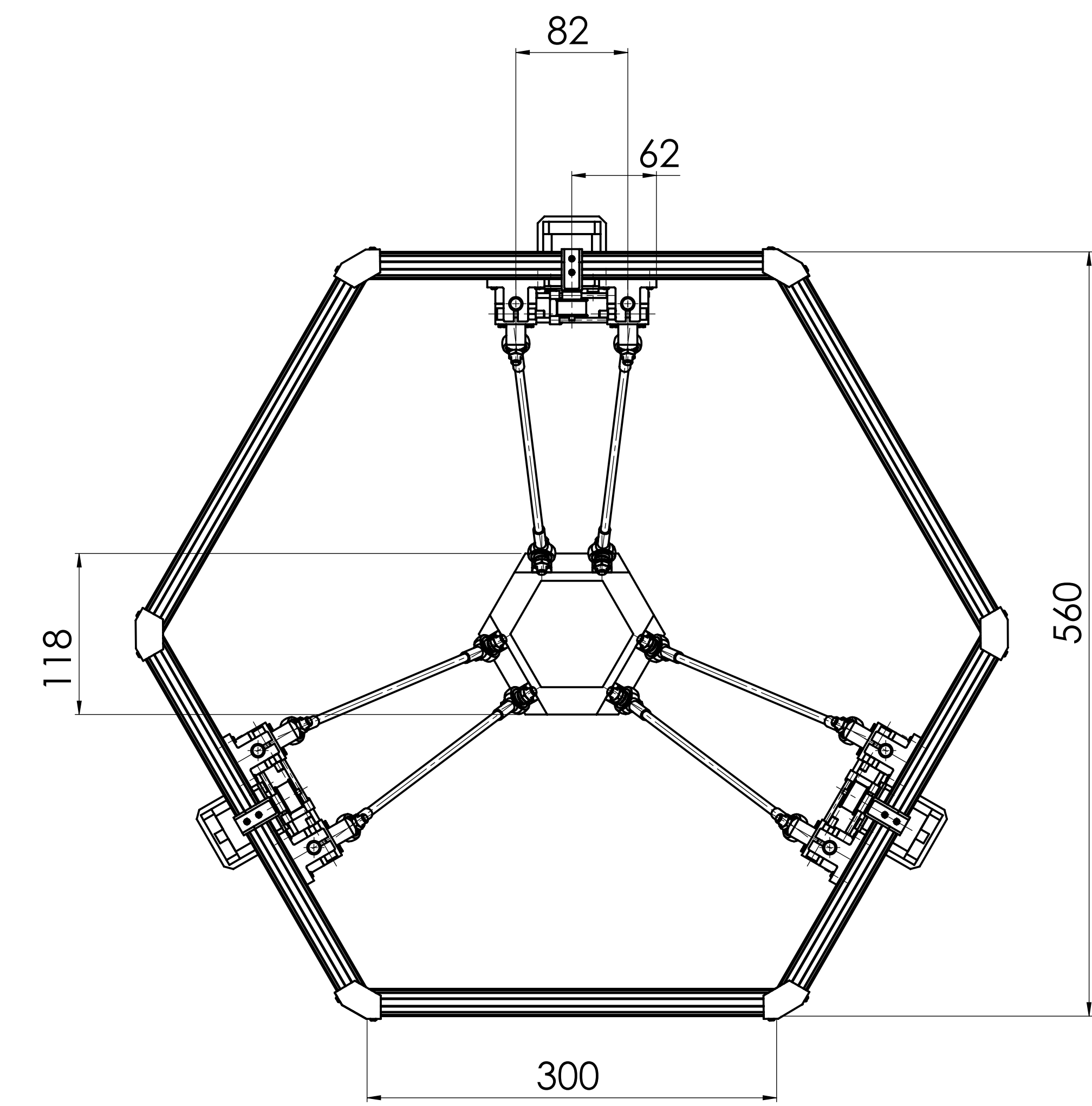
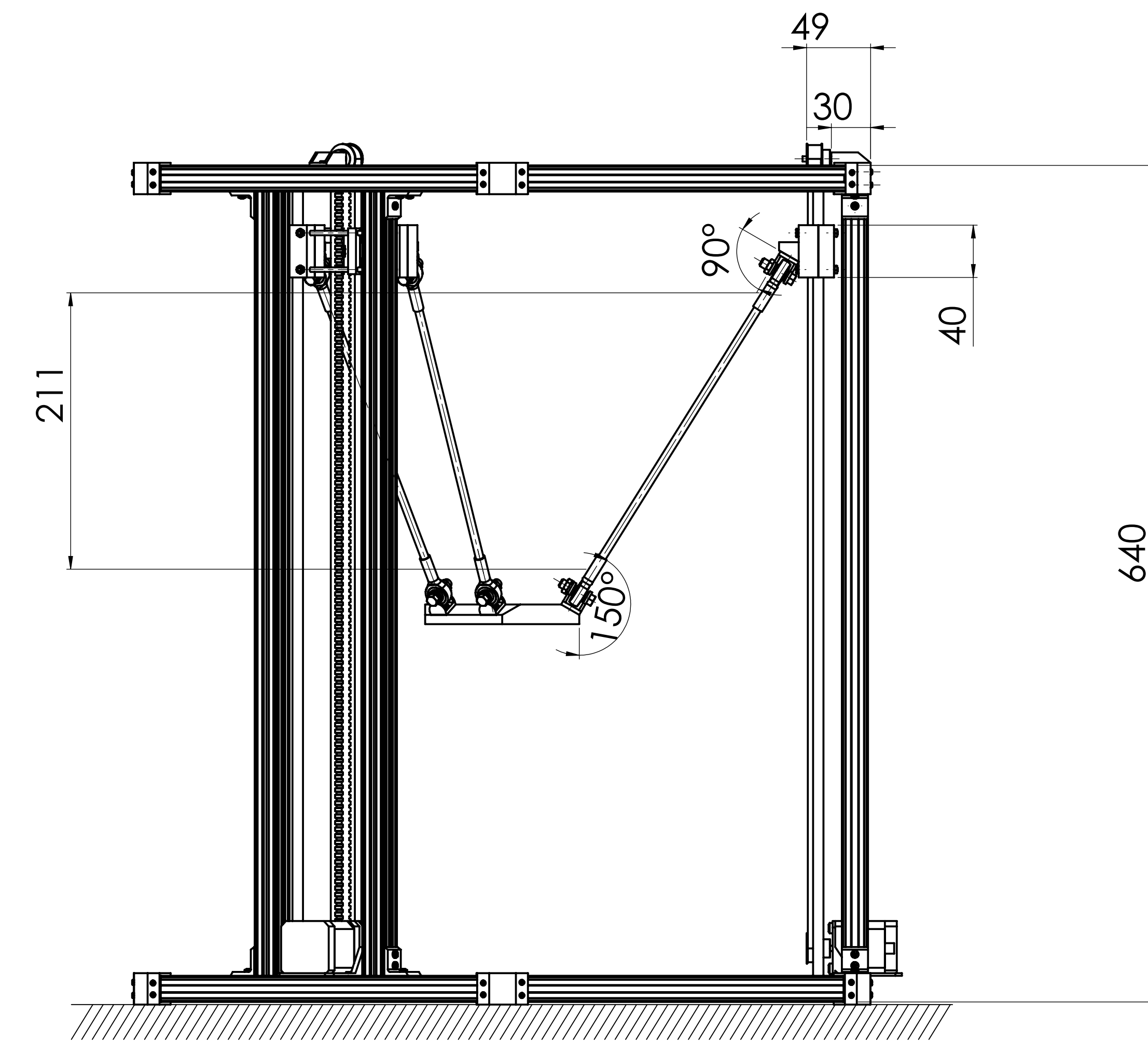
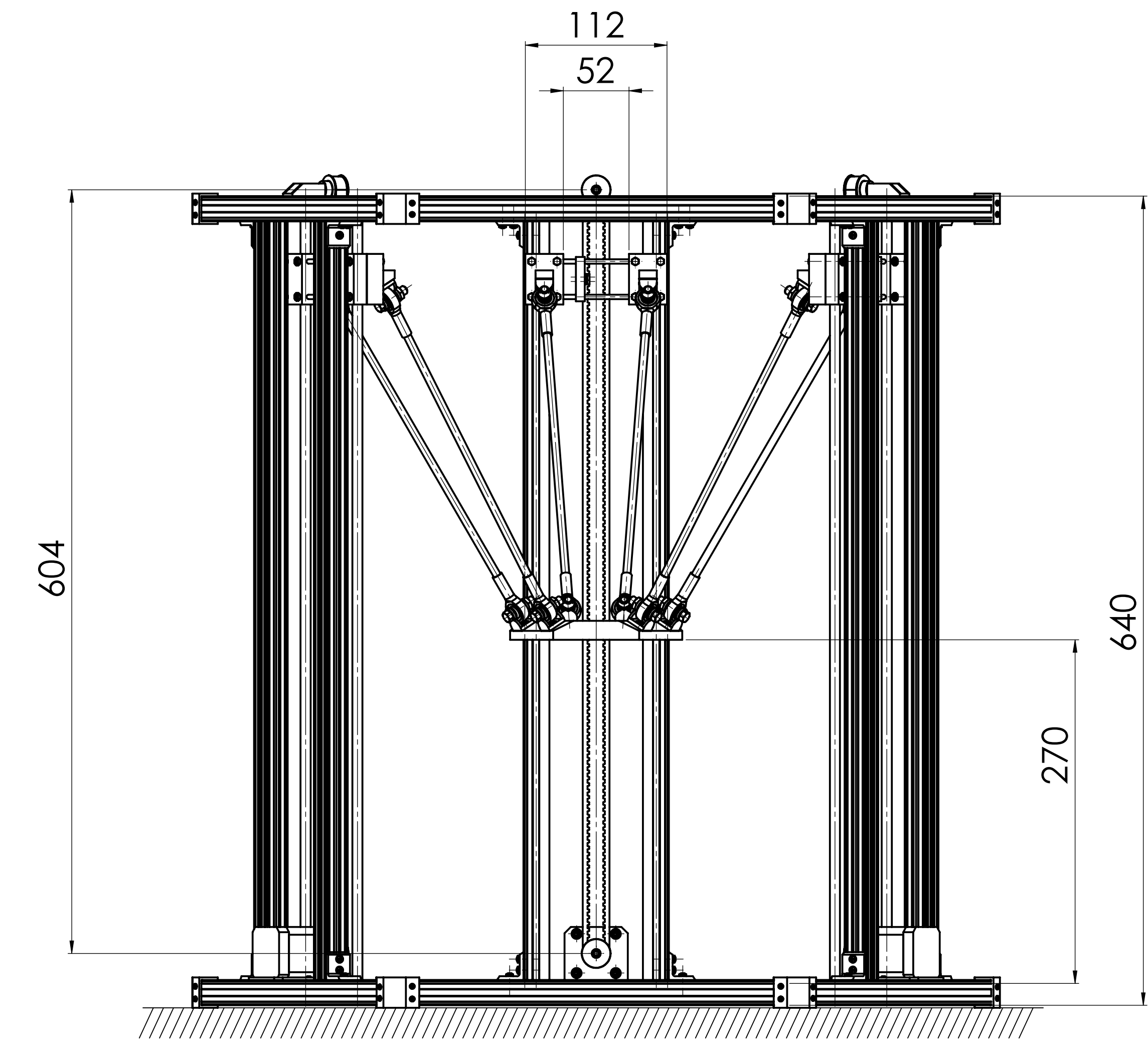
- [16] Yeshmukhametov, A. 2017. Design and Kinematics of Serial/Parallel Hybrid Robot. *Journal from 3rd International Conference on Control, Automation, and Robotics*. ResearchGate (Yeshmukhametov, 2017).

## **APPENDIX**

<i>Format</i>	<i>Zone</i>	<i>Position</i>	<i>Mark</i>	<i>Name</i>	<i>Amount</i>	<i>Note</i>
				<u>Documentation</u>		
A1			<b>VGTU BM 19 27 02 01 00 AD</b>	<b>Assembly of Delta robot</b>	<b>1</b>	
				<u>Details</u>		
			5 <b>VGTU BM 19 27 02 01 01</b>	closure for bearing(front)	3	
			6 <b>VGTU BM 19 27 02 01 02</b>	closure for bearing(back)	3	
			11 <b>VGTU BM 19 27 02 01 03</b>	Link	6	
			12 <b>VGTU BM 19 27 02 01 04</b>	Pulley holder	3	
			14 <b>VGTU BM 19 27 02 01 05</b>	Nema stand	3	
			16 <b>VGTU BM 19 27 02 01 06</b>	Clamp for profiles	12	
			26 <b>VGTU BM 19 27 02 01 07</b>	Belt clamp	3	
			31 <b>VGTU BM 19 27 02 01 08</b>	Polyring	1	
			34 <b>VGTU BM 19 27 02 01 09</b>	Profile support	12	
			7 <b>VGTU BM 19 27 02 01 10</b>	Holder	12	
			8 <b>VGTU BM 19 27 02 01 11</b>	Carriage holder	12	
Owner <b>VG TU MPfuc-15</b>		Compiled <b>A.Muthusami</b>	Document type <b>Specification</b>	Mark <b>VG TU BM 19 27 02 00 00 TS</b>		
		Checked <b>S.Petkevicius</b>	Title <b>Assembly Drawing</b>	Rev. <b>A</b>	Date <b>2019.05.29</b>	Lan. <b>en</b>
						Sheet <b>1/3</b>

<i>Format</i>	<i>Zone</i>	<i>Position</i>	<i>Mark</i>	<i>Name</i>	<i>Amount</i>	<i>Note</i>			
				<u><b>Standard Parts</b></u>					
		1		Aluminium profile 20× 300mm	12				
		2		Aluminium profile 20× 600mm	6				
		3		Linear shaft	6				
		4		Linear bearing	6				
		9		Spherical joint part	12				
		10		Outer ring or spherical joint	12				
		13		GT5mm pulley	6				
		15		NEMA 17	3				
		17		ISO 4762 M5 x 30 - 22N	6				
		18		ISO - 4034 - M5 - N	12				
		19		ISO 4014 - M3 x 30 x 12-N	24				
		20		ISO 1580 - M2 x 8 - 8N	55				
		21		ISO 1580 - M2 x 6 - 6N	23				
		22		ISO 4762 M5 x 30 - 22N	6				
		23		ISO 14583 - M4 x 5 x 3.6 - 4.8-N	12				
		24		ISO 1580 - M2.5 x 8 - 8N	24				
		25		GT5 mm Belt	3				
		27		ISO 1580 - M1.6 x 6 - 6N	12				
		28		ISO 1580 - M1.6 x 5 - 5N	6				
<b>VG TU MPfuc-15</b>		Compiled <i>A.Muthusami</i>	Document type <i>Specification</i>	Mark <b>VG TU BM 19 27 02 00 00 TS</b>					
		Checked <i>S.Petkevicius</i>	Title <i>Assembly Drawing</i>	Rev. <b>A</b>	Date <b>2019.05.29</b>	Lan. <b>en</b>			
				Sheet	<b>2/3</b>				

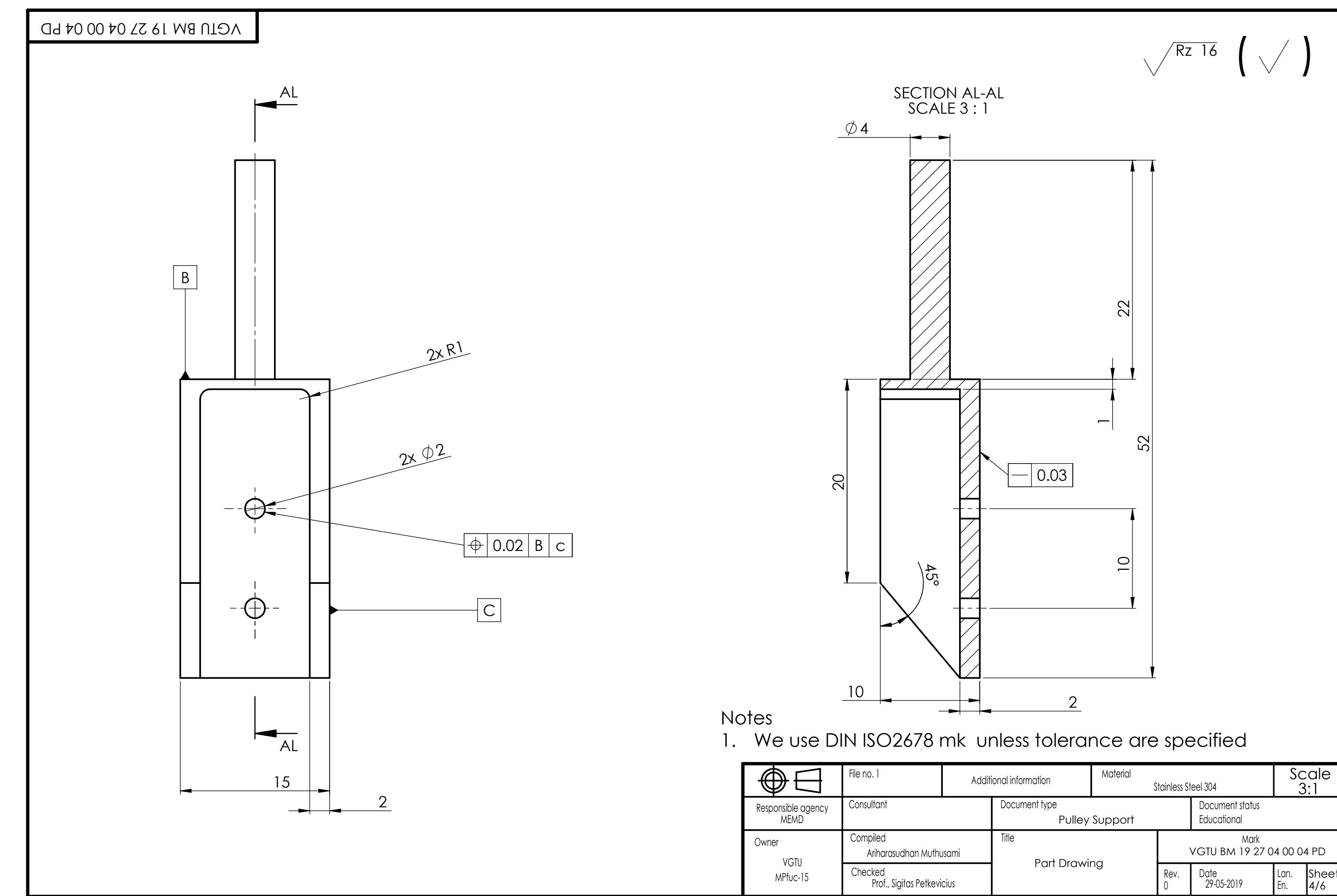
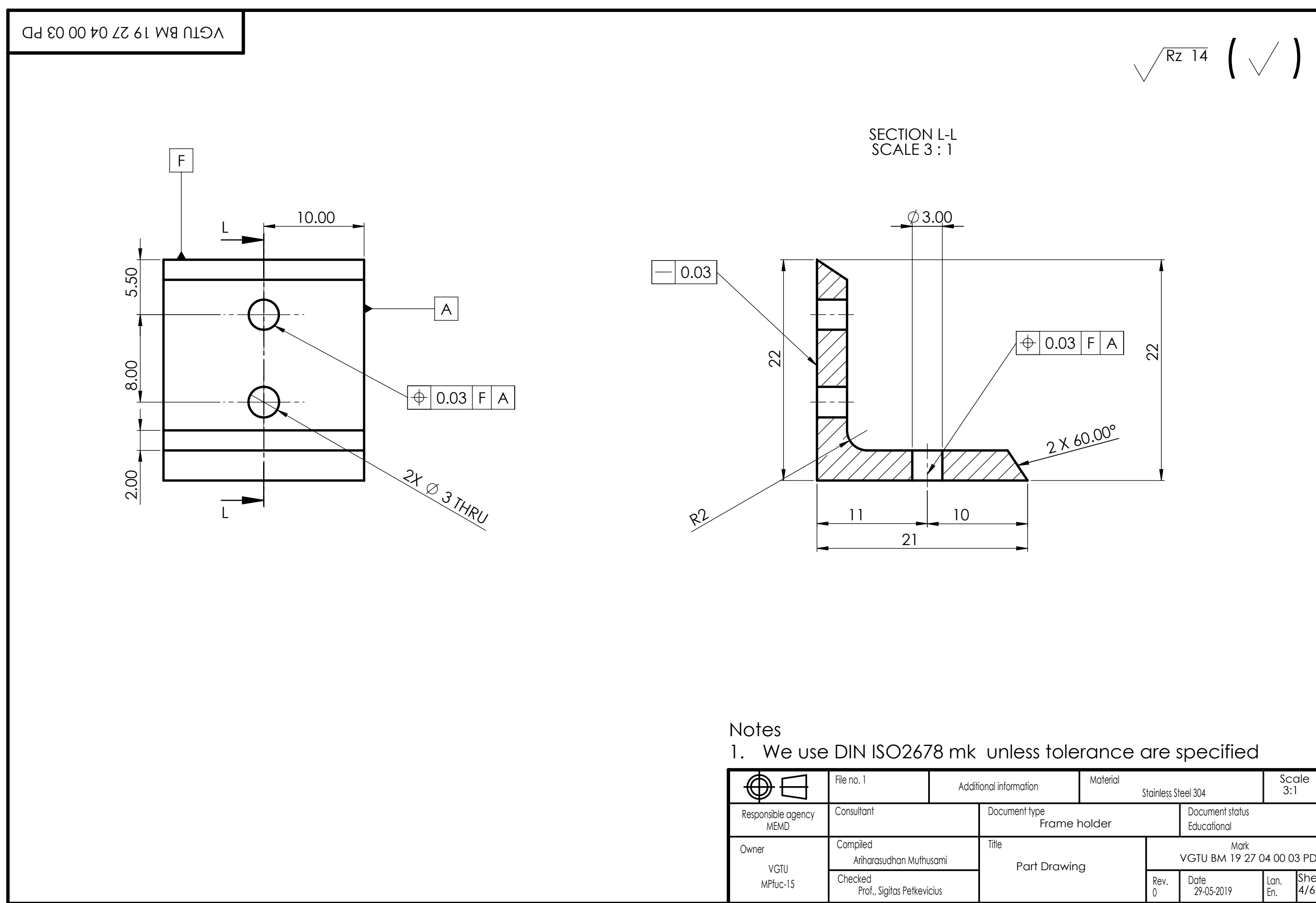
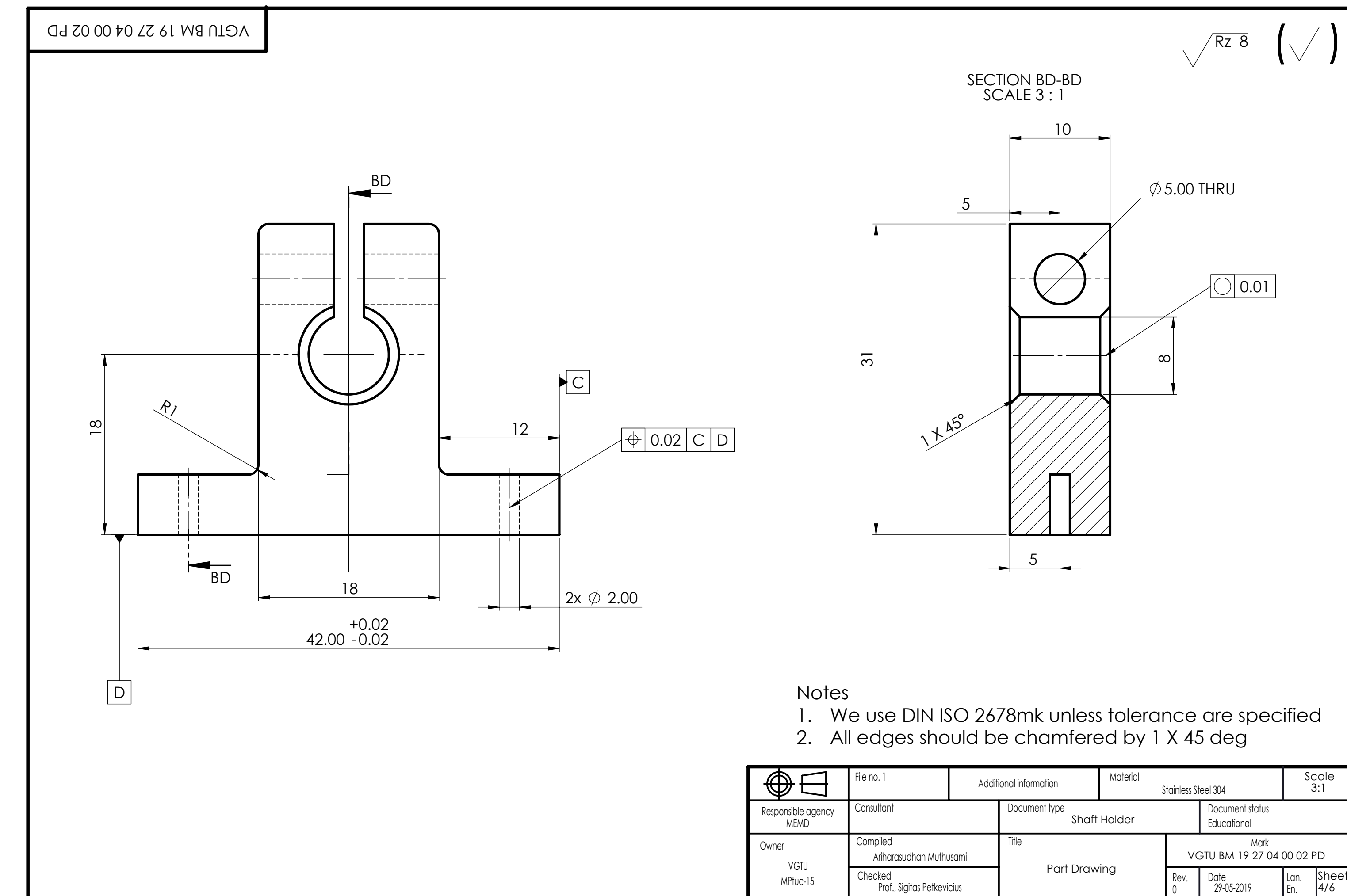
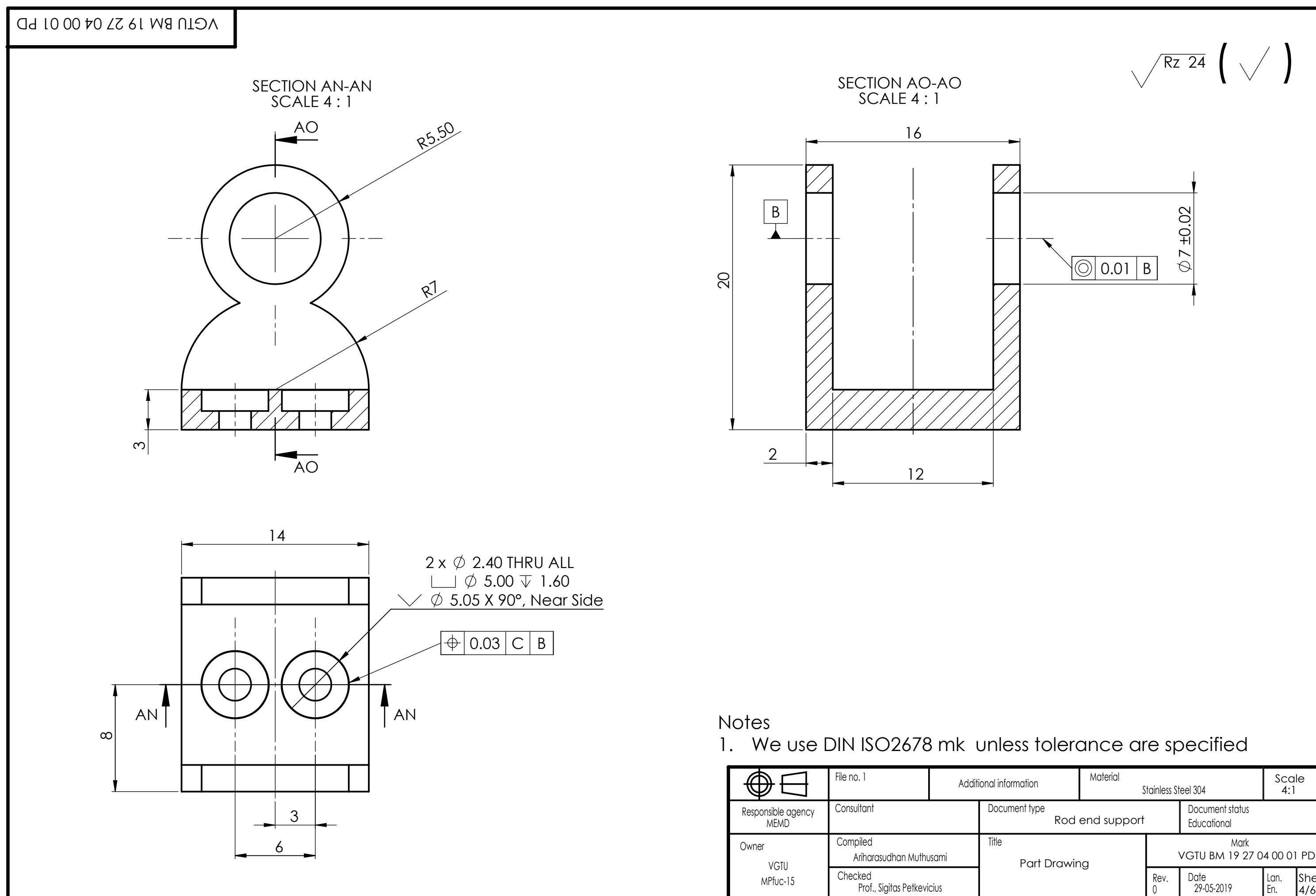




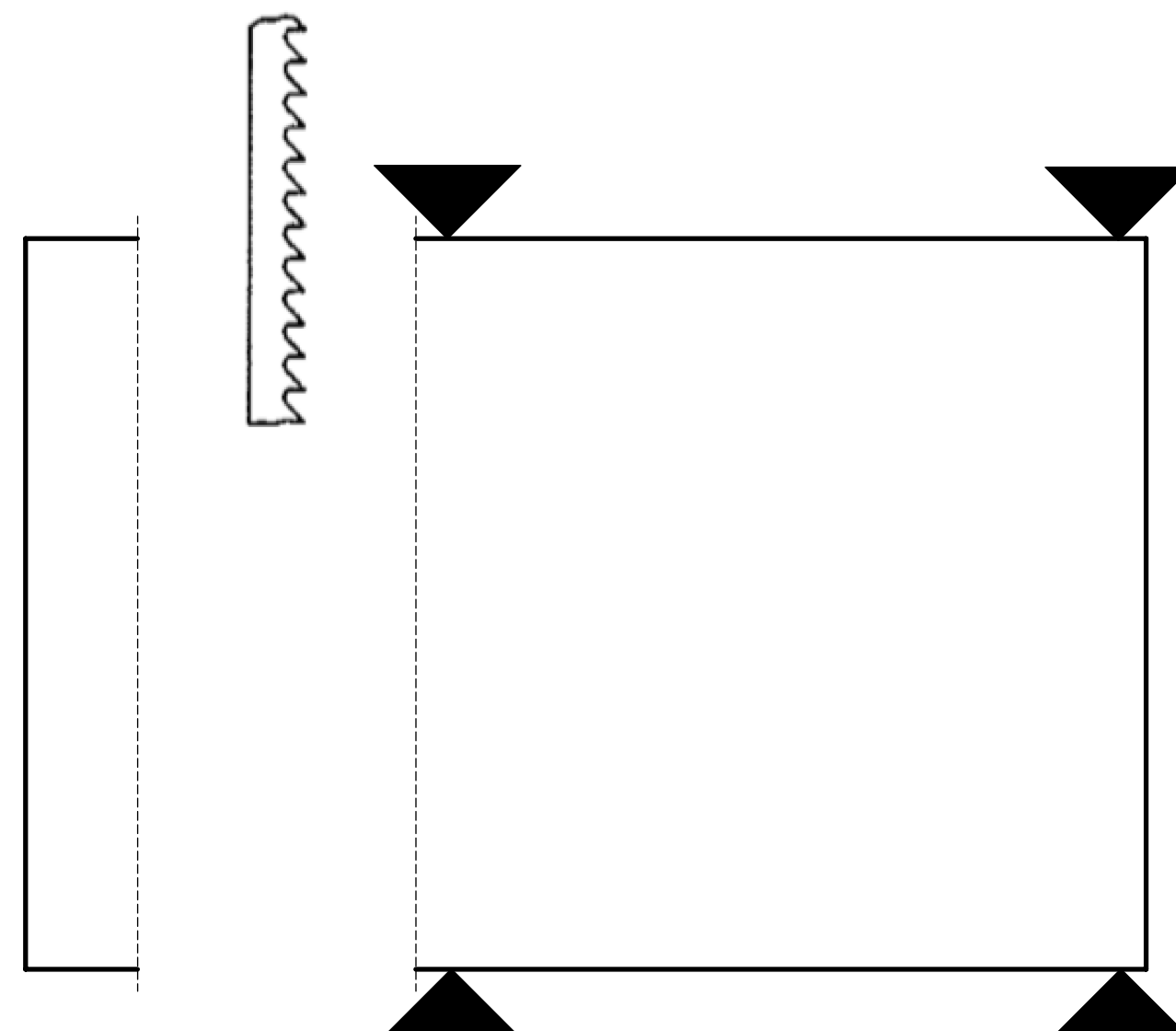
**Technical Information**

- Reference dimension
- For other details see attached 3d model
- Linear shafts and bearings have to be lubricated.
- Machine should be operated on flat level and rigid surface.
- Part names are given separately.
- Do not use above 12 voltage of supply.
- Avoid strong magnetic environment.
- Maximum speed upto 1.5m/s.
- Refer ISO 10218 for environmental safety requirements.
- Maximum payload of 1.5 kilograms.

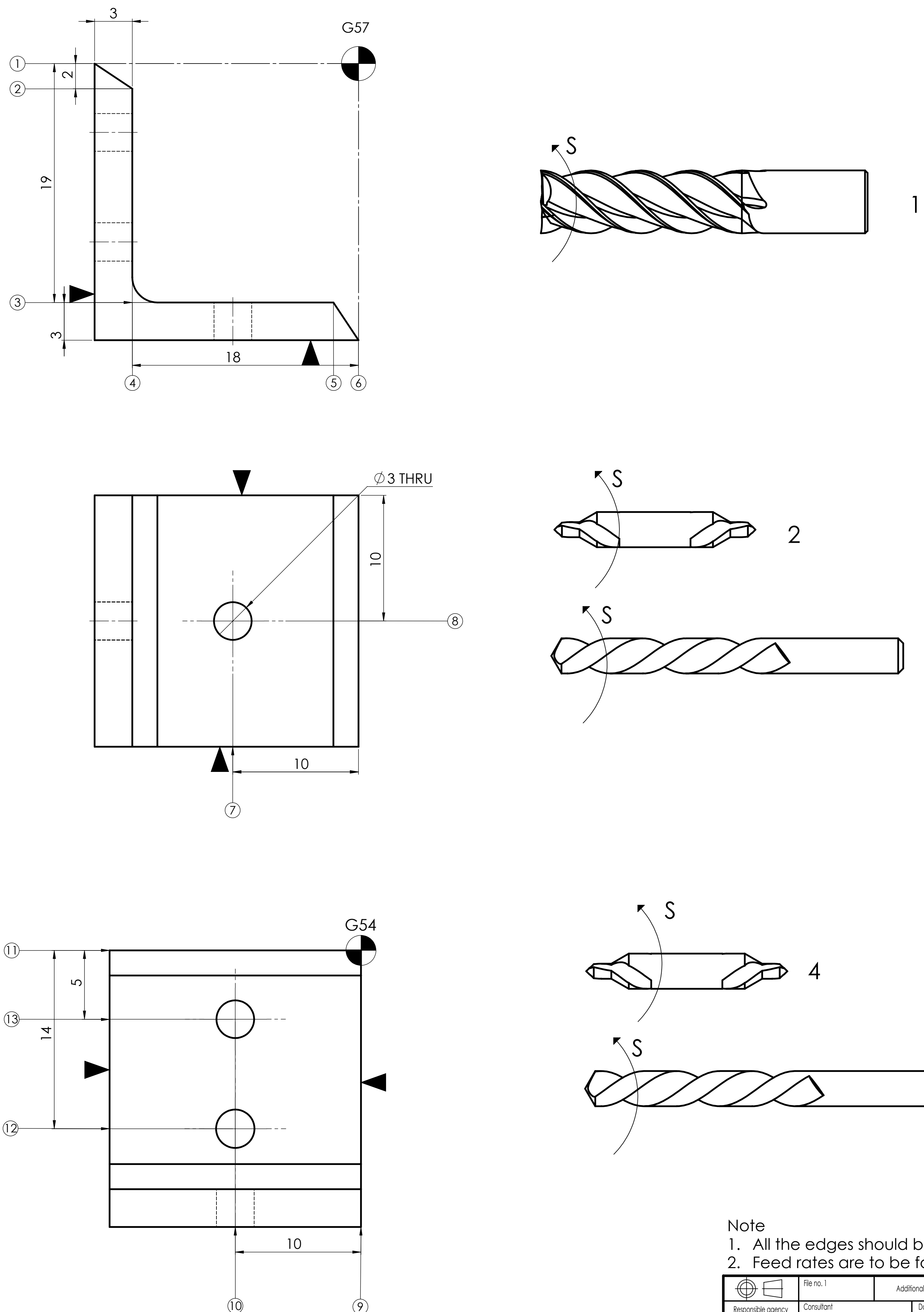
File no. 1	Additional information	Material	Scale
Responsible agency MEMD	Consultant	Document type General Drawing	Document status Educational
Owner VG TU MPfuc-15	Compiled Anilraasudhan Muthusami Checked Prof. Sigitas Pelevicius	Title Design of Delta robot	Mark VG TU BM 19 27 01 00 00 GD
	Rev. 0	Date 29-05-2019	Lan. En. Sheet 1/6



CNC Vertical milling center "HAAS Minimill" coordination sheet			
Part number:	Frame holder	Operator:	Ariharasudhan.M
Part material:	Aluminium 1060 alloy	Date of issue:	2019-05-05
part drawing marking:	MBP.122.434.005.004	Due date:	2019-06-04
Operation number:		Part count:	1
Operation name:	Milling, drilling, tapping		
Program name:	O08041		
Dimensions:	300 X 500 X10		
Holding device:	Vise		
Operation content			
Step no.	Step details		
1	End milling of point 1 to 6		
2	Center drilling of point 7 and 8 dimensions		
3	Drilling of dia 3mm of dimensions 7 and 8		
4	Center drilling of point 9 to 13 dimensions		
5	Drilling of dia 3mm for points 9 to 13 dimesions		



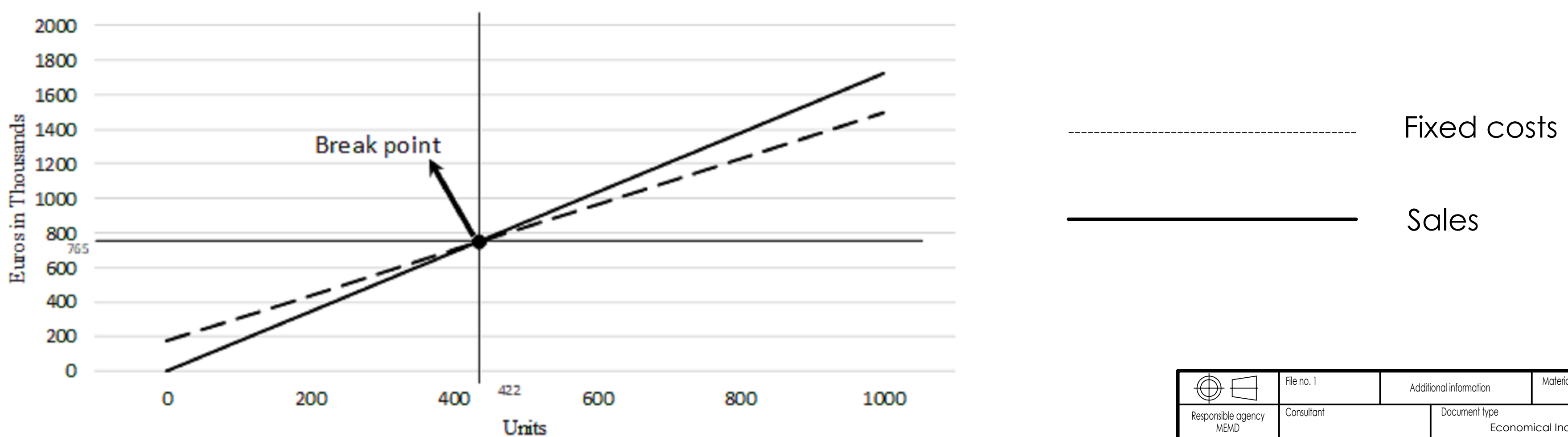
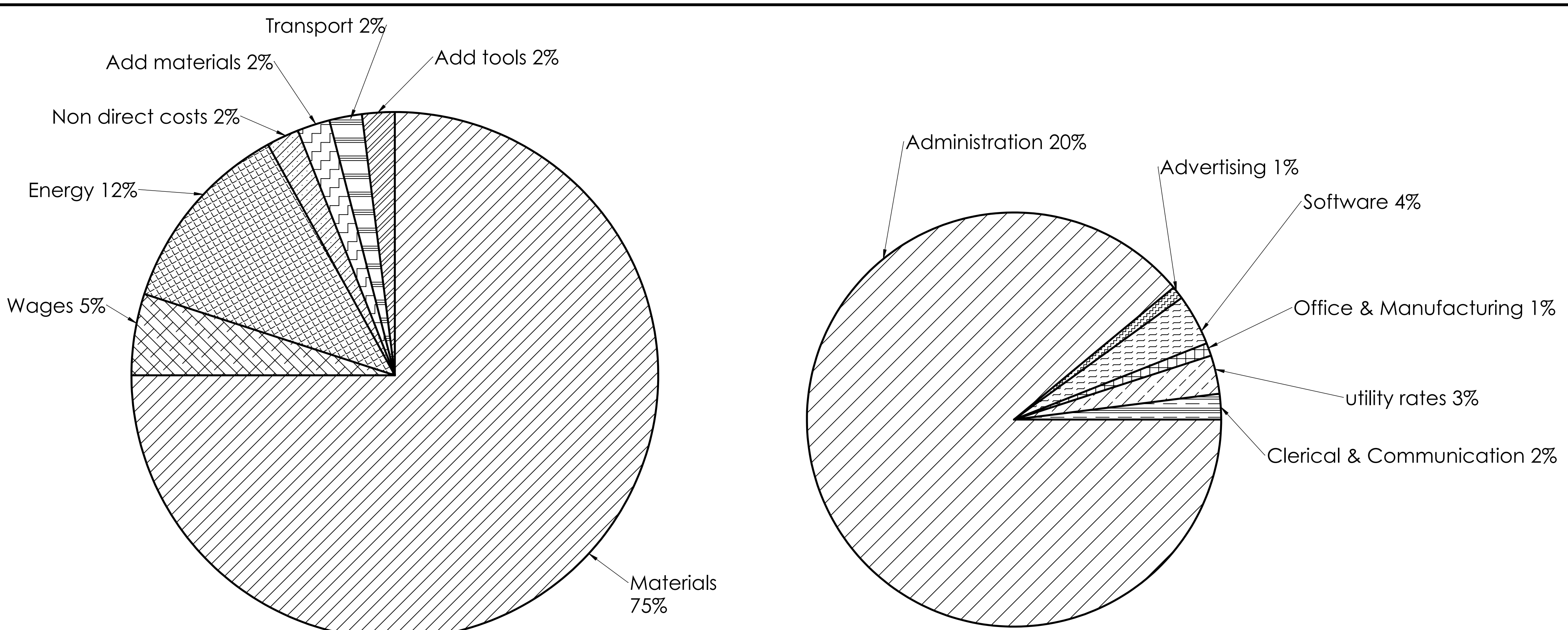
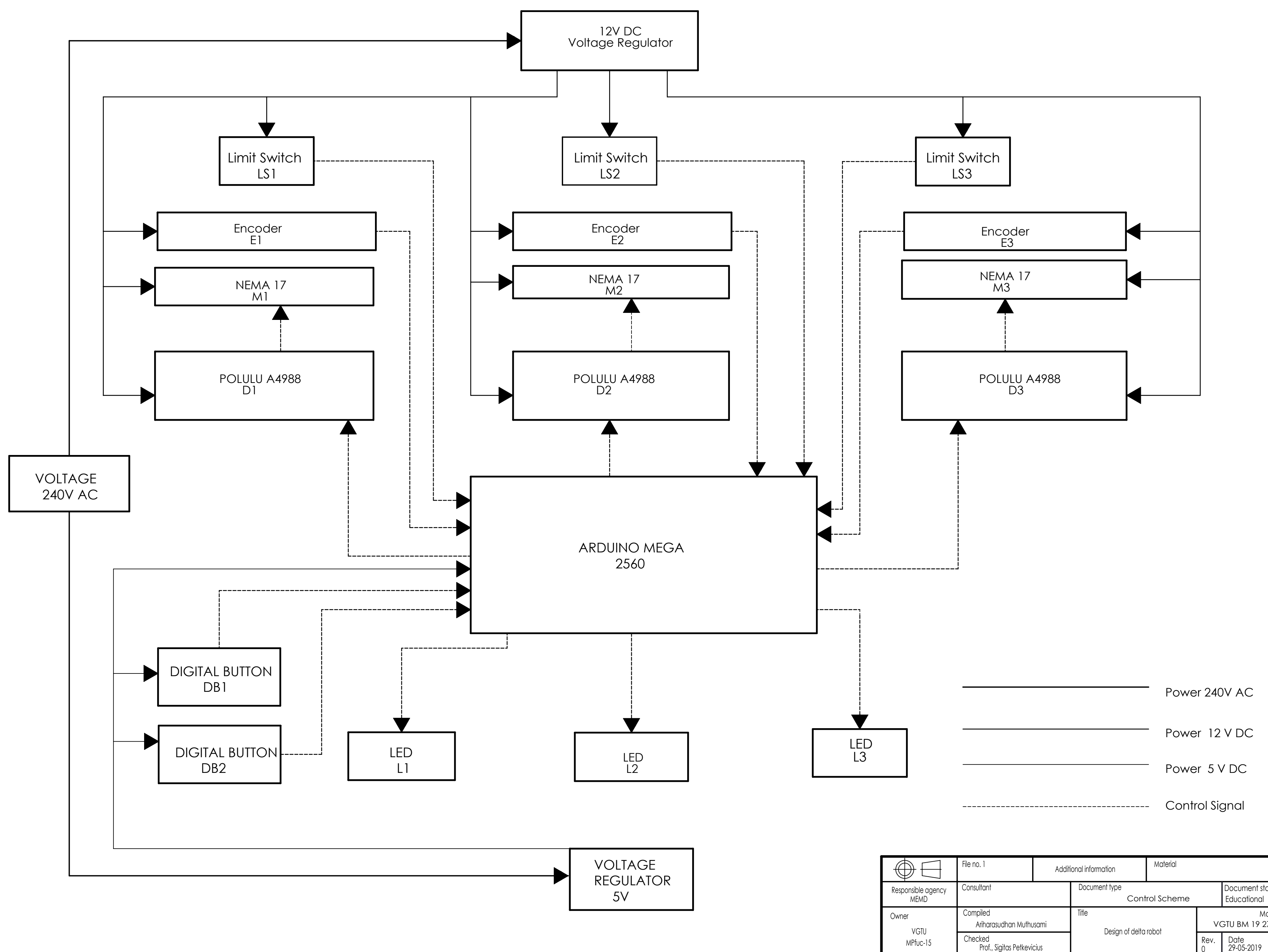
Tool number	vc m/min	vf mm/min	fz mm/t	n rev/min	ap, min	tp, min
1	205	1412.64	0.0327	10800	3	-
2,4	50	640	0.06	1500	1	0.58
3,5	182	2125.2	0.22	1300	14	

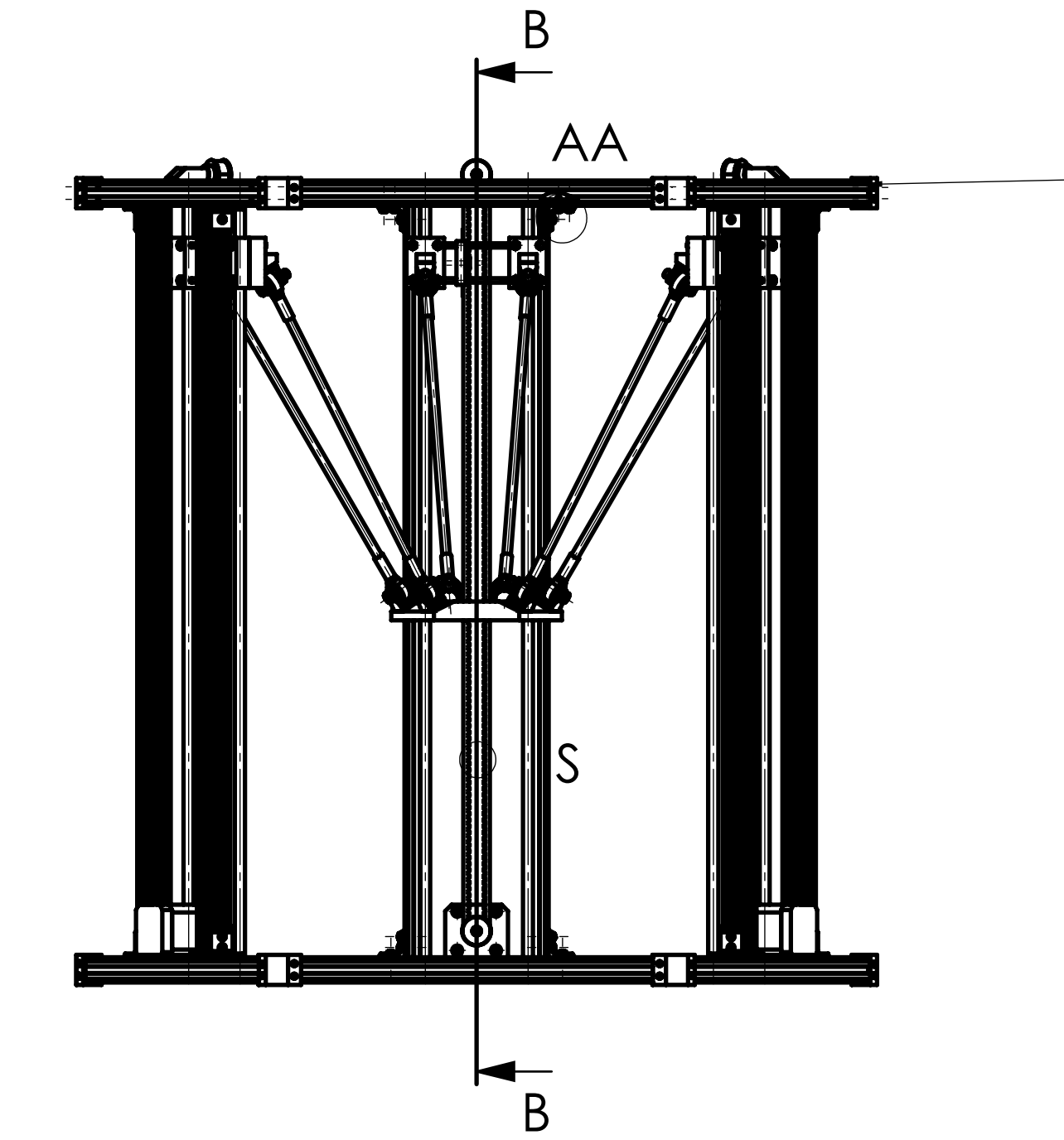
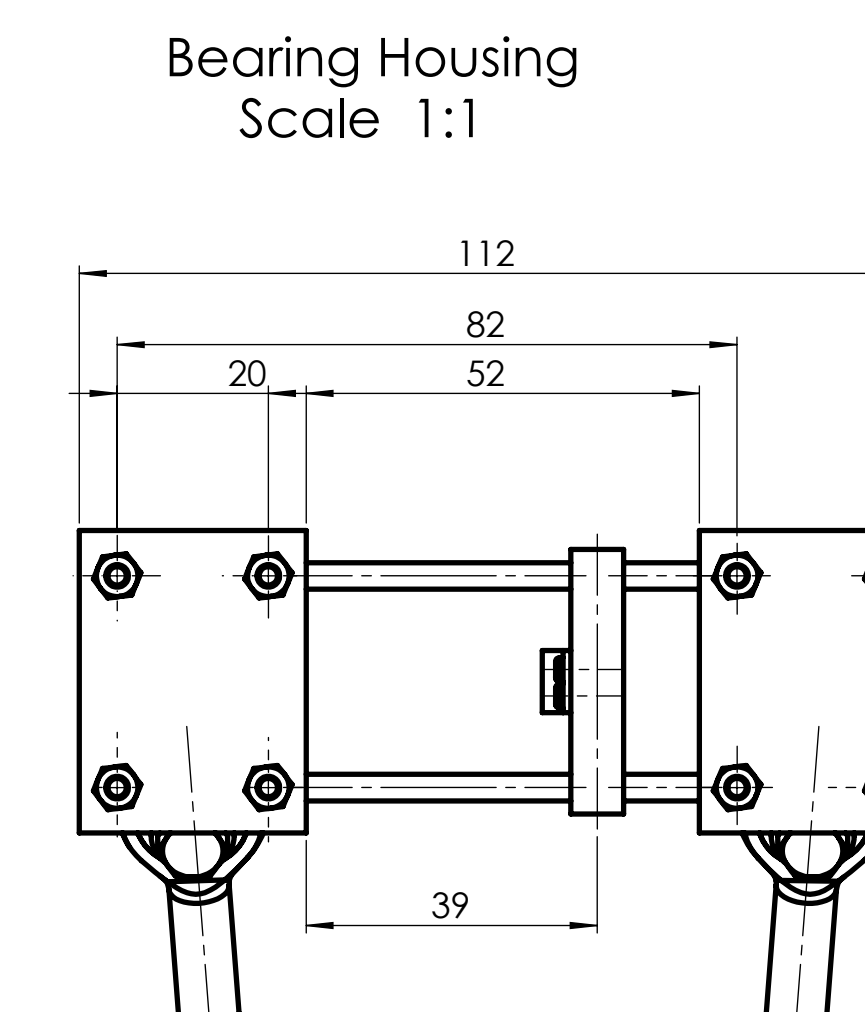
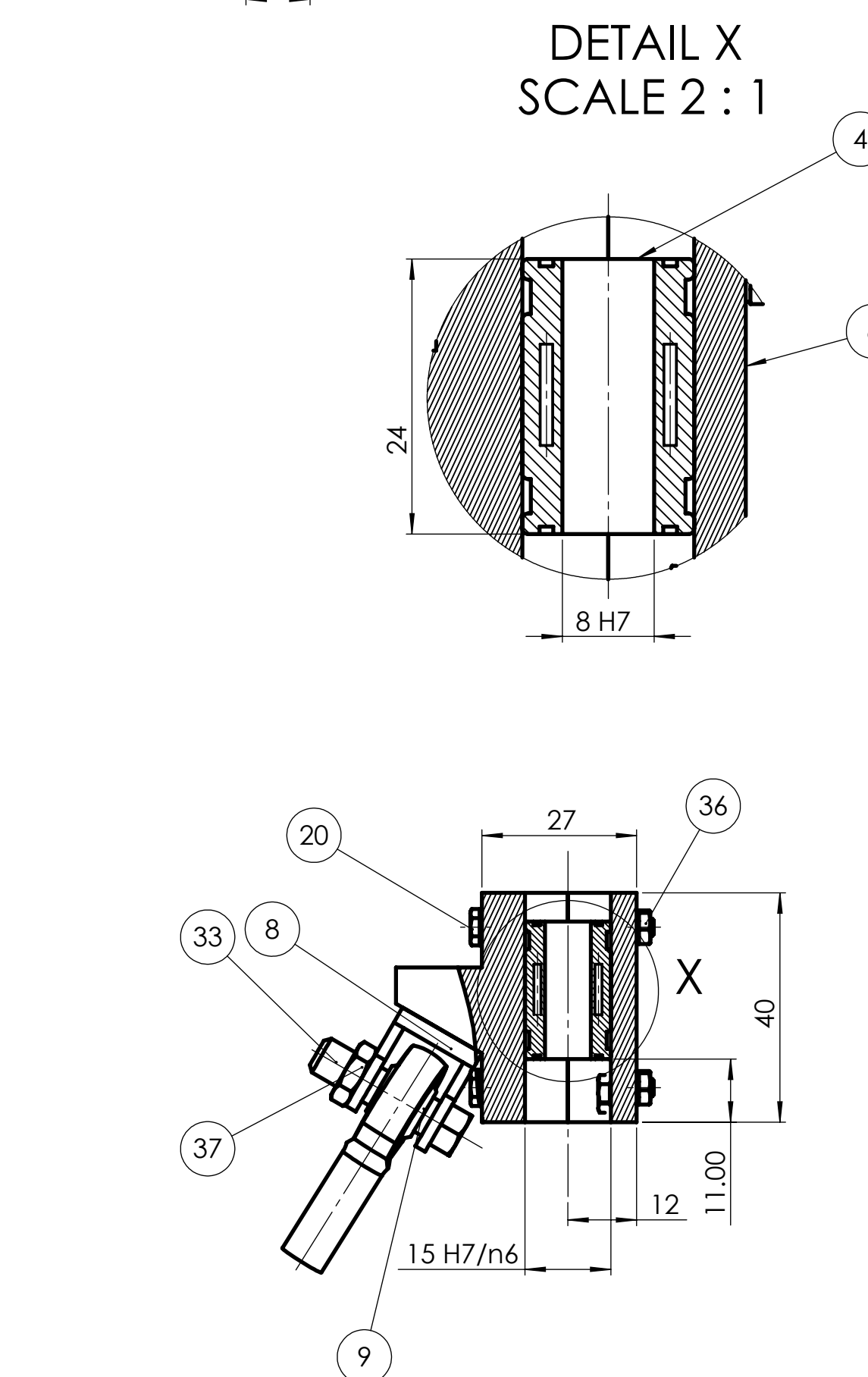
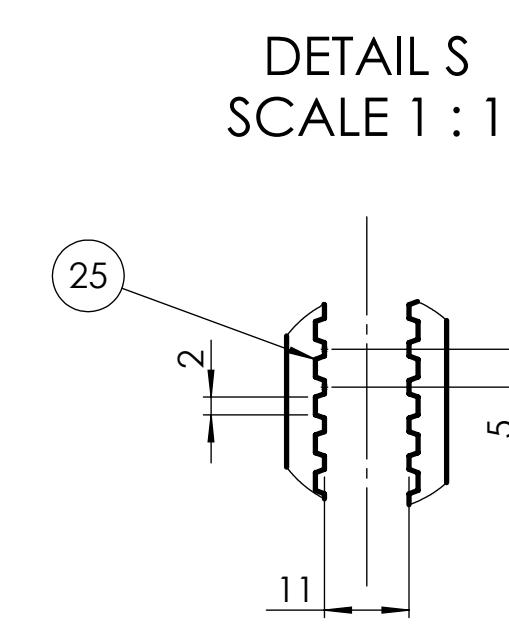
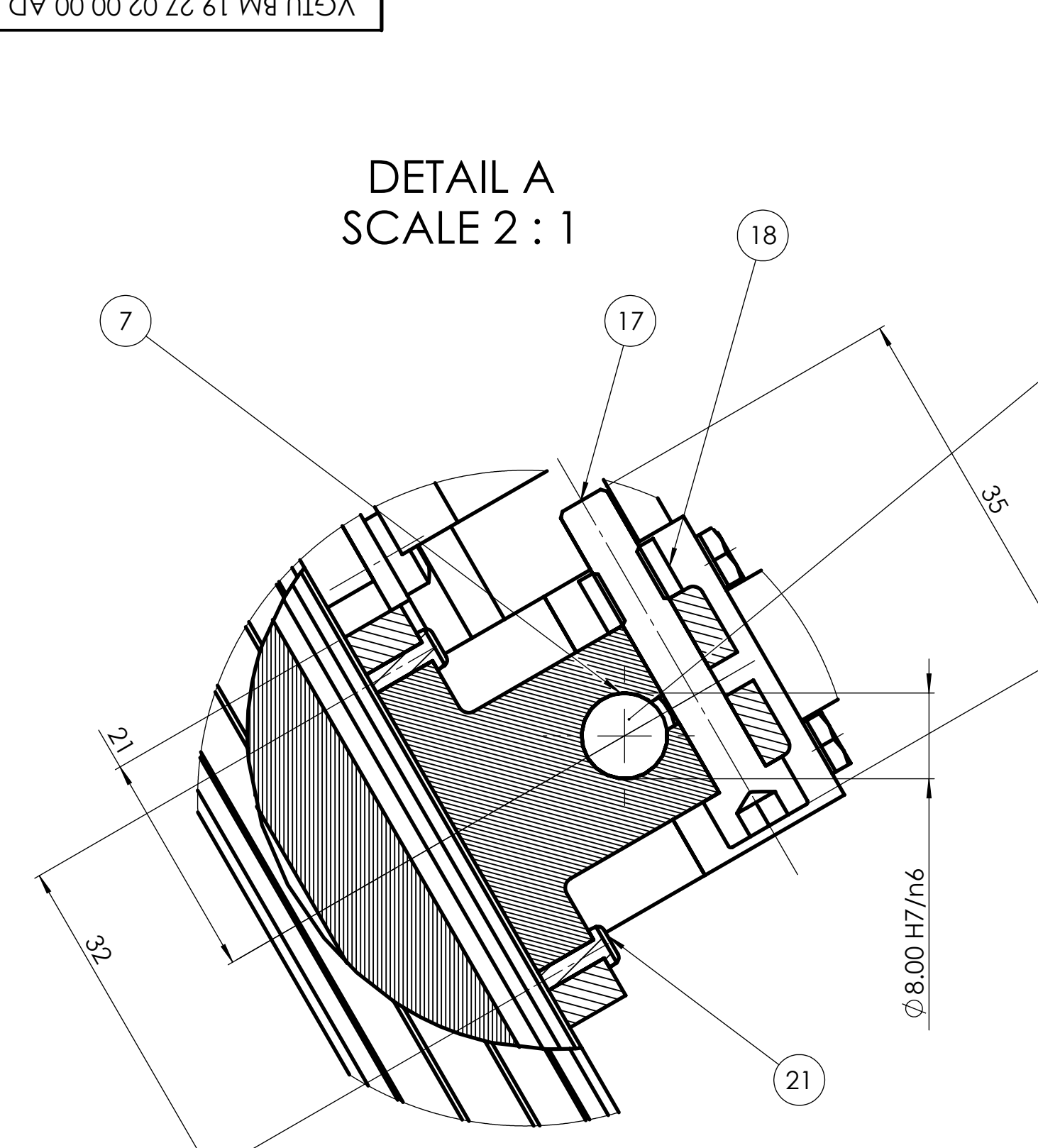


## Note

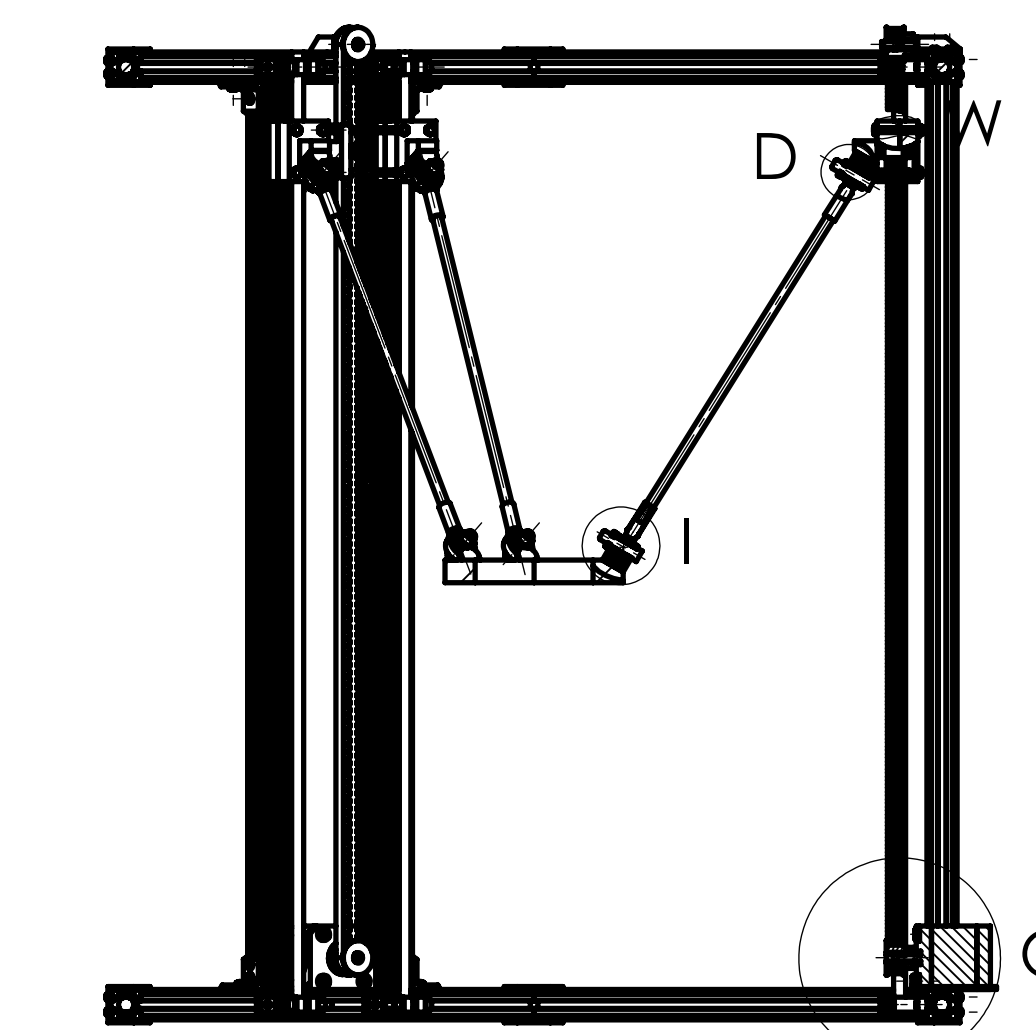
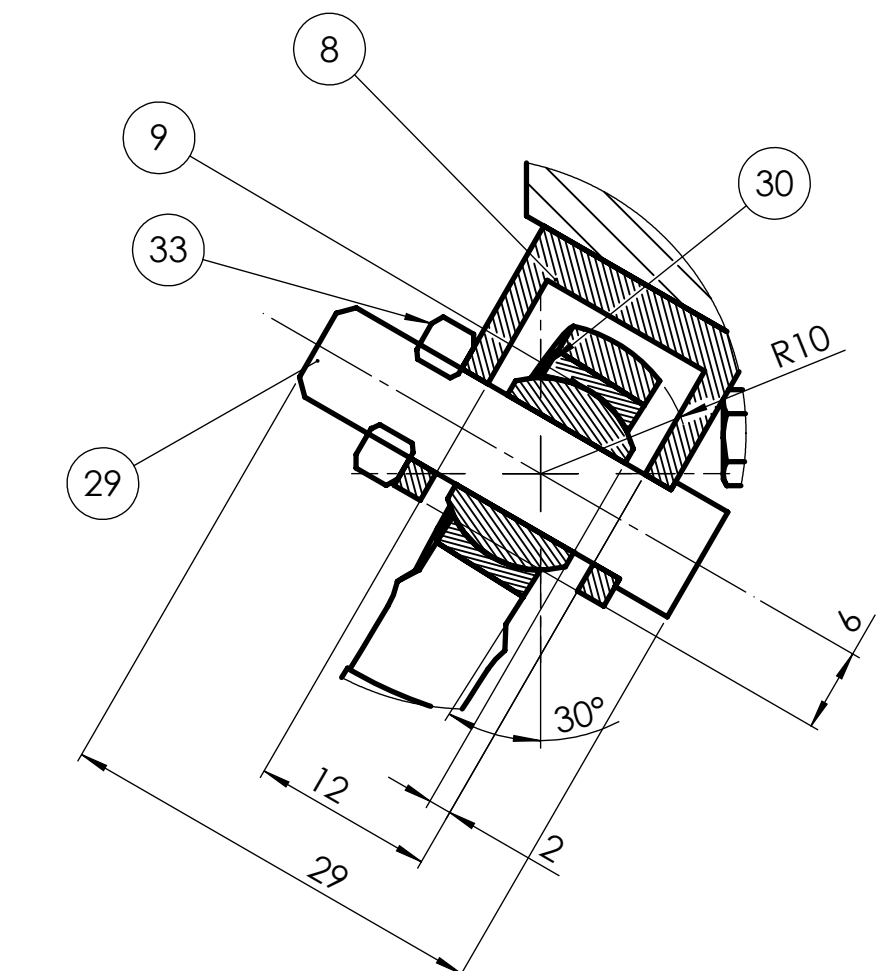
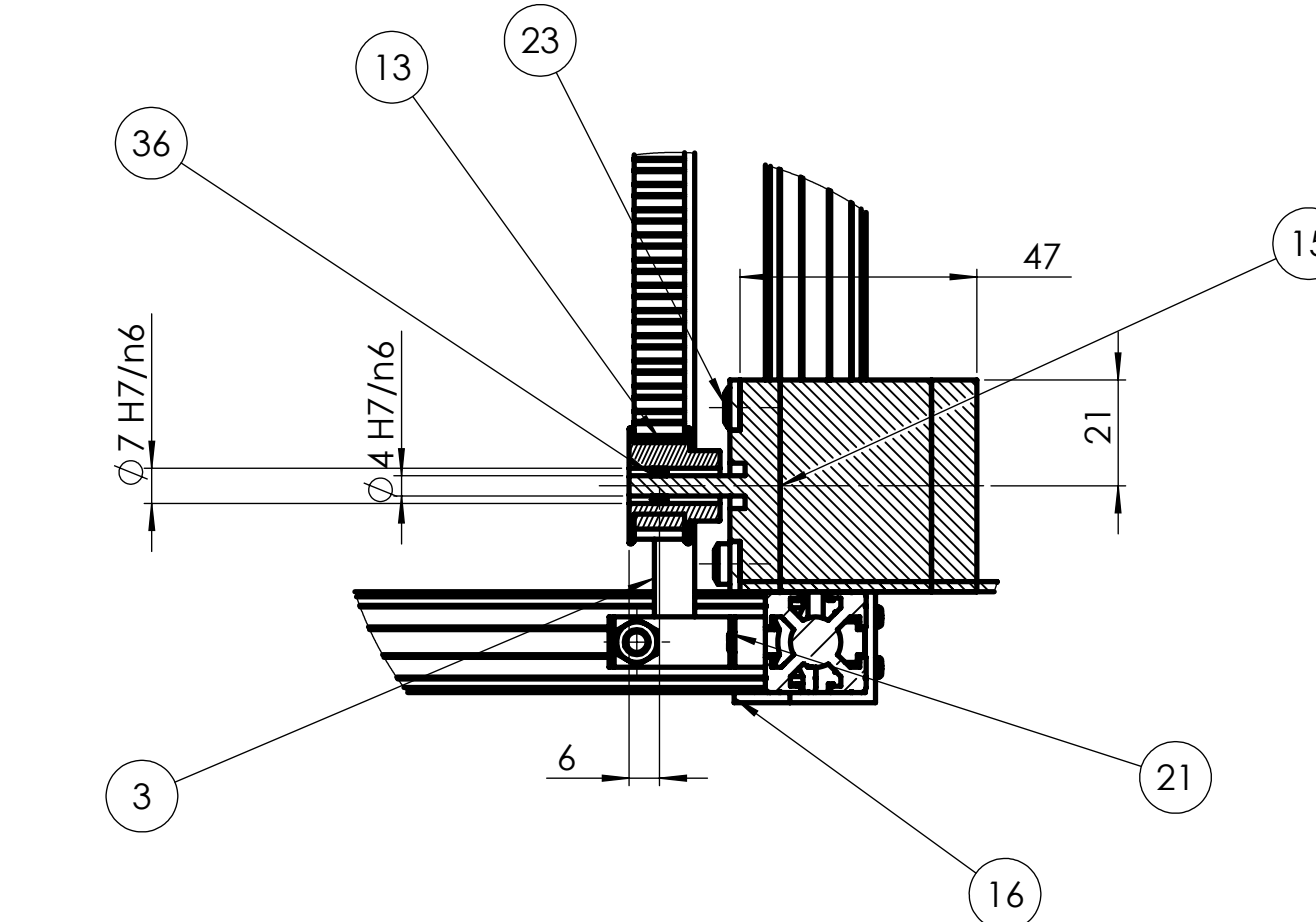
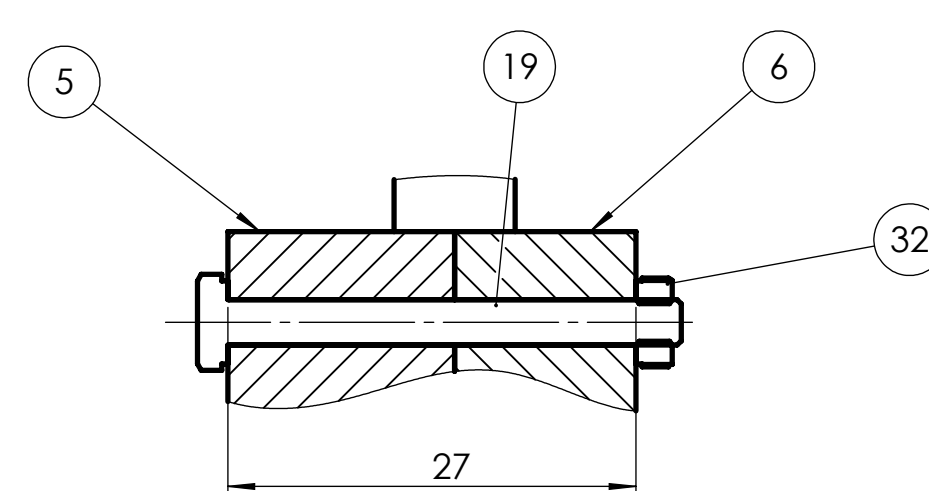
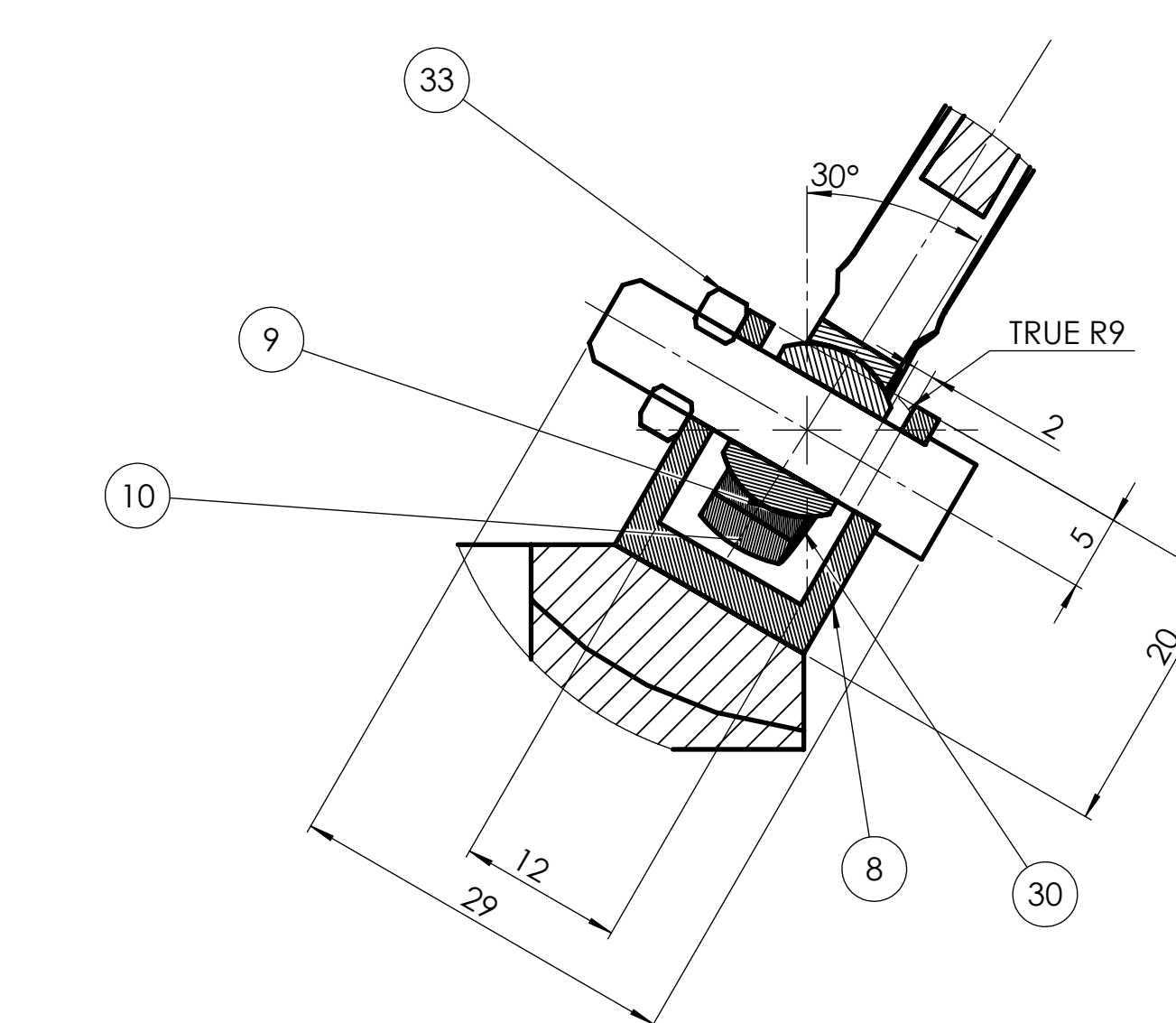
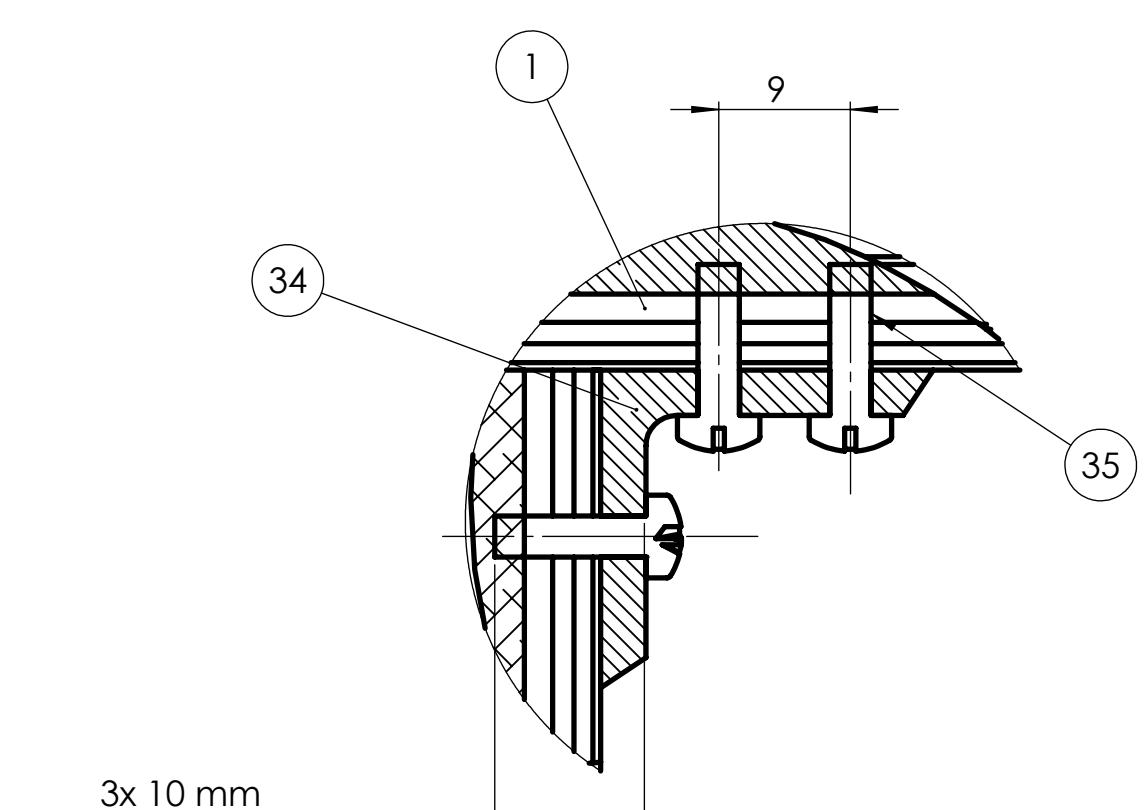
- All the edges should be chamfered 2 x 45 deg.
- Feed rates are to be followed through table

File no. 1	Additional information	Material	Scale
Responsible agency MEMD	Consultant	Document type	Stainless Steel 304
Owner VG TU MPfuc-15	Compiled Ariharasudhan Muthusami Checked Prof. Sigitas Pelevicius	Frame Holder Technological Sketches	Educational
Rev. 0	Date 29-05-2019	Mark VG TU 19 27 03 00 00 TD	Sheet 3/6





SECTION B-B

DETAIL D  
SCALE 2 : 1DETAIL O  
SCALE 2 : 3DETAIL W  
SCALE 2 : 1DETAIL I  
SCALE 2 : 1DETAIL AA  
SCALE 2 : 1

	File no. 1	Additional information	Material	Scale
Responsible agency MEMD	Consultant	Document type	Document status	
Owner	Compiled Anilraasudhan Muthusami	Assembly Drawing	Educational	
	Checked Prof. Sigitas Pekevicius	Title Design of Delta Robot	Mark VG TU BM 19 27 02 00 00 AD	
Rev. 0	Date 28-05-2019	Design	Lon. En.	Sheet 2/6